UNIVERSITAT ROVIRA I VIRGILI
ELECTROCHEMICALLY DEPOSITED METAL NANOSTRUCTURES FOR APPLICATIONS IN GENOSENSORS
Tesfaye Refera Soreta
ISBN:978-84-692-9758-2/DL:T-206-2010

Doctoral Thesis

Tesfaye Refera Soreta

Electrochemically Deposited Metal Nanostructures for Applications in Genosensors

Universitat Rovira I Virgili

Department of Chemical Engineering

UNIVERSITAT ROVIRA I VIRGILI
ELECTROCHEMICALLY DEPOSITED METAL NANOSTRUCTURES FOR APPLICATIONS IN GENOSENSORS
Tesfaye Refera Soreta
ISBN:978-84-692-9758-2/DL:T-206-2010

UNIVERSITAT ROVIRA I VIRGILI
ELECTROCHEMICALLY DEPOSITED METAL NANOSTRUCTURES FOR APPLICATIONS IN GENOSENSORS
Tesfaye Refera Soreta
ISBN:978-84-692-9758-2/DL:T-206-2010

UNIVERSITAT ROVIRA I VIRGILI
ELECTROCHEMICALLY DEPOSITED METAL NANOSTRUCTURES FOR APPLICATIONS IN GENOSENSORS
Tesfaye Refera Soreta
ISBN:978-84-692-9758-2/DL:T-206-2010

UNIVERSITAT ROVIRA I VIRGILI
ELECTROCHEMICALLY DEPOSITED METAL NANOSTRUCTURES FOR APPLICATIONS IN GENOSENSORS
Tesfaye Refera Soreta
ISBN:978-84-692-9758-2/DL:T-206-2010

Tesfaye Refera Soreta

Electrochemically Deposited Metal Nanostructures for Applications in Genosensors

DOCTORAL THESIS

Supervisors: Dr. Ciara K. O´Sullivan
Dr. Olivier F. Y. Henry
Dr. Jörg Strutwolf

Department of Chemical Engineering

UNIVERSITAT ROVIRA I VIRGILI

TARRAGONA

2009

UNIVERSITAT ROVIRA I VIRGILI
ELECTROCHEMICALLY DEPOSITED METAL NANOSTRUCTURES FOR APPLICATIONS IN GENOSENSORS
Tesfaye Refera Soreta
ISBN:978-84-692-9758-2/DL:T-206-2010

UNIVERSITAT ROVIRA I VIRGILI
ELECTROCHEMICALLY DEPOSITED METAL NANOSTRUCTURES FOR APPLICATIONS IN GENOSENSORS
Tesfaye Refera Soreta
ISBN:978-84-692-9758-2/DL:T-206-2010

UNIVERSITAT
ROVIRA I VIRGILI

Department of Chemical Engineering
Universitat Rovira i Virgili
Avenguda Països Catalans, 26
43007, Tarragona, Spain.
Tel: +34-977-558740/8721
Fax: +34-977.559621/8205

Dra. Ciara K. O´Sullivan, i Dr. Olivier Henry,

CERTIFICO:

Que aquest treball, titulat "Electrochemically deposited metal nanostructures for applications in genosensors", que presenta Tesfaye Refera Soreta per a l'obtenció del títol de Doctor, ha esta realitzat sota la meva direcció al Departament Enginyeria Química d'aquesta universitat.

Tarragona,

Dra. Ciara K. O´Sullivan

Dr. Olivier Henry

UNIVERSITAT ROVIRA I VIRGILI
ELECTROCHEMICALLY DEPOSITED METAL NANOSTRUCTURES FOR APPLICATIONS IN GENOSENSORS
Tesfaye Refera Soreta
ISBN:978-84-692-9758-2/DL:T-206-2010

UNIVERSITAT ROVIRA I VIRGILI
ELECTROCHEMICALLY DEPOSITED METAL NANOSTRUCTURES FOR APPLICATIONS IN GENOSENSORS
Tesfaye Refera Soreta
ISBN:978-84-692-9758-2/DL:T-206-2010

UNIVERSITAT
ROVIRA I VIRGILI

Department of Chemical Engineering
Universitat Rovira i Virgili
Avenguda Països Catalans, 26
43007, Tarragona, Spain.
Tel: +34-977-558740/8721
Fax: +34-977.559621/8205

Dr. Ciara K. O´Sullivan and Dr. Olivier Henry,

Certify that:

The present work entitled with "Electrochemically deposited metal nanostructures for applications in genosensors", presented by Tesfaye Refera Soreta to obtain the degree of doctor by the university Rovira I Virgili, has been carried out under my supervision at the Department of Chemical Engineering.

Tarragona,

Dr. Ciara K. O´Sullivan

Dr. Olivier Henry

UNIVERSITAT ROVIRA I VIRGILI
ELECTROCHEMICALLY DEPOSITED METAL NANOSTRUCTURES FOR APPLICATIONS IN GENOSENSORS
Tesfaye Refera Soreta
ISBN:978-84-692-9758-2/DL:T-206-2010

UNIVERSITAT ROVIRA I VIRGILI
ELECTROCHEMICALLY DEPOSITED METAL NANOSTRUCTURES FOR APPLICATIONS IN GENOSENSORS
Tesfaye Refera Soreta
ISBN:978-84-692-9758-2/DL:T-206-2010

To my family

Amanuel, Elroi & Zinash

UNIVERSITAT ROVIRA I VIRGILI
ELECTROCHEMICALLY DEPOSITED METAL NANOSTRUCTURES FOR APPLICATIONS IN GENOSENSORS
Tesfaye Refera Soreta
ISBN:978-84-692-9758-2/DL:T-206-2010

UNIVERSITAT ROVIRA I VIRGILI
ELECTROCHEMICALLY DEPOSITED METAL NANOSTRUCTURES FOR APPLICATIONS IN GENOSENSORS
Tesfaye Refera Soreta
ISBN:978-84-692-9758-2/DL:T-206-2010

ACKNOWLEDGEMENT

It gives me a great pleasure to express my deepest gratitude to my supervisors Dr. Ciara K. O´Sullivan, Dr. Jörg Strutwolf and Dr. Olivier Henry who guided and motivated me throughout the whole course of this work. It was a great opportunity for me to work in the Nanobiotechnology and Bioanalysis Group (NBG) of the Department of Chemical Engineering, at the Universitat Rovira I Virgili (URV) where research in nanotechnology and biosensors is given the highest level of attention and resources are appropriately provided.

I would like to acknowledge the Universitat Rovira I Virgili (URV) for providing me a four year URV BRDI scholarship which paid for my tuition for this Ph.D study. The Jimma University, Ethiopia is also acknowledged for allowing me to have a study leave and providing financial support to my family.

I would like to thank Dr. Klaus Drese of Institut für Mikrotechnik Mainz, Germany for giving me the opportunity to undertake a short stay at the institute.

I am thankful to Ms. Barbara Vastenavond, Ms. Núria Juanpere Mitjana, Ms. Sira Durán Cothenet for their assistance in all the administrative works.

I would like to thank all members of the NBG who helped me in various forms and situations where I needed them, especially, Dr. Alex Fragoso, Dr. Pablo Lozano and Dr. Valerio Beni who should be mentioned for sharing me their wealth of research experience. I would like also to thank Dr. Nigussie Wodago Beyene and Dr. Cengiz Özalp from whom I received a lot of assistance. I would also like to thank Ms. Mercè Moncusí, Dr. Mariana Stankova and Dr. Lukas Vojkuvka of SCRiT - Unit of Microscopy and NanoMetric Techniques of the URV, for their help with scanning electron microscopy and atomic force microscopy imaging.

My greatest appreciation goes to my family, my sons Amanuel Tesfaye and Elroi Tesfaye who are patiently waiting for *Ababa* to come back home and to my wife Zinash Degife, who is shouldering alone all the loads of family responsibility and encouraging me to concentrate on my study.

UNIVERSITAT ROVIRA I VIRGILI
ELECTROCHEMICALLY DEPOSITED METAL NANOSTRUCTURES FOR APPLICATIONS IN GENOSENSORS
Tesfaye Refera Soreta
ISBN:978-84-692-9758-2/DL:T-206-2010

UNIVERSITAT ROVIRA I VIRGILI
ELECTROCHEMICALLY DEPOSITED METAL NANOSTRUCTURES FOR APPLICATIONS IN GENOSENSORS
Tesfaye Refera Soreta
ISBN:978-84-692-9758-2/DL:T-206-2010

Resumen

Las señales del biosensor se pueden mejorar diseñando específicamente las superficies del transductor con el objetivo de proporcionar el mejor entorno para el reconocimiento de moléculas. Esto es particularmente evidente en el caso de los genosensores, donde el espaciamiento y la orientación de las sondas de captura de ADN inmovilizada tienen que controlarse con mucho cuidado para maximizar la posterior hibridación de la superficie con la secuencia destino y obtener señales de unión alta. Por esta razón, los métodos de preparación de superficie de electrodos nanoestructurados son necesarios en el desarrollo de biosensores electroquímicos para mitigar los problemas relacionados con la conglomeración de las sondas de captura de superficie y la creación de un entorno adecuado para el incremento de los eventos de bioreconocimiento. Para este fin, se han investigado varios métodos de nanoestructuración de la superficie.

El primer método de nanoestructuración de la superficie estudiado se basó en la formación inicial de monocapas de moléculas autoensambladas de alcanotioles (SAM) en substratos bimetálicos, seguido de una desorción selectiva de las SAM a partir de determinados metales mediante la aplicación de potenciales de reducción del alcanotiol específico en metal. Con el fin de conseguir este objetivo, identificamos primero dos metales por su capacidad de formar las SAM de alcanotioles. Es sabido que los metales nobles como el oro, la plata, el platino y el cobre son buenos sustratos para las SAM. Sin embargo, también se estudió el paladio (Pd), que recientemente alcanzó un interés considerable por aumentar la actividad catalítica de las aleaciones. Dado que no había informes previos sobre la formación de las SAM en los sustratos de paladio electrodepositado, llevamos a cabo un completo estudio del proceso de electrodeposición de Pd y caracterizó electroquímicamente la formación de las SAM sobre el paladio.

El paladio se depositó electroquímicamente sobre el carbono vítreo (GC) y se utilizó como sustrato para la formación de las SAM. Se estudiaron los parámetros de deposición, como el baño electrolítico, pH, y los parámetros de efectos electroquímicos (magnitud del potencial o corriente aplicados, y la duración de la señal aplicada). La estructura y morfología de los depósitos de paladio se observaron mediante microscopio

ISBN:978-84-692-9758-2/DL:T-206-2010

electrónico de barrido (MEB) y se estudiaron electroquímicamente. Se prepararon dos conjuntos de electrodos paladiados para la formación de las SAM. El primer conjunto estaba compuesto de electrodos con una superficie de paladio especular, producida en condiciones galvanostáticas y potencioestáticas inferiores. La superficie de paladio del segundo conjunto de electrodos tenía una apariencia negra y no reflectante, de nuevo producida por unas condiciones galvanoestáticas y de potencial constante. Solo se observó un bloqueo menor de metilviológeno como sonda de redox para las SAM formadas en superficies de paladio brillantes, generadas tanto potencioestáticamente como galvanostáticamente. En cambio, las monocapas ensambladas en las superficies de paladio negras forman una barrera sustancial frente a la reacción redox de la sonda de redox de metilviológeno.

En una segunda etapa, se estudiaron varios métodos para la preparación de superficies de aleación, que consistieron en (i) la codeposición de paladio y oro del baño de deposición de la aleación de paladio y oro sobre los electrodos GC, (ii) la deposición electroquímica de paladio sobre electrodos de oro y (iii) la codeposición electrónica del paladio y oro sobre sustratos de silicio (100). Las superficies resultantes se caracterizaron electroquímicamente. Para las superficies de electrodos de aleaciones que se prepararon según el método (ii), se obtuvo una desorción reductiva selectiva y controlada de las SAM de 2-mercaptoetanol de los dominios de paladio de la superficie de paladio y oro.

El segundo método de nanoestructuración investigado se basó en la nucleación electroquímica secuencial de nanopartículas de metal sobre la superficie GC. Se desarrolló un método para preparar los dominios de tamaño nano para que actuaran como sustratos para la inmovilización de las SAM y se optimizó con el fin de incrementar la densidad numérica de las nanopartículas a la vez que evitaba la formación de aglomerados. Con el objeto de hacer la realización de genosensores de alta precisión, el método de nanoestructuración permite la creación de condiciones favouables para la interacción efectiva de los nanodominios de sondas de captura de ADN asociados a las nanopartículas con su secuencia destino. El método de la nucleación electroquímica secuencial conllevó un número de deposiciones electroquímicas y pasos de protección. En resumen, el primer paso de la deposición

ISBN:978-84-692-9758-2/DL:T-206-2010

electroquímica de las nanopartículas de metal sobre la superficie de GC fue seguido de la protección de las partículas por autoensamblaje de una monocapa de tiol para evitar que estas se utilizaran como germen en los pasos de deposición posteriores. En el siguiente paso de deposición, se formaron nuevas partículas en la superficie de GC debido a la acción aislante de las SAM sobre las partículas depositadas en el paso anterior. Se estudiaron las condiciones óptimas respecto al tamaño de partículas, distribución y densidad numérica mediante la variación de los parámetros de deposición como la potencial de deposición, el tiempo de deposición y la concentración del baño de deposición. Para distinguir las superficies electroactivas de carbono vítreo de las superficies de nanopartículas de oro, se utilizó un tiol marcado electroactivo que adsorbió químicamente de manera selectiva las nanopartículas de metal.

En un principio, estudiamos la deposición secuencial de las nanopartículas de oro y después extendimos la metodología desarrollada a la deposición secuencial de las nanopartículas de paladio. Se observó un incremento de señales de ferroceno superior en las nanopartículas de oro depositadas secuencialmente comparadas con la masa de oro. Además, la deposición secuencial del paladio usando las SAM protectoras de alcanotiol ferrocenil demostró un incremento de señales de ferrocenil superior a las nanopartículas de oro. El incremento de señales podría estar asociado a las propiedades únicas de las nanopartículas que podrían realizar procesos de autoensamblaje de monocapas con base de tiol más efectivas en las nanopartículas que en los metales.

Finalmente, se demostró la nanoestructruación de la superficie de electrodos utilizando nanopartículas de oro depositadas secuencialmente para incremento de señales y mejora de la sensibilidad del biosensor de ADN. Las SAM de sonda de captura de ADN con base de tiolato 20 formada sobre la superficie nanoestructurada se emplearon para la detección de 63 bases oligonucleotidos objetivo, utilizando peroxidasa de rábano como marca enzimática. La señal electroquímica registrada se comparó con la de electrodos planos de oro, preparada por deposición electroquímica de oro sobre electrodos de carbono vítreo. Se observó una sensibilidad superior y una mejor reproducibilidad de los electrodos nanoestructurados que de los electrodos planos.

UNIVERSITAT ROVIRA I VIRGILI
ELECTROCHEMICALLY DEPOSITED METAL NANOSTRUCTURES FOR APPLICATIONS IN GENOSENSORS
Tesfaye Refera Soreta
ISBN:978-84-692-9758-2/DL:T-206-2010

Esta tesis está estructurada basándose en los artículos que se han publicado, un artículo enviado para su publicación y otro en preparación para su envío. Está compuesto de seis capítulos. El Capítulo 1 es un capítulo introductorio donde se presentan los antecedentes del estudio, la revisión bibliográfica, los objetivos del estudio y los trabajos futuros. El capítulo describe brevemente los biosensores, concretamente los biosensores electroquímicos para ADN, y una revisión bibliográfica que enfatiza la importancia de la nanoestructuración de la superficie y los distintos métodos de nanoestructuración de superficie desarrollados por los biosensores. En el Capítulo 2 se introduce el artículo sobre el estudio de la deposición electroquímica del paladio como ayuda para la formación de las SAM de alcanotioles. Los Capítulos 3 y 4 están compuestos de artículos en los que se presenta la deposición electroquímica secuencial de las nanopartículas de metal para la nanoestructuración de superficie y el incremento de las SAM electroactivas enlazadas a la superficie. El Capítulo 5 es un artículo que presenta el método de nanoestructuración de superficie usando la desorción reductiva selectiva a partir de superficie de aleación de paladio y oro. Finalmente, el capítulo 6 presenta un artículo que describe el uso de la superficie nanoestructurada para aplicaciones de sensor electroquímico para ADN.

UNIVERSITAT ROVIRA I VIRGILI
ELECTROCHEMICALLY DEPOSITED METAL NANOSTRUCTURES FOR APPLICATIONS IN GENOSENSORS
Tesfaye Refera Soreta
ISBN:978-84-692-9758-2/DL:T-206-2010

Summary

Biosensor signals can be enhanced by specifically designing transducer surfaces with the objective of providing the best environment to the recognition molecules. This is particularly evident in the case of genosensors, where spacing and orientation of immobilised DNA capture probes need to be carefully controlled to maximize subsequent surface hybridisation with the target sequence and achieve high binding signals. To address the spacing and orientation requirements, nanostructured electrode surface preparation methods can be exploited for the development of electrochemical genosensors to alleviate problems related to surface crowding of capture probes and the creation of a suitable environment for enhancement of the biorecognition events. To this end, several surface nanostructuring approaches have been investigated.

The first surface nanostructuring approach studied was based on the initial formation of self-assembled monolayers of alkanethiols (SAM) on bi-metallic substrates, followed by the selective desorption of the SAM from one of the metals by applying metal-specific alkanethiol reduction potentials. In order to realise this objective, we first identified two metals for their ability to form SAMs of alkanethiols. Noble metals such as gold, palladium, platinum, ruthenium and rhodium were evaluated. Metals were electrochemically deposited on glassy carbon (GC) and used as a substrate for SAM formation. Deposition parameters such as electrolyte bath, pH, and the effect electrochemical parameters (magnitude of the applied potential or current, and duration of the applied signal) were studied. The structure and morphology of the metal deposits were observed by scanning electron microscopy (SEM) and studied electrochemically. As there is no previous report on the formation of SAMs on palladium, we carried out a full study of the electrodeposition process and electrochemically characterised the formation of SAMs on palladium.

Palladium was electrochemically deposited under potentiostatic and galvanostatic conditions. Two sets of palladinised electrodes were prepared for SAM formation. The first set consisted of electrodes with a mirror-like palladium surface, produced under lower galvanostatic and potentiostatic conditions. The palladium surface of the second set of electrodes had a black and non-reflecting appearance, again produced by constant

ISBN:978-84-692-9758-2/DL:T-206-2010

potential and galvanostatic conditions. Only very minor blocking of methylviologen used as a redox probe was observed for the SAMs formed on shiny palladium surfaces generated both potentiostatically and galvanostaically. In contrast, monolayers assembled on the black palladium surfaces formed a substantial barrier against the redox reaction of methylviologen redox probe. Similar study was conducted for electrochemical deposition of platinum, ruthenium, gold and rhodium and the formation of alkanethiol SAMs on the substrates.

In a second step, various methods for the preparation of mixed metal surfaces were studied, which consisted in (i) the electrochemical deposition of palladium on gold electrode the des, (ii) the co-deposition of palladium and gold from palladium-gold mixed deposition bath on GC electrodes, and (iii) the co-sputtering of palladium and gold onto silicon (100) substrates. The resulting surfaces were electrochemically characterised. and controlled selective reductive desorption of SAM of 2-mercaptoethanol from palladium domains of the palladium-gold surface was achieved. Electrochemical DNA biosensors were constructed using these substrates and their performances compared to that of plain gold electrodes. For the biosensor configuration studied, the mixed metal substrates did not show improvement as compared to plain gold electrodes.

The second nanostructuring approach investigated was based on sequential electrochemical nucleation of metal nanoparticles on glassy carbon surface. A method was developed to prepare nano-sized domains to act as substrates for the immobilisation of SAMs and optimized in order to increase nanoparticles number density while preventing the formation of aggregates. With the objective of realising highly sensitive genosensors, the nanostructuring approach allowes the creation of favourable conditions for the effective interaction of nanodomains of DNA capture probes attached to the nanoparticles with their target sequence.

The sequential electrochemical nucleation approach involved a number of electrochemical deposition and protection steps. Briefly, the first stage of electrochemical deposition of the metal nanoparticles on the glassy carbon surface was followed by protection of the particles by self-assembling of a thiol monolayer to

ISBN:978-84-692-9758-2/DL:T-206-2010

prevent them from being used as seeds in subsequent deposition steps. In the next deposition step, new particles were formed on the glassy carbon surface due to the insulating action of the SAM on the particles deposited in the previous step. Optimal conditions regarding particle size, distribution and number density were studied by varying deposition parameters like deposition potential, deposition time and concentration of the deposition bath. An electroactive labelled thiol that selectively chemisorbed onto the metal nanoparticles was used to distinguish the glassy carbon electroactive surface from the gold nanoparticle surface.

We initially studied the sequential deposition of gold nanoparticles and further extended the developed methodology to the sequential deposition of palladium nanoparticles. A higher ferrocene signal enhancement was recorded when using sequentially deposited gold nanoparticles as compared to that recorded when using planar gold electrodes. Furthermore, sequential deposition of palladium using ferrocenyl alkanethiol protective SAM showed markedly higher ferrocenyl signal enhancement (57.5 μC after fifth round) than gold nanoparticles (7.2 μC after fifth round) with the overall enhancement factor close to 48 fold when comparing the palladium nanostructured surface with the planar gold electrodes (1.2 μC) routinely used in electrochemical genosensors. The signal enhancement can be attributed to the unique properties of nanoparticles with the higher surface ratio of surface atoms not only making the self-assembling processes of thiol-based monolayers more effective on the nanoparticles than on bulk metals, but also contributing to signal enhancement due to the inherent enhanced catalytic activity.

Finally, electrode surface nanostructuring using sequentially deposited gold nanoparticles for signal enhancement and improving sensitivity of DNA biosensor was demonstrated. SAMs of 20 base thiolated DNA capture probe formed on the nanostructured surface were employed for the detection of a 63 bases oligonucleotides model target using horseradish peroxidase as enzymatic label. The electrochemical signal recorded was compared against a gold planar electrode prepared by electrochemical deposition of gold on glassy carbon electrode and higher sensitivity was observed for the nanostructured electrodes for detection of the target DNA with a sandwich assay using horseradish peroxidase enzyme label. Nanostructured electrode prepared following three rounds of deposition exhibited sensitivity of 44.89 (nA/nM)

ISBN:978-84-692-9758-2/DL:T-206-2010

and linear range 0.53 nM to 25 nM, where as for the plain gold electrodes sensitivity was 13.67 nA/nM with a linear range extending from 5.22 nM to 25 nM. In another approach, for detection of ferrocene labelled target, the nanostructured electrode for three rounds of gold nanoparticles sequential deposition resulted in a 3.5 fold signal enhancement in comparison to the signal recorded using a plain gold electrode.

This thesis is organized based on articles that have been published, one article submitted for publication and one article under preparation for submission. It is composed of six chapters. Chapter 1 is an introductory chapter where the backgrounds of the study, literature review, the objectives of the study, and the future works are presented. The chapter briefly describes biosensors, specifically electrochemical DNA biosensors, and a literature review that emphasizes on the importance of surface nanostructuring and the different surface nanostructuring approaches so far developed for genosensors. In Chapter 2, the article on study of electrochemical deposition of palladium as a support for formation of SAM of alkanethiols is presented. Chapter 3 is an article that presents the surface nanopatterning approach using selective reductive desorption from a mixed metal surface of palladium-gold. Chapter 4 and 5 consist in articles in which sequential electrochemical deposition of metal nanoparticles for surface nanostructuring and enhancement of surface bound electroactive SAMs are presented. Finally, Chapter 6 presents an article that describes the application of nanostructured surfaces for electrochemical DNA sensor.

UNIVERSITAT ROVIRA I VIRGILI
ELECTROCHEMICALLY DEPOSITED METAL NANOSTRUCTURES FOR APPLICATIONS IN GENOSENSORS
Tesfaye Refera Soreta
ISBN:978-84-692-9758-2/DL:T-206-2010

List of abbreviations

A	Area, of an electrode
AFM	Atomic force microscopy
DNA	Deoxyribonucleic acid, either a single stand or a double strand
E	Voltage or potential
e^-	An electron
GC	Glassy carbon electrode
h	Thickness of a metal deposit
i	Current
i_{ct}	Faradic current (charge transfer current)
i_{dl}	Capacitive current (double layer charging current)
i_g	Total galvanostatic current
IUPAC	International union of pure and applied chemistry
M	Represents a metal
M^{n+}	Metallic ion with positive charge of n
n	Number of electrons transferred
PCR	Polymerase Chain Reaction
Q	Charge
Γ	Surface coverage of self-assembled monolayer of alkanethiol on a substrate
ρ	Density of a metal
Redox-	Reduction-oxidation reaction
RNA	Ribonucleic acid
SAM	Self-assembled monolayer
SEM	Scanning electron microscopy
SPM	Scanning probe microscopy
STM	Scanning tunnelling microscopy
t	Time
UPD	Under potential deposition
V	Volume of metal deposit
w	Weight of metal deposit
W	Atomic weight (g/mol)

UNIVERSITAT ROVIRA I VIRGILI
ELECTROCHEMICALLY DEPOSITED METAL NANOSTRUCTURES FOR APPLICATIONS IN GENOSENSORS
Tesfaye Refera Soreta
ISBN:978-84-692-9758-2/DL:T-206-2010

List of publications derived from the thesis

1. Tesfaye Refera Soreta, Jörg Strutwolf, Ciara K. O´Sullivan, Electrochemically Deposited Palladium as a Substrate for Self-Assembled Monolayers, Langmuir, 2007, 23, 10823 – 10830.

2. Tesfaye Refera Soreta, Jörg Strutwolf, Ciara K. O´Sullivan, Electrochemical Fabrication of Nanostructured Surfaces for Enhanced Response, ChemPhysChem, 2008, 9, 920 – 927.

3. Tesfaye Refera Soreta, Jörg Strutwolf, Olivier Henry, Ciara K. O´Sullivan, Electrochemical Surface Structuring with Palladium Nanoparticles for Signal Enhancement, submitted to Langmuir.

4. Tesfaye Refera Soreta, Jörg Strutwolf, Olivier Y.F. Henry, Ciara K. O´Sullivan, Electrochemical Surface Nanopatterning by Selective Reductive Desorption from Mixed Metal Surfaces, Electrochimica Acta, 2009 In press.

5. Tesfaye Refera Soreta, Jörg Strutwolf, Olivier Y.F. Henry, Ciara K. O´Sullivan, Electrochemical Surface Nanostructuring for Enhancement of Signal of DNA Biosensors, Article in preparation.

UNIVERSITAT ROVIRA I VIRGILI
ELECTROCHEMICALLY DEPOSITED METAL NANOSTRUCTURES FOR APPLICATIONS IN GENOSENSORS
Tesfaye Refera Soreta
ISBN:978-84-692-9758-2/DL:T-206-2010

Table of Contents

UNIVERSITAT ROVIRA I VIRGILI
ELECTROCHEMICALLY DEPOSITED METAL NANOSTRUCTURES FOR APPLICATIONS IN GENOSENSORS
Tesfaye Refera Soreta
ISBN:978-84-692-9758-2/DL:T-206-2010

UNIVERSITAT ROVIRA I VIRGILI
ELECTROCHEMICALLY DEPOSITED METAL NANOSTRUCTURES FOR APPLICATIONS IN GENOSENSORS
Tesfaye Refera Soreta
ISBN:978-84-692-9758-2/DL:T-206-2010

Chapter 1

Introduction

UNIVERSITAT ROVIRA I VIRGILI
ELECTROCHEMICALLY DEPOSITED METAL NANOSTRUCTURES FOR APPLICATIONS IN GENOSENSORS
Tesfaye Refera Soreta
ISBN:978-84-692-9758-2/DL:T-206-2010

UNIVERSITAT ROVIRA I VIRGILI
ELECTROCHEMICALLY DEPOSITED METAL NANOSTRUCTURES FOR APPLICATIONS IN GENOSENSORS
Tesfaye Refera Soreta
ISBN:978-84-692-9758-2/DL:T-206-2010

Chapter 1
Introduction

1. Introduction

1.1. Introduction to electrochemical DNA biosensors

1.1.1. Definition of electrochemical biosensor

According to the International Union of Pure and Applied Chemistry (IUPAC) recommendation[1], an electrochemical biosensor is defined as *"a self-contained integrated device which is capable of providing specific quantitative or semi-quantitative analytical information using a biological recognition element which is retained in direct spatial contact with an electrochemical transduction element"*. Biosensors may be classified according to the biological specificity-conferring mechanism or to the mode of physico-chemical signal transduction. The biorecognition material can be classified as bioaffinity recognition elements and biocatalytic recognition elements. The bioaffinity recognition can be based for example on antibody-antigen interaction, formation of double stranded DNA at DNA modified surfaces, or the use of synthetic receptors such as molecularly imprinted polymers and aptamers. Biocatalytic-based biosensors mostly exploit enzymes, however the application of whole cells or tissue as biocatalysts has been reported[2-4].

The detection of target biochemical molecules by means of traditional analytical methods can be slow and time consuming. On the other hand, biosensors offer the possibility of rapid, *in-situ* analysis[5]. Furthermore, biosensors can be designed to exhibit high selectivity based on the inherent properties of the immobilised biocomponents. The biological recognition element that is attached to the transducer surface selectively interacts with the analyte present in a complex sample matrix, thus eliminating the requirement for separation and/or preconcentration of the analyte.

1.1.2. Electrochemical DNA biosensors

DNA biosensors are based on the attachment of capture single stranded DNA probes onto a surface and the detection of surface hybridisation events with the complementary

ISBN:978-84-692-9758-2/DL:T-206-2010

target sequence present in the sample. Based on the Watson-Crick base pairing principle (i.e. adenine pairing with thymine and guanine with cytosine)[6-10], highly specific and sensitive DNA biosensing strategies have been developed. Consequently, new DNA biosensor technologies continue to be intensively investigated because of their promise for rapid and low cost DNA testing. Sensors have been developed based on, for example on electrochemical[11-27], optical[28-33], mass sensitive[34] and acoustic wave[35, 36] for transduction of the surface hybridisation event. Some of the applications of these sensors include, identification of pathogens[6, 37], gene expression monitoring[38], diagnosis of genetic disorders[39, 40], investigation of DNA damage[41] and bio-analysis of environmental pollution[42]. In a genetic analysis, the DNA from the sample is first extracted, and subsequently regions of interest are further chemically amplified by polymerase chain reaction (PCR) (Scheme 1). This approach yields sufficient quantities of analyte DNA for detection[37]. The development of microfluidic systems for the integration of these steps into a simple miniaturised device will reduce laboratory sample preparation and analysis time, human interaction with the different processes involved, as well as reagent and equipment costs [43].

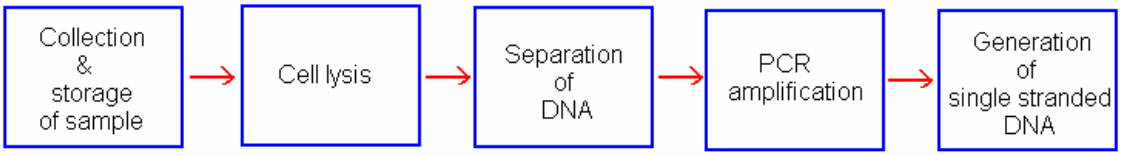

Scheme 1. Schematic representation of sample preparation for DNA analysis

1.1.3 Advantages of electrochemical DNA biosensors

Optical detection methods have found wide spread application for real-time or near real-time genosensors applications[6, 44-46]. The detection of DNA hybridisation on microarrays usually involves detecting the signal generated by the binding of a reporter probe (fluorescent, chemiluminescent, colorimetric) to the target DNA sequence. For example, for fluorophore labelled targets, fluorescence scanning is carried out to obtain the complete hybridisation pattern on microarrays DNA biosensors. However, the application of electrochemical methods to the sensing of biologically related species

ISBN:978-84-692-9758-2/DL:T-206-2010

provide significant advantages over optical biosensors[16, 47, 48]. Specifically, the advantages of electrochemical biosensors include: speed, sensitivity, and low-cost-mass-power requirements of electrochemical detection[49] as well as the relatively high stability and environmental insensitivity of electroactive labels; and the availability of electroactive labels with non-overlapping redox potentials for the simultaneous detection of multiple DNA targets[50].

1.2. Electrochemical detection of the hybridisation event

Label-free electrochemical biosensing devices can monitor sequence-specific hybridisation processes either (i) directly, based on the intrinsic DNA electroactivity[51, 52] or (ii) indirectly, by measuring changes in the electrical properties of the electrode–solution interface such as conductivity[53-55], capacitance[37] or impedance[56-59].

Label-free biosensors have the advantage of not requiring electroactive marker groups to be linked to either the target or to the probe simplifying the detection of the hybridisation event. For example, label-free electrochemical detection systems for DNA have been reported where the electrode was impedimetrically characterised[58, 60-66] in the presence of a redox system such as hexacyanoferrate(II)/hexacyanoferrate(III) before and after DNA hybridisation. Surface hybridisation resulted in an increased blocking of access of the redox marker hexacyanoferrate(II)/hexacyanoferrate(III) with an increase in charge transfer resistance after DNA duplex formation. Further enhancement in signal has been achieved after binding of a negatively charged molecule (e.g. rose Bengal) to the formed DNA duplex[63]. However, electrochemical impedance spectroscopy is highly susceptible to any change at the electrode surface, which can lead to a lack of reliability and reproducibility problems. Good control of the electrode-electrolyte interface is thus required to achieve reliable and reproducible measurements.

Non-covalent electroactive markers that interact in a different way with single strands and double strands of DNA can be also be used for labeless detection of surface hybridisation event. The interaction of these electroactive labels with DNA are typically electrostatic in cases where charged labels are used or alternatively based on molecular

ISBN:978-84-692-9758-2/DL:T-206-2010

interaction / intercalation. These electroactive labels are either metal complexes[58, 67-72] or organic compounds like daunomycin[13, 27], methylene blue[73, 74] or Hoechst 33258 [75]. The use of non-covalent markers offers the advantage of label-free detection of surface hybridisation of targeted DNA sequences with the immobilised probes.

Electroactive marker groups can be covalently linked to the immobilised probe[16] or to the target[76] in order to monitor the hybridisation event. Ferrocene and methylene blue[16, 43, 77-79], Pt(II) complex[80], colloidal nanoparticles[81] have been used as electroactive markers.

Electroactive marker labelled detection of DNA typically generates low level hybridisation signals that require complicated background current subtraction. Signal enhancement based on the use of colloidal nanoparticles has been reported to overcome low sensor sensitivity. The various strategies for the use of colloidal nanoparticles for signal enhancement to monitor the hybridisation event has been well reviewed by Merçoci et al.[81] and Fang et al.[82]. As an example, Wang et al.[83] reported a method in which the gold nanoparticle labels linked to target DNA were covered with silver by precipitation and the accumulated silver being detected by electrochemical stripping offering 83 fold signal enhancement as compared to detection without silver accumulation.

Alternatively, enhancement of hybridisation signals can be achieved though the use of enzyme labels, linked directly to a reporter DNA strand[84, 85] or indirectly through biotin–avidin[86, 87] links where the enzyme catalyses the conversion of a substrate to an electrochemically detectable product. Multiple signal enhancement strategy using enzyme labels combined with biometalisation[88, 89] has been reported to achieve even lower detection limits. For example, a detection limit of 2.5 picomolar target DNA concentration has been reported using this approach[89].

UNIVERSITAT ROVIRA I VIRGILI
ELECTROCHEMICALLY DEPOSITED METAL NANOSTRUCTURES FOR APPLICATIONS IN GENOSENSORS
Tesfaye Refera Soreta
ISBN:978-84-692-9758-2/DL:T-206-2010

1.3. Probe DNA immobilisation

The most common way of attaching DNA capture probes to the transducer surface is via the use of thiol link modified probe DNA molecules that interacts with a gold surface through the sulphur atom of the thiol group.

Herne et al.[90] gave a detailed account of the structure of surface attached probes and the impact of the probes distribution and orientation on the efficiency of hybridisation reactions using x-ray photospectroscopy and P^{32} radiolabelled study. Their studies highlighted the following important points that are the basis for the state-of-the art platform for sequence specific DNA biosensors.

a) By immobilisation of thiolated capture probes solution on a surface, the probes can be adsorbed on the surface "specifically" through the sulphur atom and "non-specifically" through the nucleotide bases. The major contribution for surface adsorption of the probe comes from the specific adsorption. The non-specific adsorption of the probe laterally on the substrate can be effectively removed by immobilising aqueous solution of "back-filler" such as 6-mercaptohexanol, effectively forcing the DNA probes to be properly oriented for subsequent hybridisation.
b) The buffer concentration has a profound influence on the success of adsorption of thiolated probe on gold surface. It was suggested that higher buffer concentration such as 1 M KH_2PO_4 could give better coverage of the probes on the gold surface as the high ionic strength is believed to suppress the intermolecular electrostatic repulsion between neighbouring strands of DNA molecules.

Alternative approaches for anchoring of DNA probes at surfaces based on biotin functionalized probes to surface immobilised streptavidin/avidin[91-94] and covalent linking of the capture probe to functionalised surfaces[95-99] have been reported. DNA probes can be also directly attached to positively charged surfaces electrostatically as result of its negatively charged phosphate-rich backbone[100]. The choice of method for

ISBN:978-84-692-9758-2/DL:T-206-2010

surface attachment depends on the nature of the transducer surface used in the biosensor construction.

Glassy carbon electrodes have been widely used in the construction of electrochemical DNA hybridisation biosensors in combination with different oligonucleotides immobilisation methods, such as (i) via entrapment[55, 78, 101, 102] or covalent attachment to the polymer film[78, 101, 102]; (ii) by covalent attachment on functionalized glassy carbon electrodes,[71, 73] with carbon nanotubes[27, 103], or gold nanoparticles[104] (iii) by electrostatic adsorption on gold colloid modified surfaces[105], and (iv) by direct adsorption of oligonucleotides onto pre-oxidized glassy carbon electrodes[58]. Electrostatic adsorption of DNA results in multipoint attachment of the DNA probe to the surface and therefore can influence the efficiency of hybridisation with the target. Direct adsorption of DNA onto glassy carbon surface is a physical adsorption process that may also influence the stability of the surface bound probes.

In this work, glassy carbon electrodes modified with electrochemically deposited metal nanoparticles (gold and palladium) were used as a substrate for attachment of alkanethiols and to investigate its use as a substrate for thiolated DNA probes.

1.4. Surface nanostructuring for enhancing the hybridisation event

In the development of DNA biosensors, one of the main issues to be addressed is the control of immobilisation of the DNA probes on the surface. Factors such as surface density, orientation and conformation of the immobilised DNA probes can affect the DNA biosensor performance[106, 107]. A probe DNA SAM with a very high packing density may not be very useful for hybridisation, since there may not be enough space between immobilised DNA probes to allow hybridisation with the target sequence[108] due to steric hindrance as well as electrostatic interactions between probe molecules that prevent target binding[109]. A very low probe density is also not favourable as the signal that can be extracted could be so small that detection may be difficult.

ISBN:978-84-692-9758-2/DL:T-206-2010

Controlling the surface coverage of the probe DNA is an important factor in maximizing hybridisation efficiency. In DNA biosensors the signal for the determination of a particular target is mainly affected by the efficiency of the hybridisation event (base pairing of the immobilised probe to the target). The hybridisation process is affected by the electrostatic repulsion between the hybridising strands of the DNA and the density of the probes on the transducer surface. One of the most commonly employed methods to control the surface coverage of DNA probes is the creation of a mixed SAM of the thiolated probe and a backfiller such as 6-mercaptohexanol.

The fundamental aspects of heterogeneous hybridisation, such as the kinetics of diffusion and adsorption of DNA molecules on solid supports need to be well understood in order to explain the hybridisation of a target to surface attached probes. Chan et al.[110] raised the following practical questions in the design and use of immobilised probe arrays: What probe density is optimal? How long should the probes and targets be? What degree of non-specific adsorption is permissible? What concentration of target is best? and, how these parameters may influence the capture (or hybridisation) rate. They recommended that for rapid and efficient hybridisation, the solution-phase (target) DNA diffusing to the probe-covered surface should be small (ideally 100 bases or less). A large distance between surface probes in low-density probes could allow fast hybridisation and also decrease the probability of multiple partial matches by a large target (bridging) and the resulting incorrect hybrid formation. The model they used for the hybridisation of target to surface attached probe was, diffusion of the target from immobilised solution to surface to be non-selectively adsorbed on the surface followed by surface diffusion of the adsorbed targets to the probe. Therefore, the conditions that permit good efficiency with sparse coverage are those that allow surface diffusion of the target from a non-selective but adsorptive region to the sparsely dispersed probes. Therefore, they recommended that, conditions conducive to surface diffusion should be created and the probe should be uniformly distributed rather than being clustered in island regions. An optimal method for generating probe surfaces should therefore allows for controlling the space around each

ISBN:978-84-692-9758-2/DL:T-206-2010

probe individually to reduce probe-probe interaction while maximizing the density of probes[109].

Consequently rates of hybridisation have been found to decrease with increasing surface probe density [107, 111-113]. Erickson et al.[114] and others[31, 107, 115-118] have also investigated the influence of surface probe density on fully complementary and single-base pair mismatched 20-mer oligonucleotide strands. Peterson et al.[107] found that probe density is a controlling factor for the efficiency of target capture as well as for the kinetics of the target/probe hybridisation. They found that, in the lowest probe density cases (2 x 10^{12} probe DNA molecules/cm^2), 100% of probes could be hybridised, whereas at higher probe density (12 x 10^{12} probe DNA molecules/cm^2) the efficiencies drop to about 10% with a considerable decrease in the kinetics of the hybridisation process.

Methods for controlling probe oligonucleotide surface density

Surface nanostructuring is used to control surface density of the probes in order to create appropriate spacing for effective hybridisation. *Top-down* and *bottom-up* fabrication approaches have been reported for the preparation of substrates for controlling the surface density of probe oligonucleotides.

Top-down methods begin with a pattern generated on a larger scale and reducing its lateral dimensions forming micro or nanostructures. This strategy is usually applied to the fabrication of electronic devices such as microchips, whose functions depend more on their patterns than on their dimensions and include techniques such as photolithography and electron-beam lithography. *Bottom-up* methods start with atoms or molecules and build-up to nanostructures. The growing interest in nanoscience has created a demand for a broad range of fabrication methods, with an emphasis on low-cost, convenient techniques.

Bottom-up methods can provide the smallest nanostructures that are usually generated as simple particles in suspension or on surfaces, rather than as designed, interconnected patterns. *Bottom-up* fabrication methods often mimics biological systems[119] that are built by self assembly rather than imposing order *top-down* from an external source.

ISBN:978-84-692-9758-2/DL:T-206-2010

B*ottom–up* fabrication may in the future offer a number of potentially very attractive advantages such as producing nano- or micro- structures starting from atomic size scale, the possibility of three-dimensional assembly, and the potential for inexpensive mass fabrication [119]. However, *bottom–up* fabrication demands understanding of how ordered or complex structures with predetermined geometry can be formed starting from atomic and molecular building blocks.

1.5. Self assembled monolayers

Self-assembly is an attractive choice for the immobilisation of probe molecules at surfaces, as the method is simple and allows for a number of useful attachment chemistries to be realised[120-123].

A self assembled monolayer (SAM) is a well organized monolayer formed by attachment of head group of molecule (in case of alkanethiols -SH group) with the surface of a support[124]. Self-organisation is achieved when the alkyl chains align themselves by van der Waals forces and form a compact monolayer (Figure 1).

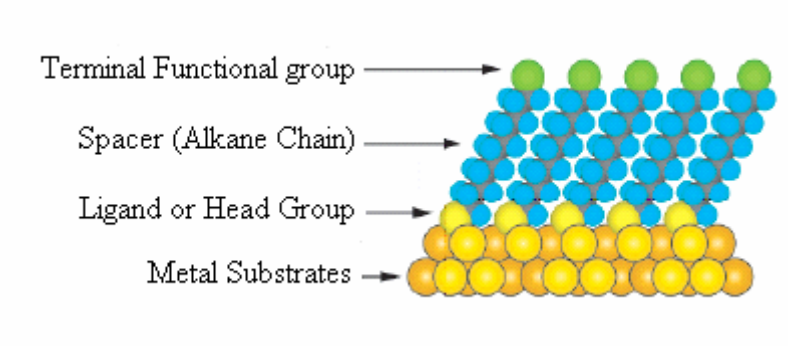

Figure 1. Schematic representation of self-assembled monolayer of alkanethiols on metal substrate (Figure taken from Love et al.[121])

SAMs spontaneously form upon exposure of the substrate to a solution containing the molecules. SAMs have become the focus of intensive investigation as they provide a facile means of defining the chemical composition and structure of a surface[122]. As a result, a number of reviews[121, 123, 125] and book chapters[120] have been devoted to the discussion of self-assembled monolayers formation, substrate preparation, surface

ISBN:978-84-692-9758-2/DL:T-206-2010

characterisation and wide area of applications (wetting, adhesion, biosensor, nanotechnology). This work aims to develop new substrates for applications in DNA biosensors based on attachment of DNA probe via formation of SAMs on metal substrates.

1.5.1. Self-assembled monolayers of alkanethiols on metals

Self-assembled monolayers of thiols, sulphides[126, 127], cyanides[128] and alkylphosphonates[129] are known to form on different substrates, but most of the work on self-assembled monolayers has focused on SAMs of alkanethiols. It is possible to find a wide range of *terminal functional groups* in the adsorbing thiolated molecule without disturbing the self-assembly process or destabilising the SAM. The high affinity of the sulphur head group for a metal substrate and the high strength of the interaction between the two is one of the reasons for the use of SAMs based on alkanethiols in biosensors.

Gold is the most widely used substrate for alkanethiols based SAMs. The first reports of SAMs formed on gold substrates were highly focused on the preparation of atomically flat, well-defined, gold surfaces. Using these surfaces some very important characteristics alkanethiols SAMs have been extracted. Gold is a noble metal that can be handled in air without the formation of an oxide surface layer, and can survive harsh chemical treatments such as those used to remove organic contaminants during cleaning. Gold electrodes may be composed of bulk gold, either polycrystalline or single crystal, or thin films deposited on various substrates. Other metals that are also used to form SAMs include palladium, platinum[130], copper[131], silver[132] and mercury[133].

Common substrates for SAMs of alkanethiols are thin films of metal, supported on silicon wafers, glass, mica, or plastic substrates prepared by physical vapour deposition methods (such as thermal or electron beam evaporation)[134, 135]. It is also possible to prepare substrates by electrochemical deposition[136-143], or electroless deposition[144-146].

ISBN:978-84-692-9758-2/DL:T-206-2010

1.5.2. Mixed SAM preparation methods

The competition between thermodynamic and kinetic control is one of the most fundamental issues in chemistry. The formation of a mixed SAM on a substrate remains controversial with thermodynamic and kinetic contributions not clearly defined. Alkanethiols adsorb rapidly and strongly onto gold surfaces, which would suggest that kinetic control might dominate. It is also known that the compositions of mixed SAMs formed by the adsorption of two or more thiols from the liquid phase tend to be enriched with the component favoured by thermodynamics[147]. In relation to mixed SAMs, the situation may be simply stated: kinetic factors favour the formation of a random mixture of adsorbates, while thermodynamics favours the formation of phase-separated domains of different adsorbates. Such questions may be of critical importance in fundamental investigations that use them as model surfaces. As Herne et al.[90] and others have reported, creating a mixed SAM of thiolated DNA probe and a diluter alkanethiol is important to control the surface coverage of thiolated probe density on a surface and to achieve the required spacing for hybridisation so that electrostatic repulsion can be minimised.

1.5.2.1. Immobilisation solution controlled methods

A) Co-immobilisation from mixed alkanethiol solutions

The most common procedures for the preparation of mixed SAMs are based on control of the composition of immobilisation solution. For example, for binary mixed SAMs, when both molecules are present in the immobilisation solution, the mole fraction of each molecule in the SAM is assumed to be controlled via the mole ratio of the two molecules in the solution. In addition to mole ratio, other parameters such as the solvent, time and temperature can also be exploited to attempt controlling the distribution of the thiols[148-150]. There is a controversy whether kinetic or thermodynamic factors control the surface composition of the mixed SAM layer. It is generally accepted that kinetic factors favour the formation of a random mixture of adsorbates, while thermodynamics favours the formation of phase-separated domains of different

ISBN:978-84-692-9758-2/DL:T-206-2010

adsorbates[151]. The less soluble thiol preferentially forms SAM. High concentrations of the thiol, long adsorption times and high temperatures encourage the SAM composition to approach equilibrium with the solution. Mixed SAM prepared by this method have phase separated domains with no particular order[149, 150, 152-155]. Even for thiols of comparable length, phase separation has been noticed[156]. An example of mixed SAMs prepared in this way which is composed of a long chain alkanethiol (for example 1-hexadecanethiol) and a short thiol for example (3-mercaptopropionic acid), form phase-separated domains[157, 158] of the short thiol with dimensions greater than 100 nm^2.

This mixed SAM preparation method was reported for DNA biosensor applications[159-162] using very low mole-fraction of thiolated probe to the diluter. Various conditions should be taken into account for probe immobilisation such as control of the ionic strength of the immobilising solution or variation of the interfacial electrostatic potential of the substrate and concentration of the thiolated probe[90]. The variation of thiolated DNA probe DNA to the diluter requires optimisation to improve hybridisation with the target. The composition of the mixed SAM monolayer may not reflect the composition of the immobilisation solution. The method is commonly employed due to its simplicity, however, it has low surface reproducibility as the process is thermodynamically controlled and random phases might be formed. Recently, to address this problem for genosensors, a detailed investigation on mole ratio of the thiolated probe to the diluter has been reported. Improvement in surface reproducibility has been claimed[163].

B) Asymmetric disulphide

Homogeneously mixed monolayers of alkanethiols can be formed by the self-assembly of an asymmetric disulphide[164-168], but the surface composition of mixed monolayers constructed by this method is principally limited to 1:1 and therefore may not give the required spacing for DNA biosensor applications. Lazerges et al.[169] made a comparative study on asymmetric disulphide DNA probe against a well spaced capture probe they have prepared using quartz crystal microbalance detection system. The sensitivity of the disulphide probe was -67±6 Hz whereas the well spaced probe was -83±Hz. The well spaced DNA probe achieved 100% hybridisation efficiency which was two time higher than the disulphide probe.

ISBN:978-84-692-9758-2/DL:T-206-2010

C) Sequential immobilisation (back-filling and displacement approaches)

In sequential immobilisation, a second thiol is incorporated into an existing SAM by prolonged immersion of the substrate in the second immobilisation solution, which has been coined as "backfilling". The distribution of the two molecules may vary from intimately mixed to completely phase-separated. When the mixed SAM contains molecules of greatly differing chain length, phase separation into microscopic domains is detectable[125].

There are several reports addressing the problem of high probe density by dilution of the capturing probe density on the surface to create the space required for attachment (hybridisation) of the complementary target[109, 170]. When following the so called back-filling approach[171, 172], a thiolated single stranded probe DNA is first immobilised on gold surface. After formation of a probe monolayer, a diluter thiol such as 6-mercaptohexanol is immobilised to orientate the chemisorbed probes for hybridisation.

Despite the fact that this backfilling approach is the most commonly used approach in electrochemical DNA sensor application using thiolated DNA probes[90], the problem of surface reproducibility remains[173]. Immobilisation solution controlled mixed SAMs preparations have low control over composition and distribution of the monolayer domains. An alternative approach is required to prepare controlled well-defined mixed SAMs to overcome the problems encountered in DNA sensor applications or other applications where molecular level surface structuring is needed.

1.5.2.2. Reductive desorption

In a strongly alkaline solution, SAM of alkanethiols desorbs at very negative potentials (Equation 1).

$$\mathbf{M}\,|\,S(CH_2)_mX + ne^- \Leftrightarrow \mathbf{M}\,| + {}^-S(CH_2)_mX \qquad (1)$$

The reductive desorption process of alkanethiols from the electrode surface can be monitored by cyclic voltammetry scans to high negative potentials in argon saturated

ISBN:978-84-692-9758-2/DL:T-206-2010

strongly aqueous alkaline solution such as 0.5 M NaOH. The sharp reductive peak(s) due to desorption can be observed and the peak potential gives important information regarding the coverage and stability of the SAM whilst the reductive desorption peak area estimated after subtraction of the background current, indicates the surface coverage of the SAM; the reductive desorption peak potential gives information on stability of the SAM. The intermolecular stabilisation of longer alkanethiol SAMs by Van der Waals force is reflected in a desorption peak at more negative potentials. The reductive desorption peak of SAMs of shorter alkanethiols like 3-mercaptopropionic acid formed on gold electrode (-0.8 V) is more positive than that of longer alkanethiols like 1-hexadecanethiol (-1.1 V) as measured using Ag/AgCl reference electrode[174].

The reductive desorption approach has been used for decreasing surface DNA probe density. Partial electrochemical reductive desorption of immobilised thiolated probe has been reported as a methodology to control the packing density of the DNA monolayers[108]. Combinations of variations in the number of electrochemical desorption cycles and changes in immobilisation time were used to control the density of the immobilised DNA probes.

In another approach, a mixed SAM of 3-mercaptopropionic acid and 6-mercaptohexanol was formed using the co-immobilisation method. The 3-mercaptopropionic acid domains were selectively desorbed and thiolated single stranded DNA adsorbed on the exposed gold surface, resulting a mixed SAM of thiolated probe and 6-mercaptohexanol (Scheme 2). The mixed SAM formed using the method resulted in a quartz crystal microbalance signal amplification of one order of magnitude over SAMs containing only the thiolated single stranded DNA, signifying a much improved hybridisation efficiency[175].

ISBN:978-84-692-9758-2/DL:T-206-2010

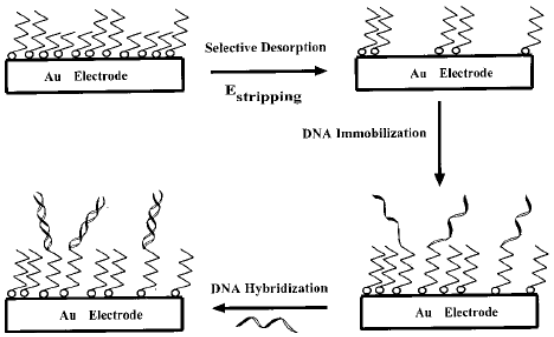

Scheme 2. Representation of selective desorption of a short alkanethiol in a mixed SAM for the subsequent attachment of thiolated DNA probe and hybridisation with its target (Figure taken from Satjapipat et al.[175])

1.5.2.3 Denaturing surface immobilised duplex

For oligonucleotides, it could be possible to optimise the spacing between probe molecules by forming SAM of probe-target pairs and later denaturing the immobilised pairs. For example, a probe can be bound to the surface pre-hybridised with the target oligonucleotides that can then be removed by thermally denaturing the hybridised probe-target, leaving a well-spaced probe array. This strategy was used to optimise sensor response, and resulted in marked improvement in both the amount of target captured and the kinetics of target capture[107].

1.5.2.4. Substrate controlled mixed SAM preparation methods

The preparation of mixed SAMs based on the control of the substrate rather than the composition of immobilisation solution has recently been reported[176]. The property of the substrate is rationally designed and specifically structured prior to exposure to pure immobilising solution. To date substrate controlled preparation of mixed SAM has been demonstrated using two approaches.

A) Underpotential deposition of metal on gold

A short alkanethiol solution is immobilised to form a SAM on gold that is partially covered with lead. The method used to get sub monolayer of lead atoms on gold electrode is called under potential deposition (UPD). The electrochemically deposited

ISBN:978-84-692-9758-2/DL:T-206-2010

lead is anodically stripped from the electrode surface and the electrode is immersed into the second alkanethiol to form mixed SAM[176, 177] (Scheme 3).

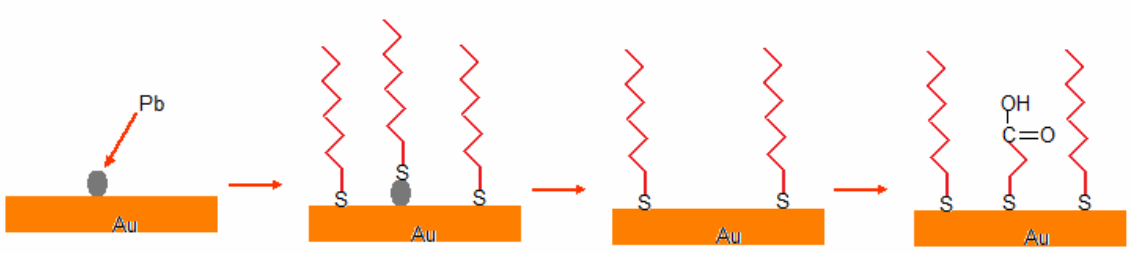

Scheme 3. Substrate controlled mixed alkanethiol SAM preparation using underpotential deposition of lead on gold. (Figure adapted from Shimazu et al.[176])

The domain size and distribution was controlled by the area of exposed gold surfaces after the lead desorption. This method did not consider reorganisation of the already formed SAM to occupy the exposed gold surface after removal of UPD lead. To date, there is no demonstration of the application of the technique for an optimal spatial orientation for DNA sensor applications.

B) Selective reductive desorption from poly crystalline gold

Reductive desorption (Equation 1) of SAMs of some thiols and disulphides from polycrystalline gold (poly-Au) electrodes may show more than one desorption peak[178-181] and these peaks are due to separated desorption waves related to the desorption from (111), (100) and (110) crystal planes of a polycrystalline gold[142, 182].

This concept has been exploited for the selective desorption of alkanethiols from one of the three low index faces of polycrystalline gold and the subsequent formation of SAMs of longer chain alkanethiols on the exposed space to obtain mixed SAMs on polycrystalline gold and using the gold surface catalysed reduction of oxygen the percentage coverage of these low index sub-domains on polycrystalline gold has been estimated[142]. Recently, the attachment of thiolated DNA probe after selective reductive desorption of 3-mercaptopropionic acid from polycrystalline gold has been reported[183].

ISBN:978-84-692-9758-2/DL:T-206-2010

1.5.3. Electrochemical characterisation methods of SAM

1.5.3.1. Blocking the access of redox probe to electrode surface

An electrochemical reaction at an electrode is a heterogeneous reaction process that occurs at the electrode-electrolyte interface. The rate of electrochemical reactions depend either on mass transfer of the ions from bulk of the solution to the electrode surface (diffusion limited) or on the rate of the heterogeneous electron transfer (kinetically limited). When a SAM of alkanethiols forms, the alkyl chains align themselves and create a densely packed structure of hydrocarbon chains. This structure hinders the approach of ions and molecules from solution to the electrode surface and as a result the electrochemical process at the electrode will be reduced[121, 122, 125]. This blocking behaviour is used to estimate the compactness of a SAM and to evaluate defects on the surface. Longer alkanethiol chains have better blocking capacity than shorter thiol SAM as they form more compact and thicker blocking monolayers. The blocking capacity of a monolayer can be estimated by comparing the peak current after SAM formation (i_{SAM}) to that of the signal before SAM formation (i_{bare}). For example, Equation 2 can be used to estimate percent blocking capacity of a SAM ($\%i_{dec}$) towards a redox probe.

$$\%i_{dec} = \left(\frac{(i_{bare} - i_{SAM})}{i_{bare}} \right) * 100\% \qquad (2)$$

1.5.3.2 Redox probes attached SAMs

Redox probes can be linked to the terminal functional group of an alkanethiol and upon self-assembling a redox active monolayer can be created. The redox centres serve as a sensitive and non-destructive probe to study the structure of SAMs. The length of the alkyl chain determines the spacing between the electrode and the redox centre. The coverage of the redox centre on the electrode surface is obtained from the cyclic voltammetry of the linked redox probe. Cyclic voltammetery allow for studying oxidation and reduction processes at an electrode in electrochemical cell by applying a triangular potential-time sweep with a given sweep rate to the electrode. A plot of the current–potential response is called a cyclic voltammogram. The anodic (oxidation) or

ISBN:978-84-692-9758-2/DL:T-206-2010

cathodic (reduction) peak area after subtracting the charging current baseline gives the charge for oxidation or reduction of the redox probe. The surface coverage (Γ) of the attached redox probe can be obtained from:

$$\Gamma = \frac{Q}{nFA} \qquad (3)$$

where Q is the amount of charge or peak area in coulombs, n is the number of electrons transferred in the redox half reaction, F is Faraday's constant, and A is the electrode area. The peak area is independent of the scan rate.

1.6. Nanoelectrochemistry for surface nanostructuring

Nanoelectrochemistry combines characteristics of electrochemistry (e.g., simplicity, speed, high selectivity and high sensitivity) with the unique properties of nanoparticles (e.g., electronic, optical, magnetic and catalytic).

Two main approaches have been reported for surface nanostructuring using electrochemistry[184, 185], namely:

a) Random electrochemical deposition of metal nanoparticles – is the generation of nanometric patterns with a more or less narrow size distribution without control on the spatial location of the nanostructures. Glassy carbon electrodes offer a practical advantage for creating these kind of structures as a result of the availability of random surface defect that can serve as nucleation centres during the electrochemical reduction of metal ions[186].

b) Defined electrochemical nanostructuring with metallic nanoparticles – this approach requires tools in order to minimiselocalise the electrochemical deposition process at the substrate/electrolyte interface. Scanning probe microscopy (SPM) techniques have been used for this purpose. Scanning tunnelling microscopy (STM) tips or metallised atomic force microscopy (AFM) cantilevers have also been used as miniaturised electrodes to deposit metal nanoclusters[187, 188] or to create nano-defects on a substrate[189].

ISBN:978-84-692-9758-2/DL:T-206-2010

The SPM probe is coated with metal, and the metal atoms are transferred in a controlled manner from the tip to a substrate made possible by a mechanical approaching of the SPM tip closely to the surface of a substrate and electrochemical dissolution of a pre-deposited metal on the tip and accumulation of the atoms on the surface as a result of the tunnelling current between the tip and substrate[188].

In this work, surface nanostructuring using nanoelectrochemistry based on random electrochemical deposition of metal nanoparticles for enhancing the hybridisation process is studied.

1.7. Electrochemical deposition of metals – brief introduction

Electrochemical metal deposition is one of the oldest subjects within the framework of electrochemistry where electroplating has been used for the production of different decorative and functional coatings. Metal electrodeposition takes place at electrode-electrolyte interfaces under the influence of an electric field to transform metal ion or the complex ion of a metal from the electrolyte to metal on the electrode surface[190].

1.7.1 Electrochemical nucleation

Electrochemical deposition of metal on an electrode surface involves at least three steps; (i) transfer of hydrated metal ions or complexes from bulk of solution to the electrode-electrolyte inter-phase, (ii) adsorption of these metal ions/complex on the surface, and finally (iii) charge transfer at the surface resulting form the reduced form[191].

The electrochemical deposition of metal starts with electrochemical transfer of ions to the atomic scale surface (defect) structure of the electrode. A metal ion M^{n+} that is transformed from solution into the ionic metal lattice is represented as:

UNIVERSITAT ROVIRA I VIRGILI
ELECTROCHEMICALLY DEPOSITED METAL NANOSTRUCTURES FOR APPLICATIONS IN GENOSENSORS
Tesfaye Refera Soreta
ISBN:978-84-692-9758-2/DL:T-206-2010

$$M^{n+}_{(hydrated)\,(solution)} \rightarrow M^{n+}_{(hydrated)\,(surface)} \quad (4)$$

Deposition/dissolution process are strongly minimiselocalised at a small number of ‘‘active sites’’, which are also known as “kink sites” (Figure 2) on the metal surface[192].

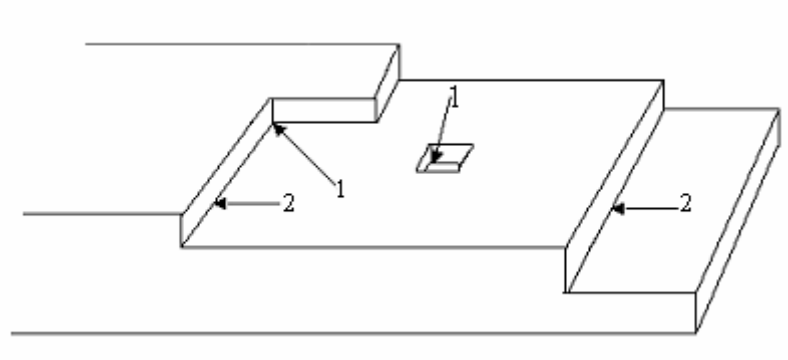

Figure 2. Nucleation sites for electrochemical metal deposition (1) kinks and (2) steps

Fundamental aspects of electrocrystallisation of metals are directly related to the nucleation and crystal growth. The nucleation step is required for the initiation of a new crystal (three-dimensional nucleation) and on which the crystal growth by the formation of new layers[190]. Plieth et al.[193] described the growth of a metallic layer as a process where discharge of hydrated metal ions and incorporation of the atom to the kink sites[190] takes place simultaneously or discharge of the metal ions takes place at steps and then the atoms diffuse to kink sites. At a kink site the atom is bound to the crystal by exactly half the bonds as in a crystal lattice. An atom at a kink site has two possibilities. It can leave the kink site by separation from the crystal lattice, or another atom can be added and then it is fixed to its final place in the crystal lattice[193].

$$M^{n+}_{(hydrated)\,(surface)} + ne^{-} \Leftrightarrow M_{(surface)} \quad (5)$$

The competition between growth and nucleation determines the surface morphology and properties of the electrodeposited surface.

ISBN:978-84-692-9758-2/DL:T-206-2010

In this work, electrochemical deposition of metals on glassy carbon substrate is studied. A glassy carbon electrode is electrochemically inert in wide potential window and has an amorphous structure with a random distribution of active sites for nucleation[186]. Electrochemical deposition of metals was performed by galvanostatic and potentiostatic techniques[49].

1.7.2. Galvanostatic and potentiostatic techniques

In the galvanostatic technique the current between the working electrode and auxiliary (counter) electrode is held constant (galvanostatic) with a current source, and the potential between the working electrode and the reference electrode is determined as a function of time with the potential being the measured variable (Figure 3).

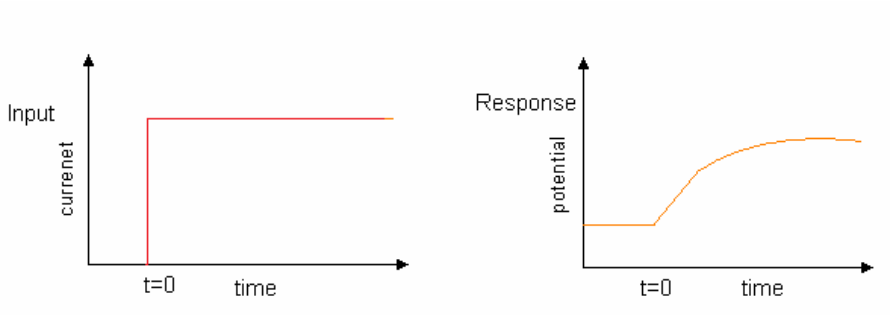

Figure 3. Variation of potential with time in galvanostatic methods

When a constant current is applied to the system, the current is used for two processes at the electrode surface, charging the double layer capacitance up to the potential at which the electrode reaction can proceed with a measurable extent and to carry out electrode reaction (charge transfer). Thus the total galvanostatic current density i_g is given by

$$i_g = i_{dl} + i_{ct} \qquad (6)$$

Where, i_{dl} is the capacitive and i_{ct} is the faradic current. Therefore, the charge consumed for reduction of the metal (which is also related to the amount of metal deposited) is obtained by subtracting the capacitive double layer charge from the total charge consumed. The charge can be calculated with a simple relation:

$$Q = i_{ct}t \qquad (7)$$

ISBN:978-84-692-9758-2/DL:T-206-2010

One of the disadvantages of galvanostatic techniques is that double-layer charging effects are larger and occur throughout the experiment [49]. This could make determination of the contribution of double layer charging more difficult.

In potentiostatic techniques a constant potential at working electrode is applied and the variation of current with time is monitored (Figure 4). In this case, the charge for the metal ion reduction is calculated by integrating the area under the current versus time curve within the limits of the initial to final deposition time.

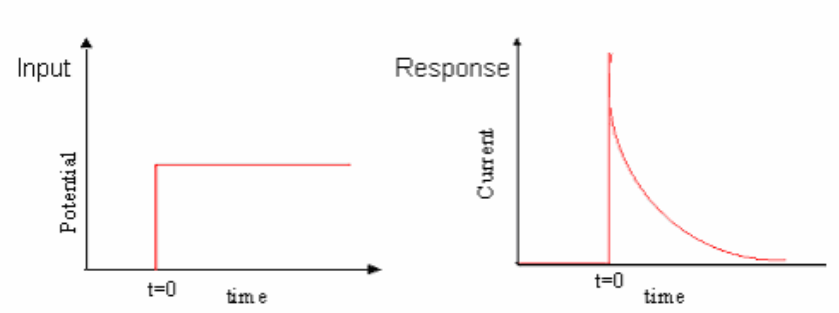

Figure 4. Variation of current with time in potentiostatic method

Programmed multiple potential steps can be applied to control particle nucleation and growth during electrochemical deposition process. It has been demonstrated that electrochemical deposition of silver nanoparticles on carbon electrodes by applying an over-potential of -500 mV to the metal formal reduction potential for short time ($5x10^{-3}$ to $5x10^{-2}$ seconds) to initiate nucleation followed by a final growth over-potential potential (-50 to -100 mV) can be used to deposit dimensionally uniform silver nanoparticles[194].

ISBN:978-84-692-9758-2/DL:T-206-2010

1.8. Objective of the work

In this work, we propose a nanostructured surface preparation approaches to overcome the problems encountered following mixed SAM preparation from solution that are used for electrochemical DNA sensor applications. There are reports on nanostructured electrode surface preparation approaches using gold. The most common approaches are: (i) gold electrode surface roughening using electrochemical deposition of gold on gold electrode[195]; (ii) attachment of gold colloids to SAM covered gold electrode such as cysteamine[196]; (iii) incorporation of colloidal gold into carbon paste electrode [197]; and (iv) electrochemical deposition of gold nanoparticles on glassy carbon electrodes [89, 137, 142, 198]. The nanostructured surfaces with gold nanoparticles showed enhancement of DNA biosensor signal [82, 195, 199, 200] mainly as a result of the increased surface area of the substrate. However, strategies to address probe DNA density and orientation were not given the required emphasis.

We propose nanostructuring of the substrate with the aim of enhancing surface coverage of DNA probes as a result of the unique surface properties of the nanomaterials as well as purposely spacing the capture DNA probes for effective hybridisation with target and moreover exploiting the unique catalytic properties of nanostructured surfaces for signal enhancement. To realise this, nanostructured surface with isolated nanodomains was pursued. The following two approaches were undertaken:

1. Selective reductive desorption from mixed metal substrate

Mixed metallic substrates were prepared by electrochemical deposition from mixed metal solutions, metal on metal deposition or co-evaporation of metals. The metals in the final mixed metal substrate should demonstrate a difference in the strength of SAM formation and stability. The substrate will be incubated in an alkanethiol solution and SAM will be formed on all the metals of the substrate. By selective desorption of the SAM from one of the metals and adsorbing of the DNA probe, it should be possible to obtain a mixed SAM of DNA probe and alkanethiol, which can be carefully controlled by the ratio of the metals in the mixed metal monolayer (Scheme 4).

UNIVERSITAT ROVIRA I VIRGILI
ELECTROCHEMICALLY DEPOSITED METAL NANOSTRUCTURES FOR APPLICATIONS IN GENOSENSORS
Tesfaye Refera Soreta
ISBN:978-84-692-9758-2/DL:T-206-2010

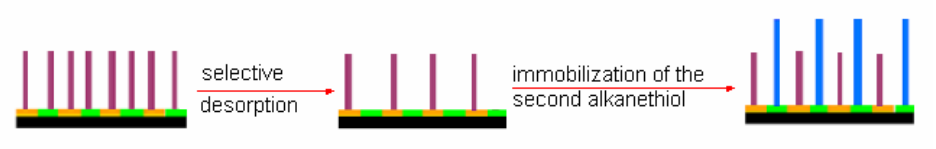

Scheme 4. Mixed SAM preparation from mixed metal substrate

2. Sequential nanoparticles deposition

Taking the advantage of a conducting carbon support known for not supporting alkanethiols SAM, metal nanoparticles were electrochemically deposited via the sequential deposition technique depicted in Scheme 5. In each deposition protection stage, the substrate is exposed to pure immobilising solution of an alkanethiol. The size and the distribution of the domains in the SAM are assumed to follow the nanoparticle size and distribution during the nanostructuring stage. To address problems with low signal of DNA hybridisation sensors due to very high dilution of probe molecules in mixed SAM preparations, a metal nanoparticles structured surface will be used to improve total surface coverage of probe molecules, whilst allowing the required spacing for effective hybridisation with target DNA and exploiting the unique catalytic properties of the electrodeposited nanoparticles.

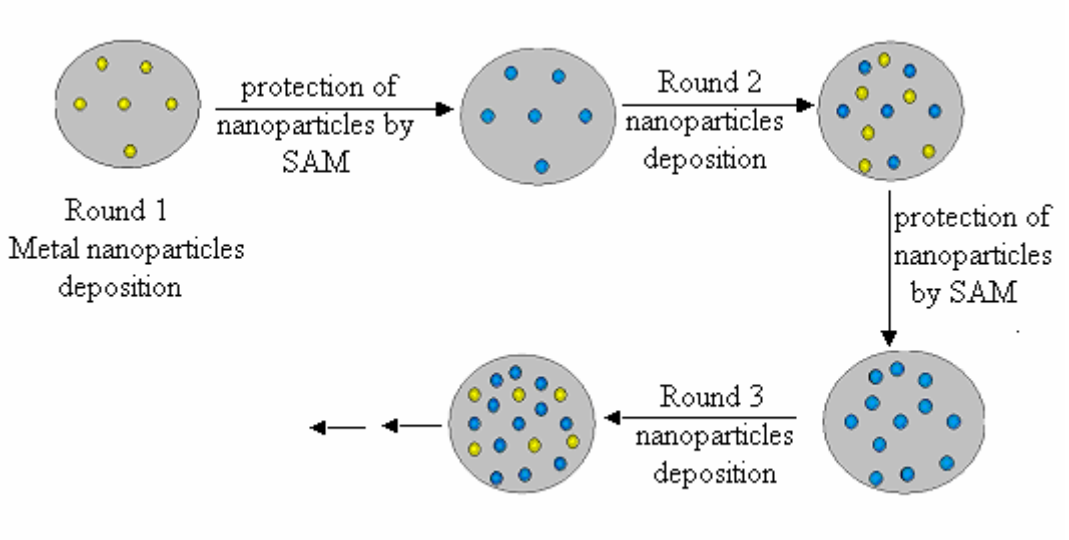

Scheme 5. Sequential electrochemical deposition of metal nanoparticles. Yellow spots represent freshly deposited metal nanoparticles; blue spots SAM protected metal nanoparticles.

ISBN:978-84-692-9758-2/DL:T-206-2010

Overall objective:

The overall objective of this work was the development of nanostructured surfaces for the formation of self assembled monolayers and to enhance readout signals of electrochemical DNA biosensors.

Sub-objectives:

- To elucidate optimum parameters for electrochemical deposition of metals for support of self assembled monolayer formation.
- To demonstrate selective reductive desorption of SAM from nanostructured mixed-metal surface.
- To elucidate a protocol for electrochemical deposition for metals nanoparticles and nano-structuring of a surface.
- To demonstrate signal enhancement and improvement of sensitivity of DNA biosensors based on the nanostructured surfaces developed in this work.

ISBN:978-84-692-9758-2/DL:T-206-2010

1.9. Highlights on the articles included in this thesis

Article 1

Title: Electrochemically Deposited Palladium as a Substrate for Self-Assembled Monolayers

Journal: *Langmuir,* **2007**, 23, 10823 - 10830

In line with the first objective of this PhD thesis, we explored metals other than the classically used gold (like palladium, platinum, rhodium and ruthenium) for developing procedures for electrochemical deposition of these metals on glassy carbon electrode to provide functional surface for the formation alkanethiol based SAMs. The article is the result of this effort that describes the optimization of electrochemical deposition of palladium from different baths (metal ion source, pH and supporting electrolyte), electrochemical deposition conditions (cyclic voltammetry, galvanostatic and potentiostatic conditions). The deposited palladium thin films were characterised by microscopic methods such as scanning electron microscopy (surface morphology) and electrochemical methods (metal loading, thickness of the deposited palladium layer). Two sets of electrodes on which palladium thin film electrodeposited were prepared for SAM formation. The first set consisted of electrodes with a mirror-like palladium surface, produced under lower galvanostatic and potentiostatic conditions. The palladium surface of the second set of electrodes had a black and non-reflecting appearance, again produced by constant potential and galvanostatic conditions. Only very minor blocking of methylviologen as a redox probe was observed for the SAMs on shiny palladium surfaces generated both potentiostatically and galvanostaically. In contrast, monolayers assembled on the black palladium surfaces form a substantial barrier against the redox reaction of methylviologen redox probe indicating a more complete palladium thin film and formation of stable alkanethiol based SAM.

Article 2

Title: Electrochemical Surface Nanopatterning by Selective Reductive Desorption from Mixed Metal Surfaces

Journal: Electrochimica Acta (in press, accepted 28 February 2009)

ISBN:978-84-692-9758-2/DL:T-206-2010

In line with sub-objective 2, a selective reduction desorption of alkanethiol from a mixed metal substrate as depicted in Scheme 4 was demonstrated. Mixed metal electrodes were prepared by electrodeposition of palladium onto gold electrodes for short deposition times. The presence of both palladium and gold atoms on the electrode surface was confirmed by electrochemical method. We demonstrated selective reductive desorption of SAM of 2-mercaptoethanol from the palladium domains of the mixed palladium-gold surface.

Article 3 and 4
Title: Electrochemical Fabrication of Nanostructured Surfaces for Enhanced Response
Journal: *ChemPhysChem,* **2008**, 9, 920 - 927

Title: Electrochemical Surface Structuring with Palladium Nanoparticles for Signal Enhancement
Journal: Submitted to *Langmuir*

In line with sub-objective 3, studies were conducted for electrochemical surface nanostructuring of carbon surface with metal particles. It is known that in a metal deposition bath at higher applied over potential and for short deposition time, metal nanoparticles can be nucleated on glassy carbon surface[201]. In this article, we have reported on a method to increase the number density of metal nanoparticles by preventing their aggregation on the glassy carbon surface through sequential deposition of metal nanoparticles. The procedure involves a number of electrochemical deposition and protection steps. The sequential deposition/protection procedure includes electrochemical deposition of the metal nanoparticles on the GC surface followed by protection of the particles by self-assembling of a thiol monolayer to prevent them from being used as seeds in the subsequent deposition step. In the next deposition step, new particles are mainly formed on the GC surface due to the insulating action of the alkanethiols SAM on the particles deposited in the previous step. Optimal conditions regarding particle size, distribution and number density were studied by varying deposition parameters like deposition potential, deposition time and concentration of the deposition bath. An electroactive labelled thiol that selectively chemisorbed onto the

ISBN:978-84-692-9758-2/DL:T-206-2010

metal nanoparticles was used to distinguish the glassy carbon electroactive surfaces from the metal nanoparticle deposits surface. A ferrocene signal enhancement of six fold was observed on sequentially deposited gold nanoparticles as compared to bulk gold. Sequential deposition of palladium using ferrocenyl alkanethiol protective SAM has showed much higher ferrocenyl signal enhancement than gold nanoparticles, demonstrating a factor of 50-fold enhancement as compared to a planar palladium surface. Furthermore, sequential deposition of palladium using ferrocenyl alkanethiol protective SAM showed markedly higher ferrocenyl signal enhancement (57.5 μC after fifth round) than gold nanoparticles (7.2 μC after fifth round). When the palladium nanostructured surface is compared with the planar gold electrodes (1.2 μC) routinely used in electrochemical genosensors, overall enhancement factor close to 48 fold was achieved. The signal enhancement can be associated with the unique properties of nanoparticles that facilitate more effective self-assembling processes of thiol based monolayers more effective on the nanoparticles than on bulk metal. We have shown that signal enhancement is not due to surface area effects, as well as the unique catalytic properties of the electrodeposited nanoparticles.

Article 5

Title: Electrochemical Surface Nanostructuring for Enhancement of Signal of DNA Biosensors

Article submitted as short communication to Biosensors & Bioelectronics

As described in the introduction part of the thesis, surface nanostructuring could enhance hybridisation efficiency of DNA biosensors and improves the sensitivity of the biosensors. In line with sub objective 4, nanostructured surface using the sequential deposition method developed was prepared. The electrochemical signal of the DNA biosensor for the different stages of nanostructuring and bulk gold electrodes was compared. Signal enhancement was observed with the first three stages of sequential deposition of gold nanoparticles, whereas the signal for the bulk gold was found to be smaller than any of the three stages of sequential deposition studied. A model, genosensors for the detection of the lymphotoxin-alpha gene was constructed by sandwich assay using horseradish peroxidase linked marker probe. The nanostructured

ISBN:978-84-692-9758-2/DL:T-206-2010

electrode prepared following three rounds of deposition exhibited sensitivity of 44.89 (nA/nM) and linear range 0.53 nM to 25 nM, where as for the plain gold sensitivity was 13.67 nA/nM and a linear range of 5.22 nM to 25 nM was obtained. In another approach, for detection of 18 bases long ferrocene labelled target, the nanostructured electrode prepare with three rounds of gold nanoparticles sequential deposition resulted in 3.5 fold signal enhancement than the plain gold electrode.

Overall, this work has contributed significantly to improvement of transducer surface which is a key element in the construction of a genosensors. At the first stage of the work, preparation and characterisation of nanostructured surfaces was studied. The high surface reactivity of the electronucleated metal nanoparticles to form alkanethiol SAMs was confirmed. Strategies to increase the particles number density were developed. Based on these findings, genosensors were constructed with improved sensitivity than routinely used gold electrodes. The reason for the observed signal enhancement was explained by the high surface reactivity of the metallic nanoparticles to strongly bind with thiolated probe DNA, and availability of suitable environment for effective hybridisation with DNA target as a result of surface nanostructuring.

ISBN:978-84-692-9758-2/DL:T-206-2010

1.10. References

1. Thevenot, D. R.; Toth, K.; Durst, R. A.; Wilson, G. S., Electrochemical biosensors: Recommended definitions and classification. *Analytical Letters* **2001,** 34, (5), 635-659.
2. D'Souza, S. F., Microbial biosensors. *Biosensors and Bioelectronics* **2001,** 16, (6), 337-353.
3. Chouteau, C.; Dzyadevych, S.; Durrieu, C.; Chovelon, J.-M., A bi-enzymatic whole cell conductometric biosensor for heavy metal ions and pesticides detection in water samples. *Biosensors and Bioelectronics* **2005,** 21, (2), 273-281.
4. Katrlík, J.; Svorc, J.; Rosenberg, M.; Miertus, S., Whole cell amperometric biosensor based on Aspergillus niger for determination of glucose with enhanced upper linearity limit. *Analytica Chimica Acta* **1996,** 331, (3), 225-232.
5. Wang, J., Survey and summary: From DNA biosensors to gene chips. *Nucl. Acids Res.* **2000,** 28, (16), 3011-3016.
6. Heller, M. J., DNA microarray technology: Devices, systems, and applications. *Annual Review of Biomedical Engineering* **2002,** 4, 129-153.
7. Wang, J., Electrochemical nucleic acid biosensors. *Analytica Chimica Acta* **2002,** 469, (1), 63-71.
8. Gooding, J. J., Electrochemical DNA Hybridisation Biosensors. *Electroanalysis* **2002,** 14, (17), 1149-1156.
9. PaleÄ□ek, E.; Jelen, F. e., Electrochemistry of Nucleic Acids and Development of DNA Sensors. *Critical Reviews in Analytical Chemistry* **2002,** 32, (3), 261 - 270.
10. Drummond, T. G.; Hill, M. G.; Barton, J. K., Electrochemical DNA sensors. *Nature Biotechnology* **2003,** 21, (10), 1192-1199.
11. Park, S. J.; Taton, T. A.; Mirkin, C. A., Array-based electrical detection of DNA with nanoparticle probes. *Science* **2002,** 295, (5559), 1503-1506.
12. Palecek, E.; Fojta, M.; Tomschik, M.; Wang, J., Electrochemical biosensors for DNA hybridisation and DNA damage. *Biosensors and Bioelectronics* **1998,** 13, (6), 621-628.
13. Marrazza, G.; Chianella, I.; Mascini, M., Disposable DNA electrochemical sensor for hybridisation detection. *Biosensors and Bioelectronics* **1999,** 14, (1), 43-51.

ISBN:978-84-692-9758-2/DL:T-206-2010

14. Boon, E. M.; Ceres, D. M.; Drummond, T. G.; Hill, M. G.; Barton, J. K., Mutation detection by electrocatalysis at DNA-modified electrodes. *Nature Biotechnology* **2000,** 18, (10), 1096-1100.
15. Gao, Z.; Tansil, N., A DNA biosensor based on the electrocatalytic oxidation of amine by a threading intercalator. *Analytica Chimica Acta* **2009,** 636, (1), 77-82.
16. Fan, C. H.; Plaxco, K. W.; Heeger, A. J., Electrochemical interrogation of conformational changes as a reagentless method for the sequence-specific detection of DNA. *Proceedings of the National Academy of Sciences of the United States of America* **2003,** 100, (16), 9134-9137.
17. Fu, X. H., Electrochemical measurement of DNA hybridisation using nanosilver as label and horseradish peroxidase as enhancer. *Bioprocess and Biosystems Engineering* **2008,** 31, (2), 69-73.
18. Chang, Z.; Pan, H.; Zhao, K.; Chen, M.; He, P. G.; Fang, Y. Z., Electrochemical DNA biosensors based on palladium nanoparticles combined with carbon nanotubes. *Electroanalysis* **2008,** 20, (2), 131-136.
19. Radi, A. E.; Sanchez, J. L. A.; Baldrich, E.; O'Sullivan, C. K., Reagentless, reusable, ultrasensitive electrochemical molecular beacon aptasensor. *Journal of the American Chemical Society* **2006,** 128, (1), 117-124.
20. Roth, K. M.; Peyvan, K.; Schwarzkopf, K. R.; Ghindilis, A., Electrochemical detection of short DNA oligomer hybridisation using the CombiMatrix ElectraSense Microarray reader. *Electroanalysis* **2006,** 18, (19-20), 1982-1988.
21. Zhu, N. N.; Chang, Z.; He, P. G.; Fang, Y. Z., Electrochemical DNA biosensors based on platinum nanoparticles combined carbon nanotubes. *Analytica Chimica Acta* **2005,** 545, (1), 21-26.
22. Kerman, K.; Kobayashi, M.; Tamiya, E., Recent trends in electrochemical DNA biosensor technology. *Measurement Science & Technology* **2004,** 15, (2), R1-R11.
23. Xu, Y.; Jiang, Y.; Cai, H.; He, P. G.; Fang, Y. Z., Electrochemical impedance detection of DNA hybridisation based on the formation of M-DNA on polypyrrole/carbon nanotube modified electrode. *Analytica Chimica Acta* **2004,** 516, (1-2), 19-27.
24. Wang, J., Nanoparticle-based electrochemical DNA detection. *Analytica Chimica Acta* **2003,** 500, (1-2), 247-257.

ISBN:978-84-692-9758-2/DL:T-206-2010

25. Cai, H.; Xu, Y.; Zhu, N. N.; He, P. G.; Fang, Y. Z., An electrochemical DNA hybridisation detection assay based on a silver nanoparticle label. *Analyst* **2002,** 127, (6), 803-808.
26. Wang, J.; Kawde, A. B., Amplified label-free electrical detection of DNA hybridisation. *Analyst* **2002,** 127, (3), 383-386.
27. Zhu, N.; Chang, Z.; He, P.; Fang, Y., Electrochemical DNA biosensors based on platinum nanoparticles combined carbon nanotubes. *Analytica Chimica Acta* **2005,** 545, (1), 21-26.
28. Piunno, P. A. E.; Krull, U. J.; Hudson, R. H. E.; Damha, M. J.; Cohen, H., Fiber optic biosensor for fluorimetric detection of DNA hybridisation. *Analytica Chimica Acta* **1994,** 288, (3), 205-214.
29. Piunno, P. A. E.; Krull, U. J.; Hudson, R. H. E.; Damha, M. J.; Cohen, H., Fiber-Optic DNA Sensor for Fluorometric Nucleic Acid Determination. *Analytical Chemistry* **2002,** 67, (15), 2635-2643.
30. Xu, X.-H.; Bard, A. J., Immobilization and Hybridisation of DNA on an Aluminum(III) Alkanebisphosphonate Thin Film with Electrogenerated Chemiluminescent Detection. *Journal of the American Chemical Society* **2002,** 117, (9), 2627-2631.
31. Peterson, A. W.; Wolf, L. K.; Georgiadis, R. M., Hybridisation of Mismatched or Partially Matched DNA at Surfaces. *Journal of the American Chemical Society* **2002,** 124, (49), 14601-14607.
32. Cao, Y. W. C.; Jin, R. C.; Mirkin, C. A., Nanoparticles with Raman spectroscopic fingerprints for DNA and RNA detection. *Science* **2002,** 297, (5586), 1536-1540.
33. Gaylord, B. S.; Heeger, A. J.; Bazan, G. C., DNA detection using water-soluble conjugated polymers and peptide nucleic acid probes. *Proceedings of the National Academy of Sciences of the United States of America* **2002,** 99, (17), 10954-10957.
34. Okahata, Y.; Kawase, M.; Niikura, K.; Ohtake, F.; Furusawa, H.; Ebara, Y., Kinetic measurements of DNA hybridisation an an oligonucleotide-immobilised 27-MHz quartz crystal microbalance. *Analytical Chemistry* **1998,** 70, (7), 1288-1296.

ISBN:978-84-692-9758-2/DL:T-206-2010

35. Hook, F.; Ray, A.; Norden, B.; Kasemo, B., Characterisation of PNA and DNA immobilization and subsequent hybridisation with DNA using acoustic-shear-wave attenuation measurements. *Langmuir* **2001,** 17, (26), 8305-8312.
36. Zhang, H.; Tan, H. W.; Wang, R. H.; Wei, W. Z.; Yao, S. Z., Immobilization of DNA on silver surface of bulk acoustic wave sensor and its application to the study of UV-C damage. *Analytica Chimica Acta* **1998,** 374, (1), 31-38.
37. Berney, H.; West, J.; Haefele, E.; Alderman, J.; Lane, W.; Collins, J. K., A DNA diagnostic biosensor: development, characterisation and performance. *Sensors and Actuators B-Chemical* **2000,** 68, (1-3), 100-108.
38. Horakova-Brazdilova, P.; Fojtova, M.; Vytras, K.; Fojta, M., Enzyme-linked electrochemical detection of PCR-amplified nucleotide sequences using disposable screen-printed sensors. Applications in gene expression monitoring. *Sensors* **2008,** 8, (1), 193-210.
39. Patolsky, F.; Lichtenstein, A.; Willner, I., Highly sensitive amplified electronic detection of DNA by biocatalyzed precipitation of an insoluble product onto electrodes. *Chemistry-a European Journal* **2003,** 9, (5), 1137-1145.
40. Alfonta, L.; Bardea, A.; Khersonsky, O.; Katz, E.; Willner, I., Chronopotentiometry and Faradaic impedance spectroscopy as signal transduction methods for the biocatalytic precipitation of an insoluble product on electrode supports: routes for enzyme sensors, immunosensors and DNA sensors. *Biosensors & Bioelectronics* **2001,** 16, (9-12), 675-687.
41. Oliveira Brett, A. M.; Diculescu, V. C.; Chiorcea-Paquim, A. M.; Serrano, S. H. P.; Merkoçi, S. A. a. A., Chapter 20 DNA-electrochemical biosensors for investigating DNA damage. In *Comprehensive Analytical Chemistry*, Elsevier: 2007; Vol. Volume 49, pp 413-437.
42. Bagni, G.; Osella, D.; Sturchio, E.; Mascini, M., Deoxyribonucleic acid (DNA) biosensors for environmental risk assessment and drug studies. *Analytica Chimica Acta* **2006,** 573, 81-89.
43. Kim, J.; Johnson, M.; Hill, P.; Gale, B. K., Microfluidic sample preparation: cell lysis and nucleic acid purification. *Integrative Biology* **2009,** 1, (10), 574-586.
44. Willner, I., Bioelectronics: Biomaterials for Sensors, Fuel Cells, and Circuitry. *Science* **2002,** 298, (5602), 2407-2408.

ISBN:978-84-692-9758-2/DL:T-206-2010

45. Bowtell, D. D. L., Options available - from start to finish - for obtaining expression data by microarray. *Nature Genetics* **1999,** 21, 25-32.
46. Winzeler, E. A.; Schena, M.; Davis, R. W., Fluorescence-based expression monitoring using microarrays. *Expression of Recombinant Genes in Eukaryotic Systems* **1999,** 306, 3-+.
47. Kuhr, W. G., Electrochemical DNA analysis comes of age. *Nature Biotechnology* **2000,** 18, (10), 1042-1043.
48. Fritz, J.; Cooper, E. B.; Gaudet, S.; Sorger, P. K.; Manalis, S. R., Electronic detection of DNA by its intrinsic molecular charge. *Proceedings of the National Academy of Sciences of the United States of America* **2002,** 99, (22), 14142-14146.
49. A.J. Bard, L. R. F., *Electrochemical Methods: Fundamentals and Applications*. 2nd ed.; John Wiely& Sons: 2001.
50. Brazill, S. A.; Kim, P. H.; Kuhr, W. G., Capillary Gel Electrophoresis with Sinusoidal Voltammetric Detection: A Strategy To Allow Four-â€œColorâ€ DNA Sequencing. *Analytical Chemistry* **2001,** 73, (20), 4882-4890.
51. Wang, J.; Kawde, A.-N., Pencil-based renewable biosensor for label-free electrochemical detection of DNA hybridisation. *Analytica Chimica Acta* **2001,** 431, (2), 219-224.
52. Wang, J.; Kawde, A. N.; Sahlin, E., Renewable pencil electrodes for highly sensitive stripping potentiometric measurements of DNA and RNA. *Analyst* **2000,** 125, (1), 5-7.
53. Thompson, L. A.; Kowalik, J.; Josowicz, M.; Janata, J., Label-free DNA hybridisation probe based on a conducting polymer. *Journal of the American Chemical Society* **2003,** 125, (2), 324-325.
54. Cha, J.; Han, J. I.; Choi, Y.; Yoon, D. S.; Oh, K. W.; Lim, G., DNA hybridisation electrochemical sensor using conducting polymer. *Biosensors and Bioelectronics* **2003,** 18, (10), 1241-1247.
55. Wang, J.; Jiang, M.; Fortes, A.; Mukherjee, B., New label-free DNA recognition based on doping nucleic-acid probes within conducting polymer films. *Analytica Chimica Acta* **1999,** 402, (1-2), 7-12.
56. Souteyrand, E.; Cloarec, J. P.; Martin, J. R.; Wilson, C.; Lawrence, I.; Mikkelsen, S.; Lawrence, M. F., Direct detection of the hybridisation of synthetic homo-

ISBN:978-84-692-9758-2/DL:T-206-2010

oligomer DNA sequences by field effect. *Journal of Physical Chemistry B* **1997,** 101, (15), 2980-2985.

57. Alfonta, L.; Willner, I.; Throckmorton, D. J.; Singh, A. K., Electrochemical and quartz crystal microbalance detection of the cholera toxin employing horseradish peroxidase and GM1-functionalized liposomes. *Analytical Chemistry* **2001,** 73, (21), 5287-5295.
58. de la Escosura-Muñiz, A.; González-García, M. B.; Costa-García, A., DNA hybridisation sensor based on aurothiomalate electroactive label on glassy carbon electrodes. *Biosensors and Bioelectronics* **2007,** 22, (6), 1048-1054.
59. Gheorghe, M.; Guiseppi-Elie, A., Electrical frequency dependent characterisation of DNA hybridisation. *Biosensors and Bioelectronics* **2003,** 19, (2), 95-102.
60. Keighley, S. D.; Estrela, P.; Li, P.; Mighorato, P., Optimization of label-free DNA detection with electrochemical impedance spectroscopy using PNA probes. *Biosensors & Bioelectronics* **2008,** 24, (4), 906-911.
61. Jin, Y., Label-free monitoring of site-specific DNA cleavage by EcoRI endonuclease using cyclic voltammetry and electrochemical impedance. *Analytica Chimica Acta* **2009,** 634, (1), 44-48.
62. Zhou, N.; Yang, T.; Jiang, C.; Du, M.; Jiao, K., Highly sensitive electrochemical impedance spectroscopic detection of DNA hybridisation based on Aunano-CNT/PANnano films. *Talanta* **2009,** 77, (3), 1021-1026.
63. Kafka, J.; Pänke, O.; Abendroth, B.; Lisdat, F., A label-free DNA sensor based on impedance spectroscopy. *Electrochimica Acta* **2008,** 53, (25), 7467-7474.
64. Park, J.-Y.; Kwon, S. H.; Park, J. W.; Park, S.-M., Label-free detection of DNA molecules on the dendron based self-assembled monolayer by electrochemical impedance spectroscopy. *Analytica Chimica Acta* **2008,** 619, (1), 37-42.
65. Degefa, T. H.; Kwak, J., Electrochemical impedance sensing of DNA at PNA self assembled monolayer. *Journal of Electroanalytical Chemistry* **2008,** 612, (1), 37-41.
66. Li, A.; Yang, F.; Ma, Y.; Yang, X., Electrochemical impedance detection of DNA hybridisation based on dendrimer modified electrode. *Biosensors and Bioelectronics* **2007,** 22, (8), 1716-1722.

ISBN:978-84-692-9758-2/DL:T-206-2010

67. Li, F.; Chen, W.; Tang, C.; Zhang, S., Recent development of interaction of transition metal complexes with DNA based on biosensor and its applications. *Talanta* **2008,** 77, (1), 1-8.
68. Wang, J.; Rivas, G.; Cai, X.; Dontha, N.; Shiraishi, H.; Luo, D.; Valera, F. S., Sequence-specific electrochemical biosensing of M. tuberculosis DNA. *Analytica Chimica Acta* **1997,** 337, (1), 41-48.
69. Hongtao, Z.; Huangxian, J., Biosensor for Hepatitis B Virus DNA PCR Product and Electrochemical Study of the Interaction of Di(2,2prime-bipyridine)osmium(III) with DNA. *Electroanalysis* **2004,** 16, (19), 1642-1646.
70. Nojima, T.; Yamashita, K.; Takagi, A.; Takagi, M.; Ikeda, Y.; Kondo, H.; Takenaka, S., Direct detection of single nucleotide polymorphism (SNP) with genomic DNA by the ferrocenylnaphthalene diimide-based electrochemical hybridisation assay (FND-EHA). *Analytical Sciences* **2003,** 19, (1), 79-83.
71. Kara, P.; Ozkan, D.; Kerman, K.; Meric, B.; Erdem, A.; Ozsoz, M., DNA sensing on glassy carbon electrodes by using hemin as the electrochemical hybridisation label. *Analytical and Bioanalytical Chemistry* **2002,** 373, (8), 710-716.
72. Aoki, H.; Umezawa, Y., Trace analysis of an oligonucleotide with a specific sequence using PNA-based ion-channel sensors. *Analyst* **2003,** 128, (6), 681-685.
73. Teh, H. F.; Gong, H.; Dong, X.-D.; Zeng, X.; Lai Kuan Tan, A.; Yang, X.; Tan, S. N., Electrochemical biosensing of DNA with capture probe covalently immobilised onto glassy carbon surface. *Analytica Chimica Acta* **2005,** 551, (1-2), 23-29.
74. Henry, O. Y. F.; Acero Sanchez, J. L.; Latta, D.; O'Sullivan, C. K., Electrochemical quantification of DNA amplicons via the detection of non-hybridised guanine bases on low-density electrode arrays. *Biosensors and Bioelectronics* **2009,** 24, (7), 2064-2070.
75. Hashimoto, K.; Ito, K.; Ishimori, Y., Microfabricated disposable DNA sensor for detection of hepatitis B virus DNA. *Sensors and Actuators B: Chemical* **1998,** 46, (3), 220-225.
76. Umek, R. M.; Lin, S. W.; Vielmetter, J.; Terbrueggen, R. H.; Irvine, B.; Yu, C. J.; Kayyem, J. F.; Yowanto, H.; Blackburn, G. F.; Farkas, D. H.; Chen, Y.-P.,

ISBN:978-84-692-9758-2/DL:T-206-2010

Electronic Detection of Nucleic Acids: A Versatile Platform for Molecular Diagnostics. *J Mol Diagn* **2001,** 3, (2), 74-84.

77. Nakayama, M.; Ihara, T.; Nakano, K.; Maeda, M., DNA sensors using a ferrocene-oligonucleotide conjugate. *Talanta* **2002,** 56, (5), 857-866.
78. Xu, C.; Cai, H.; He, P. G.; Fang, Y. Z., Electrochemical detection of sequence-specific DNA using a DNA probe labeled with aminoferrocene and chitosan modified electrode immobilised with ssDNA. *Analyst* **2001,** 126, (1), 62-65.
79. Xu, C.; He, P.; Fang, Y., Electrochemical labeled DNA probe for the detection of sequence-specific DNA. *Analytica Chimica Acta* **2000,** 411, (1-2), 31-36.
80. Hernandez-Santos, D.; Gonzalez-Garcia, M. B.; Costa-Garcia, A., Genosensor based on a Platinum(II) complex as electrocatalytic label. *Analytical Chemistry* **2005,** 77, (9), 2868-2874.
81. Merkoçi, A.; Aldavert, M.; Marín, S.; Alegret, S., New materials for electrochemical sensing V: Nanoparticles for DNA labeling. *TrAC Trends in Analytical Chemistry* **2005,** 24, (4), 341-349.
82. Fang, Y. Z.; Xu, Y.; He, P. G., DNA Biosensors Based on Metal Nanoparticles. *Journal of Biomedical Nanotechnology* **2005,** 1, (3), 276-285.
83. Wang, J.; Polsky, R.; Xu, D. K., Silver-enhanced colloidal gold electrochemical stripping detection of DNA hybridisation. *Langmuir* **2001,** 17, (19), 5739-5741.
84. Zhang, Y.; Kim, H.-H.; Heller, A., Enzyme-Amplified Amperometric Detection of 3000 Copies of DNA in a 10-Î¼L Droplet at 0.5 fM Concentration. *Analytical Chemistry* **2003,** 75, (13), 3267-3269.
85. Zhang, Y.; Pothukuchy, A.; Shin, W.; Kim, Y.; Heller, A., Detection of âˆ¼103 Copies of DNA by an Electrochemical Enzyme-Amplified Sandwich Assay with Ambient O2 as the Substrate. *Analytical Chemistry* **2004,** 76, (14), 4093-4097.
86. Abad-Valle, P.; Fernández-Abedul, M. T.; Costa-García, A., Genosensor on gold films with enzymatic electrochemical detection of a SARS virus sequence. *Biosensors and Bioelectronics* **2005,** 20, (11), 2251-2260.
87. Azek, F.; Grossiord, C.; Joannes, M.; Limoges, B.; Brossier, P., Hybridisation Assay at a Disposable Electrochemical Biosensor for the Attomole Detection of Amplified Human Cytomegalovirus DNA. *Analytical Biochemistry* **2000,** 284, (1), 107-113.

ISBN:978-84-692-9758-2/DL:T-206-2010

88. Hwang, S.; Kim, E.; Kwak, J., Electrochemical Detection of DNA Hybridisation Using Biometalisation. *Analytical Chemistry* **2004,** 77, (2), 579-584.

89. Martinez-Paredes, G.; Gonzalez-Garcia, M. B.; Costa-Garcia, A., Genosensor for SARS Virus Detection Based on Gold Nanostructured Screen-Printed Carbon Electrodes. *Electroanalysis* **2009,** 21, (3-5), 379-385.

90. Herne, T. M.; Tarlov, M. J., Characterisation of DNA Probes Immobilised on Gold Surfaces. *J. Am. Chem. Soc.* **1997,** 119, (38), 8916-8920.

91. Tashiro, H.; Kondoh, Y.; Kitsunai, T.; Takenaka, S.; Matsumoto, K.; Nojima, T. Manufacturing highly sensitive sensor device comprising organic thin films is useful for detecting trace amounts of substances e.g. biomolecules or other organic material. EP1208909-A; EP1208909-A2; US2002081715-A1; JP2002153272-A; CA2363820-A1, 2002.

92. Davis, C. B.; Shamansky, L. M.; Rosenwald, S.; Stuart, J. K.; Kuhr, W. G.; Brazill, S. A., Independently-addressable micron-sized biosensor elements. *Biosensors & Bioelectronics* **2003,** 18, (10), 1299-1307.

93. Yu, C. H.; Lau, L.; Lin, S. S. W.; Chan, D. K.; Wah Lin, S. S.; Cha, D. K.; Lau, L. T.; Chan, D. K. Y.; Lin, S. W. S.; Chan, K. D. New apparatus comprising a substrate formed with at least one reaction cell, which includes an aluminum oxide surface for the attachment of DNA capture probes, useful for detecting target DNA in a biological sample. WO2004015138-A1; US2004033496-A1; AU2003257367-A1; EP1552017-A1; BR200313409-A; JP2005535319-W; CN1675375-A; KR2005053614-A; US7153687-B2; US2007065872-A1; IN200705498-P1; AU2007224397-A1, 2004.

94. Tagle, D. A.; Swaroop, M.; Lovett, M.; Collins, F. S., Magnetic Bead Capture of Expressed Sequences Encoded within Large Genomic Segments. *Nature* **1993,** 361, (6414), 751-753.

95. Chen, J. H.; Zhang, J.; Wang, K.; Lin, X. H.; Huang, L. Y.; Chen, G. N., Electrochemical Biosensor for Detection of BCR/ABL Fusion Gene Using Locked Nucleic Acids on 4-Aminobenzenesulfonic Acid-Modified Glassy Carbon Electrode. *Analytical Chemistry* **2008,** 80, (21), 8028-8034.

96. Liu, T. Z.; Woudenberg, T.; Chen, J. Array electrode for detecting of biomolecules e.g. DNA or proteins, has array mechanisms having probe attached

to substrate through coupling, attachment, and aryl groups. US2005019803-A1, 2005.

97. Pirri, G.; Damin, F.; Chiari, M.; Bontempi, E.; Depero, L. E., Characterisation of a polymeric adsorbed coating for DNA microarray glass slides. *Analytical Chemistry* **2004,** 76, (5), 1352-1358.
98. Dankbar, D. M.; Gauglitz, G., A study on photolinkers used for biomolecule attachment to polymer surfaces. *Analytical and Bioanalytical Chemistry* **2006,** 386, (7-8), 1967-1974.
99. Galandova, J.; Labuda, J., Polymer interfaces used in electrochemical DNA-based biosensors. *Chemical Papers* **2009,** 63, (1), 1-14.
100. Xu, X. B.; Jindal, V.; Shahedipour-Sandvik, F.; Bergkvist, M.; Cady, N. C., Direct immobilization and hybridisation of DNA on group III nitride semiconductors. *Applied Surface Science* **2009,** 255, (11), 5905-5909.
101. Cai, H.; Wang, Y.; He, P.; Fang, Y., Electrochemical detection of DNA hybridisation based on silver-enhanced gold nanoparticle label. *Analytica Chimica Acta* **2002,** 469, (2), 165-172.
102. Zhu, N.; Cai, H.; He, P.; Fang, Y., Tris(2,2'-bipyridyl)cobalt(III)-doped silica nanoparticle DNA probe for the electrochemical detection of DNA hybridisation. *Analytica Chimica Acta* **2003,** 481, (2), 181-189.
103. Cai, H.; Cao, X.; Jiang, Y.; He, P.; Fang, Y., Carbon nanotube-enhanced electrochemical DNA biosensor for DNA hybridisation detection. *Analytical and Bioanalytical Chemistry* **2003,** 375, (2), 287-293.
104. Kang, J.; Li, X.; Wu, G.; Wang, Z.; Lu, X., A new scheme of hybridisation based on the Aunano-DNA modified glassy carbon electrode. *Analytical Biochemistry* **2007,** 364, (2), 165-170.
105. Lin, X.; Zheng, S.; Miao, Q.; Jin, B., DNA SENSOR FOR BASE MISMATCH DETECTION BASED ON A GOLD COLLOID MODIFIED GLASSY CARBON ELECTRODE. *Analytical Letters* **2002,** 35, (8), 1373 - 1385.
106. Southern, E.; Mir, K.; Shchepinov, M., Molecular interactions on microarrays. *Nature Genetics* **1999,** 21, 5-9.
107. Peterson, A. W.; Heaton, R. J.; Georgiadis, R. M., The effect of surface probe density on DNA hybridisation. *Nucl. Acids Res.* **2001,** 29, (24), 5163-5168.

ISBN:978-84-692-9758-2/DL:T-206-2010

108. Sanchez-Pomales, G.; Santiago-Rodriguez, L.; Rivera-Velez, N. E.; Cabrera, C. R., Control of DNA self-assembled monolayers surface coverage by electrochemical desorption. *Journal of Electroanalytical Chemistry* **2007,** 611, (1-2), 80-86.
109. Tokuhisa, H.; Liu, J. A.; Omori, K.; Kanesato, M.; Hiratani, K.; Baker, L. A., Efficient Biosensor Interfaces Based on Space-Controlled Self-Assembled Monolayers. *Langmuir* **2009,** 25, (3), 1633-1637.
110. Chan, V.; Graves, D. J.; McKenzie, S. E., The biophysics of DNA hybridisation with immobilised oligonucleotide probes. *Biophysical Journal* **1995,** 69, (6), 2243-2255.
111. Yguerabide, J.; Ceballos, A., Quantitative Fluorescence Method for Continuous Measurement of DNA Hybridisation Kinetics Using a Fluorescent Intercalator. *Analytical Biochemistry* **1995,** 228, (2), 208-220.
112. Wilkins Stevens, P.; Henry, M. R.; Kelso, D. M., DNA hybridisation on microparticles: determining capture-probe density and equilibrium dissociation constants. *Nucl. Acids Res.* **1999,** 27, (7), 1719-1727.
113. Henry, M. R.; Wilkins Stevens, P.; Sun, J.; Kelso, D. M., Real-Time Measurements of DNA Hybridisation on Microparticles with Fluorescence Resonance Energy Transfer. *Analytical Biochemistry* **1999,** 276, (2), 204-214.
114. Erickson, D.; Li, D.; Krull, U. J., Modeling of DNA hybridisation kinetics for spatially resolved biochips. *Analytical Biochemistry* **2003,** 317, (2), 186-200.
115. Watterson, J. H.; Piunno, P. A. E.; Wust, C. C.; Krull, U. J., Effects of Oligonucleotide Immobilization Density on Selectivity of Quantitative Transduction of Hybridisation of Immobilised DNA. *Langmuir* **2000,** 16, (11), 4984-4992.
116. Watterson, J. H.; Piunno, P. A. E.; Krull, U. J., Towards the optimization of an optical DNA sensor: control of selectivity coefficients and relative surface affinities. *Analytica Chimica Acta* **2002,** 457, (1), 29-38.
117. Watterson, J. H.; Piunno, P. A. E.; Wust, C. C.; Raha, S.; Krull, U. J., Influences of non-selective interactions of nucleic acids on response rates of nucleic acid fiber optic biosensors. *Fresenius' Journal of Analytical Chemistry* **2001,** 369, (7), 601-608.

ISBN:978-84-692-9758-2/DL:T-206-2010

118. Boncheva, M.; Scheibler, L.; Lincoln, P.; Vogel, H.; Akerman, B., Design of oligonucleotide arrays at interfaces. *Langmuir* **1999,** 15, (13), 4317-4320.
119. Brust, M.; Kiely, C. J., Some recent advances in nanostructure preparation from gold and silver particles: a short topical review. *Colloids and Surfaces a-Physicochemical and Engineering Aspects* **2002,** 202, (2-3), 175-186.
120. Ulman, A., Formation and Structure of Self-Assembled Monolayers. *Chem. Rev.* **1996,** 96, (4), 1533-1554.
121. Love, J. C.; Estroff, L. A.; Kriebel, J. K.; Nuzzo, R. G.; Whitesides, G. M., Self-assembled monolayers of thiolates on metals as a form of nanotechnology. *Chemical Reviews* **2005,** 105, (4), 1103-1169.
122. Finklea, H. O., Self-Assembled Monolayers on Electrodes. In *Encyclopedia of Analytical Chemistry*, Meyers, R. A., Ed. Wieley, New York: 2000; Vol. 11, pp 10090-10115.
123. Schreiber, F., Self-assembled monolayers: from 'simple' model systems to biofunctionalized interfaces. *Journal of Physics-Condensed Matter* **2004,** 16, (28), R881-R900.
124. Nuzzo, R. G.; Allara, D. L., Adsorption of bifunctional organic disulfides on gold surfaces. *J. Am. Chem. Soc.* **1983,** 105, (13), 4481-4483.
125. Finklea, H. O., Electrochemistry of organized monolayers of thiols and related molecules on electrodes. In *Electroanalytical Chemistry: a Series of Advances, Vol 19*, 1996; Vol. 19, pp 109-335.
126. Lee, H.; He, Z.; Hussey, C. L.; Mattern, D. L., Unsymmetrical Dialkyl Sulfides for Self-Assembled Monolayer Formation on Gold: Lack of Preferential Cleavage of Allyl or Benzyl Substituents. *Chem. Mater.* **1998,** 10, (12), 4148-4153.
127. Vaughan, R. D.; O'Sullivan, C. K.; Guilbault, G. G., Sulfur based self-assembled monolayers (SAM's) on piezoelectric crystals for immunosensor development. *Fresenius Journal of Analytical Chemistry* **1999,** 364, (1-2), 54-57.
128. Yamada, T.; Sekine, R.; Sawaguchi, T., Ultrahigh-vacuum multitechnique study of AuCN monolayers on Au(111) formed by electrochemical deposition. *Journal of Chemical Physics* **2000,** 113, (3), 1217-1227.

ISBN:978-84-692-9758-2/DL:T-206-2010

129. Gao, W.; Dickinson, L.; Grozinger, C.; Morin, F. G.; Reven, L., Order-disorder transitions in self-assembled monolayers: A C-13 solid-state NMR study. *Langmuir* **1997,** 13, (2), 115-118.
130. Laiho, T.; Lukkari, J.; Meretoja, M.; Laajalehto, K.; Kankare, J.; Leiro, J. A., Chemisorption of alkyl thiols and S-alkyl thiosulfates on Pt(111) and polycrystalline platinum surfaces. *Surface Science* **2005,** 584, (1), 83-89.
131. Azzaroni, O.; Vela, M. E.; Fonticelli, M.; Benitez, G.; Carro, P.; Blum, B.; Salvarezza, R. C., Electrodesorption potentials of self-assembled alkanethiolate monolayers on copper electrodes. An experimental and theoretical study. *Journal of Physical Chemistry B* **2003,** 107, (48), 13446-13454.
132. Li, W. J.; Virtanen, J. A.; Penner, R. M., Self-Assembly of N-Alkanethiolate Monolayers on Silver Nanostructures - Determination of the Apparent Thickness of the Monolayer by Scanning-Tunneling-Microscopy. *Journal of Physical Chemistry* **1994,** 98, (45), 11751-11755.
133. Cohen-Atiya, M.; Nelson, A.; Mandler, D., Characterisation of n-alkanethiol self-assembled monolayers on mercury by impedance spectroscopy and potentiometric measurements. *Journal of Electroanalytical Chemistry* **2006,** 593, (1-2), 227-240.
134. Collier, P. J.; Iggo, J. A.; Whyman, R., Preparation and characterisation of solvent-stabilised nanoparticulate platinum and palladium and their catalytic behaviour towards the enantioselective hydrogenation of ethyl pyruvate. *Journal of Molecular Catalysis A: Chemical* **1999,** 146, (1-2), 149-157.
135. Magnusson, M. H.; Deppert, K.; Malm, J. O.; Bovin, J. O.; Samuelson, L., Size-selected gold nanoparticles by aerosol technology. *Nanostructured Materials* **1999,** 12, (1-4), 45-48.
136. Milan Paunovic; Schlesinger, M., *Fundamentals of Electrochemical Deposition,*. Second ed.; Wiley: USA, 2006.
137. Finot, M. O.; Braybrook, G. D.; McDermott, M. T., Characterisation of electrochemically deposited gold nanocrystals on glassy carbon electrodes. *Journal of Electroanalytical Chemistry* **1999,** 466, (2), 234-241.
138. Finot, M. O.; McDermott, M. T., Characterisation of n-alkanethiolate monolayers adsorbed to electrochemically deposited gold nanocrystals on glassy carbon electrodes. *Journal of Electroanalytical Chemistry* **2000,** 488, (2), 125-132.

ISBN:978-84-692-9758-2/DL:T-206-2010

139. El-Deab, M. S.; Ohsaka, T., Quasi-reversible two-electron reduction of oxygen at gold electrodes modified with a self-assembled submonolayer of cysteine. *Electrochemistry Communications* **2003,** 5, (3), 214-219.
140. El-Deab, M. S.; Ohsaka, T., Molecular-level design of binary self-assembled monolayers on polycrystalline gold electrodes. *Electrochimica Acta* **2004,** 49, (13), 2189-2194.
141. El-Deab, M. S.; Okajima, T.; Ohsaka, T., Fabrication of phase-separated multicomponent self-assembled monolayers at gold nanoparticles electrodeposited on glassy carbon electrodes. *Journal of the Electrochemical Society* **2006,** 153, (12), E201-E206.
142. Oyama, T.; Okajima, T.; Ohsaka, T., Electrodeposition of gold at glassy carbon electrodes in room-temperature ionic liquids. *Journal of the Electrochemical Society* **2007,** 154, (6), D322-D327.
143. Soreta, T. R.; Strutwolf, J.; O'Sullivan, C. K., Electrochemically deposited palladium as a substrate for self-assembled monolayers. *Langmuir* **2007,** 23, (21), 10823-10830.
144. Hou, Z. Z.; Dante, S.; Abbott, N. L.; Stroeve, P., Self-assembled monolayers on (111) textured electroless gold. *Langmuir* **1999,** 15, (8), 3011-3014.
145. Dubrovsky, T. B.; Hou, Z. Z.; Stroeve, P.; Abbott, N. L., Self-assembled monolayers formed on electroless cold deposited on silica gel: A potential stationary phase for biological assays. *Analytical Chemistry* **1999,** 71, (2), 327-332.
146. Pham, T.; Jackson, J. B.; Halas, N. J.; Lee, T. R., Preparation and characterisation of gold nanoshells coated with self-assembled monolayers. *Langmuir* **2002,** 18, (12), 4915-4920.
147. Folkers, J. P.; Laibinis, P. E.; Whitesides, G. M., Self-Assembled Monolayers of Alkanethiols on Gold - Comparisons of Monolayers Containing Mixtures of Short-Chain and Long-Chain Constituents with Ch3 and Ch2oh Terminal Groups. *Langmuir* **1992,** 8, (5), 1330-1341.
148. Bain, C. D.; Evall, J.; Whitesides, G. M., Formation of monolayers by the coadsorption of thiols on gold: variation in the head group, tail group, and solvent. *J. Am. Chem. Soc.* **1989,** 111, (18), 7155-7164.

ISBN:978-84-692-9758-2/DL:T-206-2010

149. Folkers, J. P.; Laibinis, P. E.; Whitesides, G. M.; Deutch, J., Phase-Behavior of 2-Component Self-Assembled Monolayers of Alkanethiolates on Gold. *Journal of Physical Chemistry* **1994,** 98, (2), 563-571.
150. Bain, C. D.; Whitesides, G. M., Formation of Monolayers by the Coadsorption of Thiols on Gold - Variation in the Length of the Alkyl Chain. *Journal of the American Chemical Society* **1989,** 111, (18), 7164-7175.
151. Brewer, N. J.; Leggett, G. J., Chemical Force Microscopy of Mixed Self-Assembled Monolayers of Alkanethiols on Gold: Evidence for Phase Separation. *Langmuir* **2004,** 20, (10), 4109-4115.
152. Chen, S. F.; Li, L. Y.; Boozer, C. L.; Jiang, S. Y., Controlled chemical and structural properties of mixed self-assembled monolayers of alkanethiols on Au(111). *Langmuir* **2000,** 16, (24), 9287-9293.
153. Shon, Y. S.; Lee, S.; Perry, S. S.; Lee, T. R., The adsorption of unsymmetrical spiroalkanedithiols onto gold affords multi-component interfaces that are homogeneously mixed at the molecular level. *Journal of the American Chemical Society* **2000,** 122, (7), 1278-1281.
154. Tamada, K.; Hara, M.; Sasabe, H.; Knoll, W., Surface phase behavior of n-alkanethiol self-assembled monolayers adsorbed on Au(111): An atomic force microscope study. *Langmuir* **1997,** 13, (6), 1558-1566.
155. Stranick, S. J.; Atre, S. V.; Parikh, A. N.; Wood, M. C.; Allara, D. L.; Winograd, N.; Weiss, P. S., Nanometer-scale phase separation in mixed composition self-assembled monolayers. *Nanotechnology* **1996,** 7, (4), 438-442.
156. Kim, Y. K.; Koo, J. P.; Huh, C. J.; Ha, J. S.; Pi, U. H.; Choi, S. Y.; Kim, J., Adsorption behavior of binary mixed alkanethiol molecules on Au: Scanning tunneling microscope and linear-scan voltammetry investigation. *Applied Surface Science* **2006,** 252, (14), 4951-4956.
157. Hayes, W. A.; Kim, H.; Yue, X. H.; Perry, S. S.; Shannon, C., Nanometer-scale patterning of surfaces using self-assembly chemistry .2. Preparation, characterisation, and electrochemical behavior of two-component organothiol monolayers on gold surfaces. *Langmuir* **1997,** 13, (9), 2511-2518.
158. Hobara, D.; Ota, M.; Imabayashi, S.; Niki, K.; Kakiuchi, T., Phase separation of binary self-assembled thiol monolayers composed of 1-hexadecanethiol and 3-

mercaptopropionic acid on Au(111) studied by scanning tunneling microscopy and cyclic voltammetry. *Journal of Electroanalytical Chemistry* **1998,** 444, (1), 113-119.

159. Steichen, M.; Buess-Herman, C., Electrochemical detection of the immobilization and hybridisation of unlabeled linear and hairpin DNA on gold. *Electrochemistry Communications* **2005,** 7, (4), 416-420.
160. Ishige, Y.; Shimoda, M.; Kamahori, M., Immobilization of DNA probes onto gold surface and its application to fully electric detection of DNA hybridisation using field-effect transistor sensor. *Japanese Journal of Applied Physics Part 1-Regular Papers Brief Communications & Review Papers* **2006,** 45, (4B), 3776-3783.
161. Boozer, C.; Chen, S.; Jiang, S., Controlling DNA Orientation on Mixed ssDNA/OEG SAMs. *Langmuir* **2006,** 22, (10), 4694-4698.
162. Henry, O. Y. F.; Perez, J. G.; Sanchez, J. L. A.; O'Sullivan, C. K., Electrochemcial characterisation and hybridisation efficiency of co-assembled monolayers of PEGylated ssDNA and mercaptohexanol on planar gold electrodes. *Biosensors and Bioelectronics* In Press, Corrected Proof.
163. Keighley, S. D.; Li, P.; Estrela, P.; Mighorato, P., Optimization of DNA immobilization on gold electrodes for label-free detection by electrochemical impedance spectroscopy. *Biosensors & Bioelectronics* **2008,** 23, (8), 1291-1297.
164. Azehara, H.; Yoshimoto, S.; Hokari, H.; Akiba, U.; Taniguchi, I.; Fujihira, M., Investigation of the structure of self-assembled monolayers of asymmetrical disulfides on Au(111) electrodes by electrochemical desorption. *Journal of Electroanalytical Chemistry* **1999,** 473, (1-2), 68-74.
165. Bain, C. D.; Biebuyck, H. A.; Whitesides, G. M., Comparison of Self-Assembled Monolayers on Gold - Coadsorption of Thiols and Disulfides. *Langmuir* **1989,** 5, (3), 723-727.
166. Ishida, T.; Yamamoto, S.; Mizutani, W.; Motomatsu, M.; Tokumoto, H.; Hokari, H.; Azehara, H.; Fujihira, M., Evidence for cleavage of disulfides in the self-assembled monolayer on Au(111). *Langmuir* **1997,** 13, (13), 3261-3265.
167. Offord, D. A.; John, C. M.; Griffin, J. H., Contact-Angle Goniometry, Ellipsometry, Xps, and Tof-Sims Analysis of Gold-Supported, Mixed Self-

ISBN:978-84-692-9758-2/DL:T-206-2010

Assembled Monolayers Formed from Mixed Dialkyl Disulfides. *Langmuir* **1994,** 10, (3), 761-766.

168. Schonherr, H.; Ringsdorf, H.; Jaschke, M.; Butt, H. J.; Bamberg, E.; Allinson, H.; Evans, S. D., Self-assembled monolayers of symmetrical and mixed alkyl fluoroalkyl disulfides on gold .2. Investigation of thermal stability and phase separation. *Langmuir* **1996,** 12, (16), 3898-3904.
169. Lazerges, M.; Perrot, H.; Zeghib, N.; Antoine, E.; Compere, C., In situ QCM DNA-biosensor probe modification. *Sensors and Actuators B: Chemical* **2006,** 120, (1), 329-337.
170. Steel, A. B.; Levicky, R. L.; Herne, T. M.; Tarlov, M. J., Immobilization of nucleic acids at solid surfaces: Effect of oligonucleotide length on layer assembly. *Biophysical Journal* **2000,** 79, (2), 975-981.
171. Levicky, R.; Herne, T. M.; Tarlov, M. J.; Satija, S. K., Using Self-Assembly To Control the Structure of DNA Monolayers on Gold: A Neutron Reflectivity Study. *Journal of the American Chemical Society* **1998,** 120, (38), 9787-9792.
172. Berganza, J.; Olabarria, G.; García, R.; Verdoy, D.; Rebollo, A.; Arana, S., DNA microdevice for electrochemical detection of Escherichia coli 0157:H7 molecular markers. *Biosensors and Bioelectronics* **2007,** 22, (9-10), 2132-2137.
173. Berggren, C.; Bjarnason, B.; Johansson, G., Capacitive biosensors. *Electroanalysis* **2001,** 13, (3), 173-180.
174. Nishizawa, M.; Sunagawa, T.; Yoneyama, H., Selective desorption of 3-mercaptopropionic acid from a mixed monolayer with hexadecanethiol assembled on a gold electrode. *Journal of Electroanalytical Chemistry* **1997,** 436, (1-2), 213-218.
175. Satjapipat, M.; Sanedrin, R.; Zhou, F. M., Selective desorption of alkanethiols in mixed self-assembled monolayers for subsequent oligonucleotide attachment and DNA hybridisation. *Langmuir* **2001,** 17, (24), 7637-7644.
176. Shimazu, K.; Kawaguchi, T.; Isomura, T., Construction of mixed mercaptopropionic acid/alkanethiol monolayers of controlled composition by structural control of a gold substrate with underpotentially deposited lead atoms. *Journal of the American Chemical Society* **2002,** 124, (4), 652-661.

ISBN:978-84-692-9758-2/DL:T-206-2010

177. Shimazu, K.; Hashimoto, Y.; Kawaguchi, T.; Tada, K., Construction of mixed mercaptopropionic acid/alkanethiol monolayers on polycrystalline gold electrodes using underpotentially deposited lead as the control element. *Journal of Electroanalytical Chemistry* **2002,** 534, (2), 163-169.
178. Carvalhal, R. T.; Freire, R. S.; Kubota, L. T., Polycrystalline gold electrodes: A comparative study of pretreatment procedures used for cleaning and thiol self-assembly monolayer formation. *Electroanalysis* **2005,** 17, (14), 1251-1259.
179. El-Deab, M. S.; Arihara, K.; Ohsaka, T., Fabrication of Au(111)-like polycrystalline gold electrodes and their applications to oxygen reduction. *Journal of the Electrochemical Society* **2004,** 151, (6), E213-E218.
180. Madueno, R.; Sevilla, J. M.; Pineda, T.; Roman, A. J.; Blazquez, M., A voltammetric study of 6-mercaptopurine monolayers on polycrystalline gold electrodes. *Journal of Electroanalytical Chemistry* **2001,** 506, (2), 92-98.
181. Yang, W.; Justin Gooding, J.; Brynn Hibbert, D., Characterisation of gold electrodes modified with self-assembled monolayers of -cysteine for the adsorptive stripping analysis of copper. *Journal of Electroanalytical Chemistry* **2001,** 516, (1-2), 10-16.
182. Strutwolf, J.; O'Sullivan, C. K., Microstructures by selective desorption of self-assembled monolayer from polycrystalline gold electrodes. *Electroanalysis* **2007,** 19, (14), 1467-1475.
183. Henry, O. Y. F.; Maliszewska, A.; O'Sullivan, C. K., DNA surface nanopatterning by selective reductive desorption from polycrystalline gold electrode. *Electrochemistry Communications* **2009,** 11, (3), 664-667.
184. Leiva, E., *Nanoelectrochemistry*. Second ed.; John Wiley & Sons, Inc.: New Jersey, 2006; p 679 - 691.
185. Hugelmann, M.; Hugelmann, P.; Lorenz, W. J.; Schindler, W., Nanoelectrochemistry and nanophysics at electrochemical interfaces. *Surface Science* **2005,** 597, (1-3), 156-172.
186. Milchev, A.; Zapryanova, T., Nucleation and growth of copper under combined charge transfer and diffusion limitations - Part II. *Electrochimica Acta* **2006,** 51, (23), 4916-4921.

ISBN:978-84-692-9758-2/DL:T-206-2010

187. Li, W.; Virtanen, J. A.; Penner, R. M., Nanometer-scale electrochemical deposition of silver on graphite using a scanning tunneling microscope. *Applied Physics Letters* **1992,** 60, (10), 1181-1183.

188. Kolb, D. M.; Ullmann, R.; Will, T., Nanofabrication of Small Copper Clusters on Gold(111) Electrodes by a Scanning Tunneling Microscope. *Science* **1997,** 275, (5303), 1097-1099.

189. Andersen, J. E. T.; Zhang, J. D.; Chi, Q.; Hansen, A. G.; Nielsen, J. U.; Friis, E. P.; Ulstrup, J.; Boisen, A.; Jensenius, H., In situ scanning probe microscopy and new perspectives in analytical chemistry. *TrAC Trends in Analytical Chemistry* **1999,** 18, (11), 665-674.

190. Budevski, E.; Staikov, G.; Lorenz, W. J., Electrocrystallization: Nucleation and growth phenomena. *Electrochimica Acta* **2000,** 45, (15-16), 2559-2574.

191. Paunovic, M.; Schlesinger, M., *Fundamentals of electrochemical deposition*. 2nd ed.; Hoboken, NJ : John Wiley & Sons, cop.: 2006.

192. Magnussen, O. M.; Polewska, W.; Zitzler, L.; Behm, R. J., In situ video-STM studies of dynamic processes at electrochemical interfaces. *Faraday Discussions* **2002,** 121, 43-52.

193. Plieth, W.; Georgiev, G. S., Residence times in kink sites and Markov chain model of alloy and intermetallic compound deposition. *Russian Journal of Electrochemistry* **2006,** 42, (10), 1093-1100.

194. Penner, R. M., Metal Deposition. In *Handbook of Electrochemistry*, First edition ed.; Zoski, C. G., Ed. Elsevier: 2007; pp 661-709.

195. Fang, B.; Jiao, S.; Li, M.; Qu, Y.; Jiang, X., Label-free electrochemical detection of DNA using ferrocene-containing cationic polythiophene and PNA probes on nanogold modified electrodes. *Biosensors and Bioelectronics* **2008,** 23, (7), 1175-1179.

196. Wang, M. J.; Sun, C. Y.; Wang, L. Y.; Ji, X. H.; Bai, Y. B.; Li, T. J.; Li, J. H., Electrochemical detection of DNA immobilised on gold colloid particles modified self-assembled monolayer electrode with silver nanoparticle label. *Journal of Pharmaceutical and Biomedical Analysis* **2003,** 33, (5), 1117-1125.

ISBN:978-84-692-9758-2/DL:T-206-2010

197. Du, D.; Liu, S. L.; Chen, J.; Ju, H. X.; Lian, H. Z.; Li, J. X., Colloidal gold nanoparticle modified carbon paste interface for studies of tumor cell adhesion and viability. *Biomaterials* **2005,** 26, (33), 6487-6495.
198. El-Deab, M. S.; Okajima, T.; Ohsaka, T., Electrochemical reduction of oxygen on gold nanoparticle-electrodeposited glassy carbon electrodes. *Journal of the Electrochemical Society* **2003,** 150, (7), A851-A857.
199. Pingarron, J. M.; Yanez-Sedeno, P.; Gonzalez-Cortes, A., Gold nanoparticle-based electrochemical biosensors. *Electrochimica Acta* **2008,** 53, (19), 5848-5866.
200. Yanez-Sedeno, P.; Pingarron, J. M., Gold nanoparticle-based electrochemical biosensors. *Analytical and Bioanalytical Chemistry* **2005,** 382, (4), 884-886.
201. Sasha Gorer, H. L., Rebecca M. Stiger, Michael P. Zach, James V. Zoval, and Reginald M. Penner, *Electrodeposition of Metal Nanoparticles on Graphite and Silicon*. MARCEL DEKKER, INC.: New York, 2002; p 237 - 259.
202. Hwang, S.; Kim, E.; Kwak, J., Electrochemical detection of DNA hybridisation using biometalisation. *Analytical Chemistry* **2005,** 77, (2), 579-584.

UNIVERSITAT ROVIRA I VIRGILI
ELECTROCHEMICALLY DEPOSITED METAL NANOSTRUCTURES FOR APPLICATIONS IN GENOSENSORS
Tesfaye Refera Soreta
ISBN:978-84-692-9758-2/DL:T-206-2010

ISBN:978-84-692-9758-2/DL:T-206-2010

Chapter 2

Electrochemically Deposited Palladium as a Substrate for Self-Assembled Monolayers

UNIVERSITAT ROVIRA I VIRGILI
ELECTROCHEMICALLY DEPOSITED METAL NANOSTRUCTURES FOR APPLICATIONS IN GENOSENSORS
Tesfaye Refera Soreta
ISBN:978-84-692-9758-2/DL:T-206-2010

Electrochemically Deposited Palladium as a Substrate for Self-Assembled Monolayers

Tesfaye Refera Soreta,† Jorg Strutwolf,*,†,§ and Ciara K. O'Sullivan*,†,‡

Nanobiotechnology and Bioanalysis Group, Department of Chemical Engineering, Universitat Rovira I Virgili, Avinguda Països Catalans, 26, 43007, Tarragona, Spain, and Institució Catalana de Recerca i Estudis Avançats, Passeig Lluís Companys 23, 08010 Barcelona, Spain

Received March 8, 2007. In Final Form: July 16, 2007

The vast majority of reports of self-assembled monolayers (SAMs) on metals focus on the use of gold. However, other metals, such as palladium, platinum, and silver offer advantages over gold as a substrate. In this work, palladium is electrochemically deposited from $PdCl_2$ solutions on glassy carbon electrodes to form a substrate for alkanethiol SAMs. The conditions for deposition are optimized with respect to the electrolyte, pH, and electrochemical parameters. The palladium surfaces have been characterized by scanning electron microscopy (SEM) and the surface roughness has been estimated by chronocoulometry. SAMs of alkane thiols have been formed on the palladium surfaces, and their ability to suppress a Faradaic process is used as an indication for palladium coverage on the glassy carbon. The morphology of the Pd deposit as characterized by SEM and the blocking behavior of the SAM formed on deposited Pd delivers a consistent picture of the Pd surface. It has been clearly demonstrated that, via selection of experimental conditions for the electrochemical deposition, the morphology of the palladium surface and its ability to support SAMs can be controlled. The work will be applied to create a mixed monolayer of metals, which can subsequently be used to create a mixed SAM of a biocomponent and an alkanethiol for biosensing applications.

1. Introduction

Designing electrode surfaces on a molecular level can be achieved by the chemical adsorption of alkanethiol molecules on a metal electrode surface.[1,2] The high grade of organization and stability of self-assembled monolayers (SAMs) and the potential of the functionalization of molecules within the monolayer enable a wide range of applications of SAM-modified electrode surfaces in sensing processes (e.g., biosensors).[3−7] Gold is the most popular substrate for thiol SAMs. Gold substrates can be handled in air without any oxide surface layer formation, and can survive harsh chemical treatment to remove organic contaminants because of the noble character of gold.[1] The other coinage metals (silver and copper) and platinum have also been used as substrates for thiol SAMs.[8−10] Palladium is not often used as a substrate for SAM formation, although the properties of SAMs of alkanethiols on palladium substrates offer advantages over SAM formation on other metals.[11−15] SAMs on palladium resist corrosion by solution-phase chemical etchants, regardless of the chain length and wettability of the SAM, in contrast to gold as a substrate, where hydrophobic, well-ordered, crystalline alkane films are required. This property makes SAMs on palladium superior to SAMs on gold or SAMs on silver systems for patterning microstructures by microcontact printing.[11,13] Palladium has also been employed as a substrate for SAMs used in biotechnology.[12] For characterization of alkanethiol SAMs on Pd, a variety of surface analytical techniques have been employed: contact angle measurements, optical ellipsometry, reflection absorption infrared spectroscopy, X-ray photoelectron spectroscopy, and surface plasmon resonance.[12,14] To our knowledge, no electrochemical method has been used for the characterization of SAMs formed on Pd. We report on the use of electrodeposited palladium on glassy carbon (GC) electrodes as a substrate to support thiol-based SAMs. The blocking behavior of the longer chain alkanethiol SAMs toward a redox reaction provides an indication of the completeness of the deposited palladium layer, since thiol SAMs form stable films on palladium but are not supported on bare GC. Consequently, redox reactions occur at the bare GC subareas, while electron-transfer reactions are more or less blocked by the SAM covering palladium deposits. The adsorption behavior of thiol SAMs has implications for the formation of micro- and nanostructures based on SAM formation

* Corresponding author. E-mail: ciara.osullivan@urv.cat (C.K.O.); jorg.strutwolf@fundacio.urv.cat (J.S.). Fax: +34 977 55 9667.
† Universitat Rovira I Virgili.
‡ Institució Catalana de Recerca i Estudis Avançats.
§ Visiting scientist at the University of Tübingen, Department of Chemistry, Institute of Organic Chemistry, Auf der Morgenstelle 18, 72076 Tübingen, Germany.

(1) Finklea, H. O. Self-assembled monolayers on electrodes. In *Encyclopedia of Analytical Chemistry*; Meyers, R. A., Ed.; Wiley: New York, 2000; Vol. 11, pp 10090−10115.
(2) Ulman, A. *Chem. Rev.* **1996**, *96* (4), 1533−1554.
(3) Wink, T.; van Zuilen, S. J.; Bult, A.; van Bennekom, W. P. *Analyst* **1997**, *122* (4), R43−R50.
(4) Satjapipat, M.; Sanedrin, R.; Zhou, F. M. *Langmuir* **2001**, *17* (24), 7637−7644.
(5) Frederix, F.; Bonroy, K.; Laureyn, W.; Reekmans, G.; Campitelli, A.; Dehaen, W.; Maes, G. *Langmuir* **2003**, *19* (10), 4351−4357.
(6) Gooding, J. J.; Mearns, F.; Yang, W.; Liu, J. *Electroanalysis* **2003**, *15* (2), 81−96.
(7) Chaki, N. K.; Vijayamohanan, K. *Biosens. Bioelectron.* **2002**, *17* (1−2), 1−12.
(8) Laibinis, P. E.; Whitesides, G. M. *J. Am. Chem. Soc.* **1992**, *114* (6), 1990−1995.
(9) Laibinis, P. E.; Whitesides, G. M.; Allara, D. L.; Tao, Y. T.; Parikh, A. N.; Nuzzo, R. G. *J. Am. Chem. Soc.* **1991**, *113* (19), 7152−7167.
(10) Laibinis, P. E.; Bain, C. D.; Whitesides, G. M. *J. Phys. Chem.* **1991**, *95* (18), 7017−7021.
(11) Carvalho, A.; Geissler, M.; Schmid, H.; Michel, B.; Delamarche, E. *Langmuir* **2002**, *18* (6), 2406−2412.
(12) Jiang, X.; Bruzewicz, D. A.; Thant, M. M.; Whitesides, G. M. *Anal. Chem.* **2004**, *76* (20), 6116−6121.
(13) Love, J. C.; Wolfe, D. B.; Chabinyc, M. L.; Paul, K. E.; Whitesides, G. M. *J. Am. Chem. Soc.* **2002**, *124* (8), 1576−1577.
(14) Love, J. C.; Wolfe, D. B.; Haasch, R.; Chabinyc, M. L.; Paul, K. E.; Whitesides, G. M.; Nuzzo, R. G. *J. Am. Chem. Soc.* **2003**, *125* (9), 2597−2609.
(15) Love, J. C.; Wolfe, D. B.; Paul, K. E.; Chabinyc, M. L.; Nuzzo, R. G.; Whitesides, G. M. *Abstr. Pap. Am. Chem. Soc.* **2002**, *224*, U431−U431.

10.1021/la7006777 CCC: $37.00
Published on Web 09/12/2007

on mixed metal surfaces,[16] which may serve as substrates to allow specific attachment of bioreceptor molecules.

Electrodeposition of Pd on GC electrodes is used to obtain Pd substrates. Although coating methods such as evaporation and sputtering chemical vapor deposition are an option, electrodeposition is often used for reasons of economy and/or convenience. Electrodeposition of palladium is especially attractive because palladium is seen as a replacement for gold as a contact metal in the electronic industry, in view of its excellent resistance to corrosion and wear, good solderability, and lower density.[17,18] However, the ability of palladium to catalyze hydrogen evolution and to absorb and dissolve hydrogen[19,20] poses a significant problem for the electrodeposition of Pd from aqueous solutions (hydrogen embrittlement). The evolution of hydrogen interferes with the reduction of Pd ions at the electrode surface, resulting in cracks of the deposited metal. The term hydrogen embrittlement is used to describe a variety of fracture phenomena related to the presence of hydrogen in a metal or alloy.[21] The degree of fractured areas in a Pd layer deposited onto a GC depends on the applied deposition potential or current.

In the first part of the paper, we will concentrate on Pd deposition to create a suitable substrate for SAMs. Palladium has been deposited from a wide variety of electrolytes, which can be broadly classified as alkaline, neutral, and acidic.[21,22] The morphology and material properties of the deposited palladium is greatly affected by the deposition conditions, such as temperature, transport mode (convection), composition, the pH of the electrolyte, the electrochemical technique, and associated parameters such as the use of applied potential or current. In the reported work, we have systematically investigated the influence of some critical experimental conditions on the deposition of palladium on GC electrode surfaces from an aqueous solution of two Pd−chloro complexes. Three different acidic electrolyte solutions are tested: nitric acid, buffer solutions of citrate, and acetate. For each electrolyte, the pH was adjusted between 1 and 4, if feasible. Deposition was performed using potentiodynamic, potentiostatic, and galvanostatic experiments. In the two latter cases, the influence of applied potential and current is investigated. The morphology of the deposited palladium is characterized by scanning electron microscopy (SEM).

The optimal parameters for palladium electrodeposition depends on the desired surface morphology. It will be shown how the variation of experimental conditions can be used for controlling the brightness, smoothness, graininess, and surface coverage of the deposited palladium layer, and in the second part of this report, it will be shown how these surface properties affect the alkanethiol SAM formation.

2. Experimental Section

2.1. Reagents. Palladium was deposited from a buffered solution of $PdCl_2$ and Na_2PdCl_4 (99.9%, Aldrich). The deposition baths employed were citrate buffer (consisting of 0.03 M citric acid, 0.0082 M HCl, 0.061 M NaCl, pH 2, Fluka), acetate buffer (acetic acid, sodium acetate, pH 4.65, Riedel-de Haen), and nitric acid (65%, Scharlau). The pH of the bath was adjusted by adding a diluted sodium hydroxide (98% Scharlau) solution or diluted nitric acid. Methyl viologen (98%, Aldrich) and potassium hexacyanoferrate-(III) (99%, Aldrich) were used as redox probes. For the formation of alkanethiol-based SAMs, *n*-decanethiol (96%, Aldrich) and *n*-butanethiol (99%, Aldrich) were used. All chemicals were provided by Sigma (Barcelona, Spain) and used as received without any other treatment. The solutions were prepared with Milli-Q water (18.2 MΩ·cm).

2.2. Electrode Preparation. GC rods (Sigradur, HTW Hochtemperatur Werkstoffe, Germany) with a length of 7 cm and a diameter of 3 mm were pressed into two layers of heat-shrinking polyolefine tubes. One end of the rod, which served as the electrode surface, was polished with 0.3 μm alumina slurry (BUEHLER). Upon polishing, the electrodes were carefully rinsed with Milli-Q water and sonicated for about 15 min. The electrodes were used immediately after the cleaning procedure.

For SAMs of alkanethiols, the palladinized electrodes were immersed into a 10 mM ethanolic solution of *n*-decanthiol or *n*-butanethiol for 12 h. Afterward, the electrodes were carefully flushed with ethanol and washed with water followed by air drying.

2.3. Instrumentation. *2.3.1. Electrochemical Measurements.* Cyclic voltammetry, potential step, and current step experiments were carried out using an Autolab model PGSTAT 12 potentiostat/galvanostat controlled with the General Purpose Electrochemical System (GPES) software (Eco Chemie B.V., The Netherlands). A conventional three-electrode setup was used with the GC electrode as the working electrode and a platinum wire (BAS model MW-1032) as a counter electrode. An Ag/AgCl electrode (BAS model MF-2078) served as a reference electrode. All potentials were reported with respect to this reference electrode. A magnetic stirrer provided the convective transport during potential step and galvanostatic experiments. Prior to any measurement, the solutions in the electrochemical cell were flushed with Argon gas for 5 min. All depositions were performed from solutions containing 1.33 g/L $PdCl_2$ or Na_2PdCl_4.

Because of the limited potential window, it was not possible to use potassium hexacyanoferrate to determine the area of the palladinized electrodes, and instead methyl viologen was used. The real electrode areas, taking into account the surface roughness, were determined by chronocoulometry. The duration of the potential step was 250 ms. The real electrode area of the bare GC electrode was estimated in 0.1 M aq KCl using 0.1 mM potassium hexacyanoferrate (diffusion coefficient 7.6×10^{-6} cm^2/s) using Anson's equation.[23] The real area of the deposited palladium surfaces was measured by chronocoulometry using methyl viologen dichloride. The diffusion coefficient of methyl viologen was measured by cyclic voltammetry using a bare GC electrode, and a value of $D = 6.4 \times 10^{-6}$ cm^2/s was found. Chronocoulmetric measurements with the palladium-modified electrodes using methyl viologen allows then the estimation of the real area from which the roughness factor was calculated.

2.3.2. SEM Imaging. SEM for the characterization of palladinized surfaces on a GC electrode was carried out using a Quanta 600, FEI Company model environmental scanning electron microscope at an acceleration voltage of 20 kV and a working distance of 10 mm in a high-vacuum mode.

3. Results and Discussion

Primarily studies of electrochemical Pd deposition were performed by cyclic voltammetry in unstirred solution for all conditions under investigation. All voltammograms showed the same basic shape, but with differences in the peak potentials for the reductive palladium deposition, depending on the electrolyte, pH, and Pd source, as will be discussed later. A typical example is given in Figure 1, where the first, second, and third scan for deposition from $PdCl_2$ in citrate buffer solution at pH 3 is shown. The peak potentials can be assigned to the following electrode reactions: Palladium is reductively deposited at 125 mV (first

(16) Oyamatsu, D.; Kanemoto, H.; Kuwabata, S.; Yoneyama, H. *J. Electroanal. Chem.* **2001**, *497* (1−2), 97−105.
(17) Micklus, S. G. *Plat. Surf. Finish.* **1995**, *82*, 67.
(18) Abys, J. A. *Plat. Surf. Finish* **1999**, *86*, 108−115.
(19) Lewis, F. A. *The Palladium-Hydrogen System*; Academic Press: New York, 1967.
(20) Green, T.; Britz, D. *J. Electroanal. Chem.* **1996**, *412* (1−2), 59−66.
(21) Abys, J. A.; Dullaghan, C. A. Electrodeposition of palladium and palladium alloys. In *Modern Electroplating*; Schlesinger, M., Paunovic, M., Eds.; John Wiley & Sons: New York, 2000; pp 483−553.
(22) Rao, C. R. K.; Trivedi, D. C. *Coord. Chem. Rev.* **2005**, *249* (5−6), 613−631.
(23) Anson, F. C. *Anal. Chem.* **1966**, *38* (1), 54−57.

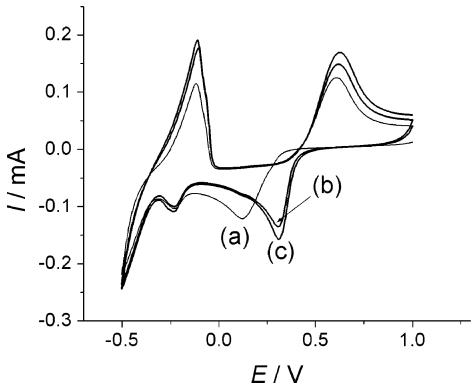

Figure 1. CVs of Pd deposition on a GC surface from a $PdCl_2$ solution in citrate buffer at pH 3: (a) first scan; (b) second scan; (c) third scan. Scan rate 50 mV/s.

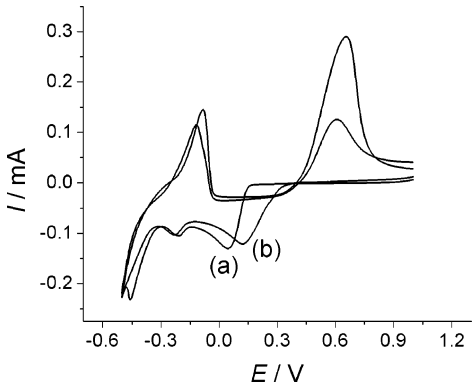

Figure 2. CV (first cyclic scan) of (a) Na_2PdCl_4 and (b) $PdCl_2$ (all conditions as in Figure 1).

scan) and 308 mV (consecutive scans). The cathodic peak at −225 mV is due to the formation of PdH_x[21] followed by a steep current increase as a result of hydrogen evolution at the negative end of the potential window. On the return scan, hydrogen is stripped off at a potential of −110 mV, and finally palladium is dissolved at 620 mV. The positive potential shift of palladium deposition process after the first scan has been observed in all electrolyte systems. It is not a concentration effect, since the deposition potential peak remains constant after the first scan. The behavior can be attributed to a nucleation effect of Pd on GC only present in the first scan. This explanation is supported by the observation of two current crossovers on the positive going scan of the first cycle, only present in the first scan.

3.1. Effect of Pd Source. The electrochemical mechanism of palladium deposition from an acid chloride system has been studied in detail.[24−29] In a chloride solution, various Pd−chloro complexes can exist, and the reduction mechanism assumes the complex dissociates sequentially to form $PdCl_2$. Only $PdCl_2$ is found to be the discharging species:[25]

$$PdCl_4^{2-} \leftrightarrow PdCl_3^{-} \leftrightarrow PdCl_2 + 2e \rightarrow Pd + 2Cl^-$$

Figure 2 shows voltammograms of the deposition from solutions prepared with $PdCl_2$ and Na_2PdCl_4. The Pd deposition peak for the more stable $PdCl_4^-$ complex is shifted by 80 mV to a more negative potential. The difference in peak potential remains constant in consecutive scans. Since interference from hydrogen co-deposition increases with more negative potential, deposition from $PdCl_2$ is thus preferable.

3.2. Effect of pH and Electrolyte. The effect of pH and electrolyte on the deposition potential of Pd was studied by cyclic voltammetry. The peak potentials for the deposition of palladium from $PdCl_2$ in three electrolyte solutions at different pH values are displayed in Table 1.

The Pd complexation ability of nitrate ions is low, even in nitric acid at very low pH values (stability constant, $\log \beta = 1.2$ at pH = 0 in aq nitric acid solution[30]), and the nitrate complexes are much less stable than those with chloride.[31] Therefore, in a pH 2 solution of $PdCl_2$ in nitric acid, Pd is present in the form of its chloro complex and we focus in the following discussion on the effect of acetate and citrate electrolytes only.

Within one sort of electrolyte solution (acetate or citrate), the potential of the deposition peak is shifted in the negative direction with increasing pH. This behavior is explained by the competition between palladium complexation by the ligand L^{n-} (acetate or citrate ion) and protonation of the ligand:

$$Pd^{2+} + nL^{m-} \Leftrightarrow PdL_n^{(mn-)+2}$$

A high proton concentration will decrease the amount of ligand ions free for the complexation of palladium ions:

$$H_mL \Leftrightarrow mH^+ + L^{m-}$$

The protonation of the ligand depends on the proton concentration and on the pK_a value of the ligand itself. The pK_{a1} value for acetic acid is 4.52, while, for citric acid, $pK_{a1} = 2.80$ and $pK_{a2} = 4.08$, indicating a higher concentration of citrate than acetate at the relevant pH values.

Since deposition from the ligand−palladium complex is energetically less favored than that from uncomplexed Pd ions, the peak potential for deposition is shifted in a negative direction with decreasing pH (within the same electrolyte).

On the other hand, hydroxide concentration plays a significant role because of the stability of hydroxo complexes. The stability constant for the reaction

$$Pd^{2+} + 2OH^- \Leftrightarrow Pd(OH)_2$$

is $\log \beta = 25.8$,[32] at pH > 3.

At higher pH values (pH > 3), stable hydroxo complexes of palladium are formed, preventing Pd deposition.

At pH > 3, the Pd deposition is limited by the formation of the stable hydroxides, which compete with the formation of Pd complexes with acetate, citrate, and nitrate, resulting in poor quality of the Pd film.

At pH 2 and 3, the complexing ability of the two ligands (acetate and citrate) listed in Table 1 can be compared. At both

(24) Bell, M. F.; Harrison, J. A. *Electroanal. Chem. Interfacial Electrochem.* **1973**, *41*, 15−25.
(25) Crosby, J. N.; Harrison, J. A.; Whitfield, T. A. *Electrochim. Acta* **1981**, *26* (11), 1647−1651.
(26) Crosby, J. N.; Harrison, J. A.; Whitfield, T. A. *Electrochim. Acta* **1982**, *27* (7), 897−902.
(27) Gimeno, Y.; Creus, A. H.; Carro, P.; Gonzalez, S.; Salvarezza, R. C.; Arvia, A. J. *J. Phys. Chem. B* **2002**, *106* (16), 4232−4244.
(28) Harrison, J. A.; Alcazar, H. B. S.; Thompson, J. *Electroanal. Chem. Interfacial Electrochem.* **1974**, *53*, 145−150.
(29) Harrison, J. A.; Hill, R. P. J.; Thompson, J. *Electroanal. Chem. Interfacial Electrochem.* **1973**, *47*, 431−440.
(30) Jorgensen, C. K.; Parthasarathy, V. *Acta Chem. Scand., Ser. A: Phys. Inorg. Chem.* **1978**, *32* (10), 957−962.
(31) Frias, E. C.; Pitsch, H.; Ly, J.; Poitrenaud, C. *Talanta* **1995**, *42* (11), 1675−1683.
(32) *Stability Constants of Metal-Ion Complexes*, 2nd ed.; Sillén, L. G., Martell, A. E., Eds.; The Chemical Society: London, 1971; p 25.

Table 1. Peak Potentials for Pd Deposition from $PdCl_2$ Using Different Electrolyte Systems and pH Values[a]

electrolyte	pH	Pd deposition peak/V
nitric acid	2	0.338
acetate	2	0.411
acetate	3	0.343
citrate	2	0.322
citrate	3	0.288
citrate	4	0.246
citrate	5	0.207

[a] The scan rate was 50 mV/s, and peak potentials are reported for the second potential cycle.

pH values, the peak potential of Pd deposition from acetate is more positive than that from citrate solution, implying that a less electrochemical driving force is necessary. This might be due to the higher pK_{a1} value of acetic acid in comparison to citric acid, resulting in lower availability of acetate ions for complexation and therefore easier electrochemical deposition from the acetate solution.

Pd was potentiodynamically deposited by cycling the potential between 0.8 and −0.5 V at a scan rate of 25 mV/s 25 times to inspect the structure and morphology of the Pd deposits by SEM. SEM images of the deposition from citrate (pH 2, 3), nitrate (pH 2), and acetate (pH 2, 3) solutions are presented in Figure 3. SEM images for deposition from citrate (pH 4 and 5) reveal a part of uncovered GC (pH 4) and the formation of isolated Pd particles (pH 5). These images are presented in the Supporting Information available for this article. The low solubility of $PdCl_2$ (hydroxide precipitation) in nitric acid at pH ≥ 3 and in acetate at pH ≥ 5 prevents deposition at these pH values. Deposition from pH 2 nitrate (Figure 3c) and pH 3 acetate (Figure 3e) did not give good coverage of the GC electrode with bare parts of the GC exposed to the solution. These media were excluded from further studies. Palladium deposition from pH 2 and 3 citrate buffer and pH 2 acetate buffer resulted in well-covered surfaces, with the pH 3 citrate system delivering the most uniform coverage, as was found by visual examination of the SEM images taken at five different locations of the surface. Therefore, for subsequent studies, the choice was palladium deposition from citrate buffer at pH 3.

3.3. Potentiostatic and Galvanostatic Deposition. Palladium was deposited by applying constant potentials between 300 and −300 mV for 60 s in stirred citrate (pH 3) solutions. As expected, the deposition at positive potentials of 300, 200, and 100 mV, which are near the deposition peak potentials of palladium (see Figure 1), resulted in isolated palladium particles on the GC surface, as shown in Figure 4A. For more negative potentials, the amount of palladium deposited on the electrode increases, improving the surface coverage. At a step potential of −100 mV, the electrode surface is shiny silver. The mirror-like appearance indicates the high reflective power of a smooth palladium layer. In contrast, at more negative potentials, −200 mV and −300 mV, the electrode appears dark and non-shiny. The SEM images reveal a complete coverage of the electrodes but with smaller crystallites in the case of deposition at −100 mV (Figure 4B). A photograph of electrodes modified with a shiny silver and black Pd layer are presented in the Supporting Information.

The finer grain size is due to a slower growth of Pd particles at less negative potentials. The size of the crystallites increases with more negative deposition potentials (see Figure 4C). However, the effect of palladium-catalyzed hydrogen evolution and adsorption has a major effect on the structure of the deposited metal layer. The hydrogen evolution process interferes with palladium deposition and becomes more prominent with decreasing potential. Increased hydrogen evolution and adsorption might inhibit the leveling observed for a deposition potential of −100 mV (leading to a bright surface), and will produce a dark porous palladium coating instead.

The galvanostatic deposition of palladium was performed at current densities of −1.4, −2.8, −4.3, −5.7, and −7.1 mA/cm^2 (equivalent to currents of 100, 200, 300, 400, and 500 μA, respectively, on a 0.071 cm^2 electrode) for 100 s. The visible appearance of the electrode was bright and shiny for the less negative current densities, but became dark and non-reflecting for current densities of −5.7 and −7.1 mA/cm^2. Assuming 100% current efficiency, an even deposition of a compact Pd layer across the electrode surface would result in a deposition thickness between 65 and 327 nm for current densities between −1.4 and −7.1 mA/cm^2. Despite the strong decrease in the current efficiency, mainly due to hydrogen evolution, a complete coverage of the electrode with Pd (the lattice constant of pure palladium is 0.33889 nm) would have been attainable. SEM images using a 30 000× magnification (Figure 5A) reveal a relatively smooth surface for a deposition current density of −1.4 mA/cm^2 (100 s). The image shows an area uncovered by Pd. Such areas are observed in many regions across the electrode and are a result of incomplete coverage and might be introduced by hydrogen evolution, a side reaction already present at low overpotential, or, alternatively, by inhomogeneities of the GC substrate. At more negative current densities (−5.7 and −7.1 mA/cm^2) a change in the morphology is observed (Figure 5B). The Pd layer is rougher and porous, in contrast to the more compact layer deposited at −1.4 mA/cm^2. The change in morphology is due to the increasing influence of hydrogen evolution and co-deposition. However, because of the increased volume of the black Pd deposit, a better coverage of the GC electrode is achieved. This observation is analogous to the behavior for potentiostatic deposition at low and high applied potentials.

Surface roughness can be defined as the difference between the real or microscopic electrode area A_m and the geometrical or projected area A_g,[33] with the roughness factor being $\rho = A_m/A_g$. The microscopic areas of bare GC surfaces and of electrodes modified with palladium deposits were estimated by chronocoulometry in the short time range. The roughness factor measured for individual bare GC electrodes varied between $\rho = 4.4$ and 6.6. The general trend is an increase in the roughness factor ρ of the palladinized electrode with increasing absolute reduction current density, that is, an increase in roughness, as confirmed by the SEM images presented in Figure 5. For a smooth shiny Pd layer deposited at −1.4 mA/cm^2 for 100 s, ρ was estimated by chronocoulometry to be 3.38 ± 0.04, while, for the black Pd layer (−7.1 mA/cm^2), a roughness factor of 56.77 ± 0.16 was estimated. As will be shown, the surface properties of the deposited palladium has an important influence on the integrity of alkanethiol-based SAMs formed on top of the metal.

3.4. SAM Formation on Palladium. The formation and stability of alkanethiol-based SAMs on palladium has been studied by nonelectrochemical methods.[13,14] In this work, the influence of a dodecanethiol SAM formed on palladium on the redox reaction of a species in bulk solution is investigated. The ability to suppress the redox reaction of, for example, potassium hexacyanoferrate, is a measure of the integrity of the SAM. One problem encountered with the electrochemical characterization of the SAM on palladium is the accessible potential window that is limited by hydrogen evolution reaction on the cathodic side

(33) Bard, A. J.; Faulkner, L. R. *Electrochemical Methods: Fundamentals and Applications*, 2nd ed.; John Wiely & Sons: New York, 2001.

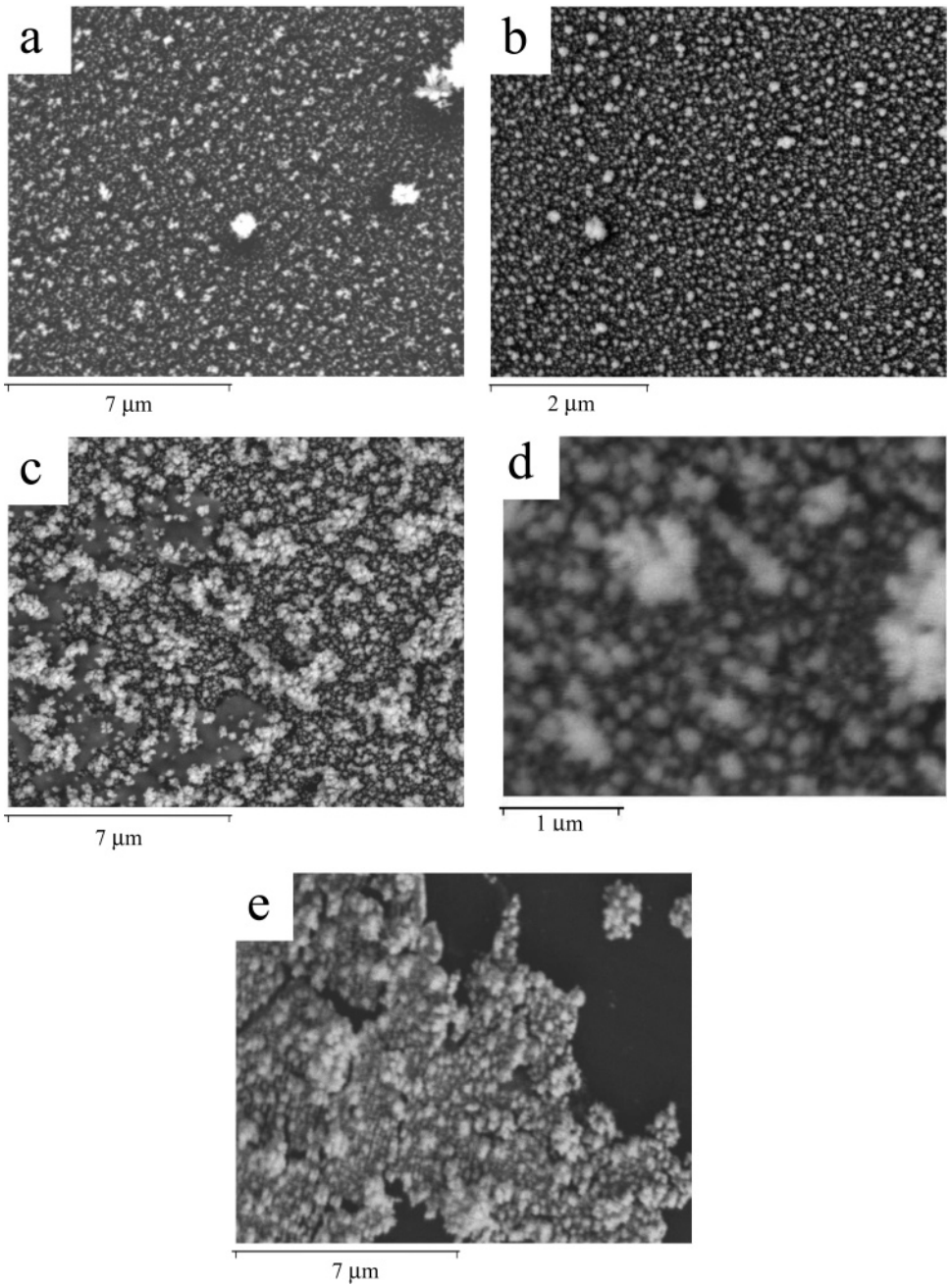

Figure 3. SEM images of palladium deposits on GC electrode by cyclic voltammetry: (a) pH 2 citrate; (b) pH 3 citrate (20 000×); (c) pH 2 HNO_3; (d) pH 2 acetate (50 000×); (e) pH 3 acetate. Magnification is 10 000× except where indicated in parentheses.

and by palladium dissolution on the anodic range. Precisely for this reason, methyl viologen was used as the redox probe instead of the more conventionally used potassium hexacyanoferrate. The electrochemistry of viologen compounds have been extensively studied by electrochemical techniques.[34] Cyclic voltammograms (CVs) showing the redox reaction of methyl viologen at GC electrodes are presented in the Supporting Information. The CV of methyl viologen (MV^{2+}) at GC electrodes exhibits two separated redox waves, which are attributed to the $MV^{2+}/MV^{+\bullet}$ ($E_{1/2} = -0.66$ V) and $MV^{+\bullet}/MV^0$ ($E_{1/2} = -1.02$ V vs Ag/AgCl) couples, respectively. The second redox wave at more negative potential is markedly affected by deposition of the neutral methyl viologen product, MV^0, unlike the first stage, $MV^{2+}/MV^{+\bullet}$, which shows the typical behavior of a reversible electron transfer without any evidence of adsorption, in agreement with other reports.[35,36] Since the first redox stage fell into the accessible potential window of the palladinized electrodes (−0.825 to −0.5V), the $MV^{2+}/MV^{+\bullet}$ redox couple was chosen for probing the integrity of SAMs formed on Pd. It was shown before that SAMs formed on gold electrodes can effectively block the $MV^{2+}/MV^{+\bullet}$ reaction.[37]

Two sets of palladinized electrodes were used for SAMs of *n*-decanethiol. The first set consists of electrodes with a mirror-like palladium surface, produced under galvanostatic (current density −1.4 mA/cm^2 for 100 s) and potentiostatic (applied potential −100mV for 60 s) conditions. The palladium surface of the second set of electrodes had a black and non-reflecting appearance, again produced by constant potential (−300 mV,

(34) Bird, C. L.; Kuhn, A. T. *Chem. Soc. Rev.* **1981**, *10* (1), 49−82.

(35) Engelman, E. E.; Evans, D. H. *Langmuir* **1992**, *8* (6), 1637−1644.
(36) Kaifer, A. E.; Bard, A. J. *J. Phys. Chem.* **1985**, *89* (22), 4876−4880.
(37) Henderson, J. I.; Feng, S.; Ferrence, G. M.; Bein, T.; Kubiak, C. P. *Inorg. Chim. Acta* **1996**, *242* (1−2), 115−124.

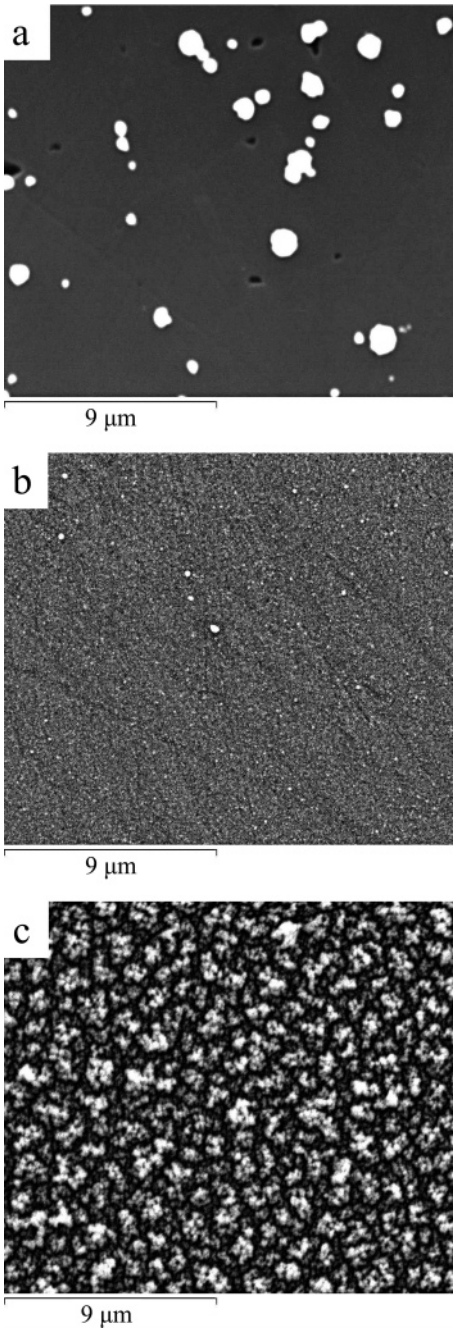

Figure 4. SEM images of palladium deposits on GC for deposition potentials (a) +0.3 V, (b) −0.1 V, and (c) −0.3 V. Magnification 8000×.

60 s) and current (−7.1 mA/cm^2, 100 s) conditions. In all cases, deposition was from a pH 3 citrate solution containing $PdCl_2$.

Examples of CVs for both kinds of electrodes using methyl viologen as a redox probe are presented in Figure 6. The CVs labeled "a" in Figure 6(i)−(iv) are recorded using the palladinized electrodes without SAM, while the CVs labeled "b" were measured with decanethiol SAM-modified Pd surfaces. Optical micrographs of the Pd surfaces are presented as insets in Figure 6(i)−(iv), showing the reflection of a 633 nm laser beam at the electrode surface. The micrographs are taken over an area of 500 × 500 μm^2. Only minor blocking of the methyl viologen redox reaction, manifested in a slight decrease of the peak currents, is observed for the SAMs on shiny palladium surfaces, both generated potentiostatically and galvanostatically. For Figure 6(i), a Pd surface produced at a deposition potential of −100 mV for 60 s was used. The highly reflective surface is characterized

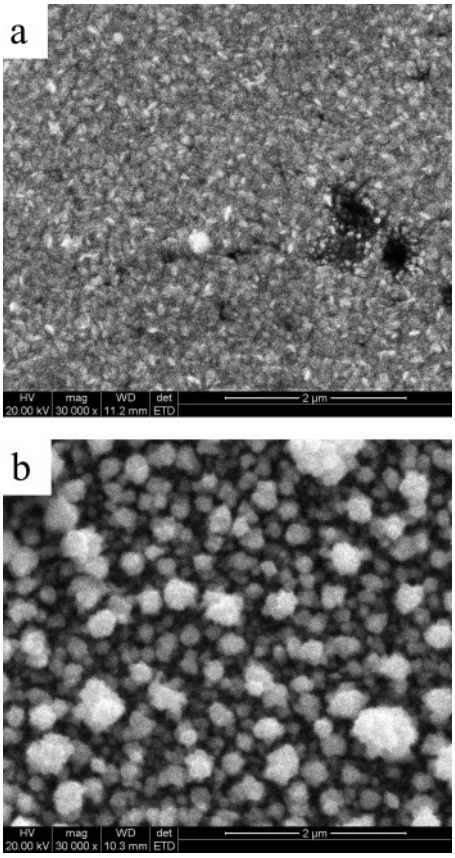

Figure 5. SEM images (magnification 30 000×) of galvanostatically deposited Pd: (a) −1.4 mA/cm^2; (b) −7.1 mA/cm^2. Deposition time 100 s.

by the bright optical micrograph, as shown in the inset of Figure 6(i). Likewise, the galvanostatically deposited Pd film (−1.4 mA/cm^2 for 100 s) shows a similar behavior (Figure 6(iii)). In contrast, monolayers assembled on the black palladium surfaces form a substantial barrier against the redox reaction, as can be seen in Figure 6(ii),(iv). The non-reflecting appearance of the Pd surface is indicated by the black micrographs. Microcracks and microholes in the shiny palladium layer, as shown in the SEM images in Figures 4B and 5A, could be the reason for the lack of blocking, since thiol-based monolayers are not assembled on GC. The redox process of methyl viologen could therefore take place at the microholes, while the *n*-decanethiol monolayer on palladium prevents redox reactions from taking place at the metal surface. This is the situation of a partially blocked electrode. However, from the size and distribution of the microholes, as shown in the SEM images, one would expect a more pronounced change in the shape of the CVs. Therefore we assume that SAM formation on the palladium of the shiny electrodes is highly incomplete, in opposition to the SAM formation on the black, non-reflecting palladium. The different behavior might be attributed to the difference in surface roughness. It is known that the quality of an alkanethiol SAM on gold improves with increasing roughness of the gold surface and the presence of crystal grain boundaries.[38,39] However, a contribution of microcracks in the thin Pd layer, as shown in Figure 5A, to the lack of blocking cannot be ruled out. The increase in roughness and thickness might be the reason that the SAM formation on the non-reflecting palladium leads to a dense blocking layer. To

(38) Creager, S. E.; Hockett, L. A.; Rowe, G. K. *Langmuir* **1992**, *8* (3), 854−861.
(39) Guo, L. H.; Facci, J. S.; McLendon, G.; Mosher, R. *Langmuir* **1994**, *10* (12), 4588−4593.

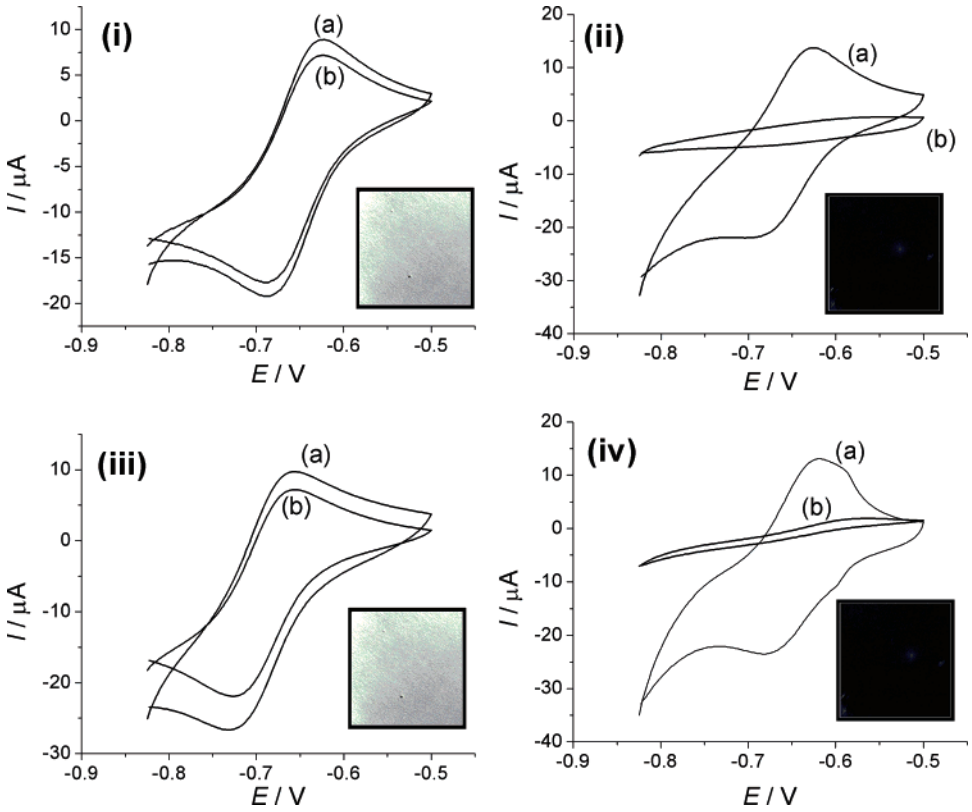

Figure 6. CVs of methyl viologen (3 mM) in 0.1 M aq KCl solution (a) before and (b) after decanethiol SAM formation. Palladium was deposited (i) potentiostatically, applied potential −100 mV (60 s); (ii) potentiostatically, applied potential −300 mV (60 s); (iii) galvanostatically, applied current density −1.4 mA/cm^2 (100 s); and (iv) galvanostatically, applied current density −7.1 mA/cm^2 (100 s). The insets are optical micrographs showing the reflection of a 633 nm laser beam scanned over an area of 500 × 500 μm^2.

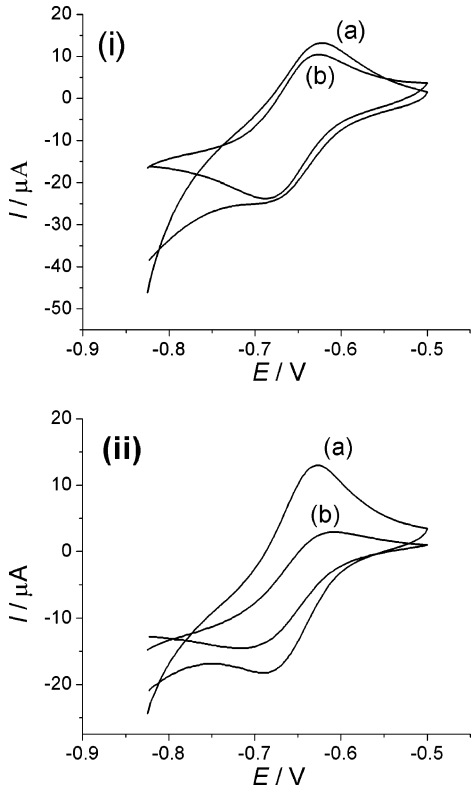

Figure 7. CVs of methyl viologen (3 mM) in 0.1 M aq KCl solution (a) before and (b) after *n*-butanethiol SAM formation. Palladium was deposited at (i) −100 mV and (ii) −300 mV for 60 s.

compare the formation of a SAM with a short- rather than long-chain alkanethiol, butanethiol was used instead of decanethiol, with the same trend being observed as shown in Figure 6. For the voltammograms shown in Figure 7(i),(ii), the Pd substrates were produced with the same conditions as in Figure 6(i),(ii), but decanethiol was replaced by butanethiol. Again, only very minor blocking is observed for the smooth Pd surface, indicated by a 5% decrease in the anodic current peak. Partial blocking can be seen for the rougher surface (Figure 7(ii)), resulting in a 57% decrease in the anodic current peak. As expected, the blocking behavior of butanethiol is not as good as that of decanethiol, since the blocking ability increases with increasing chain length.[1]

4. Conclusion

Selection of experimental conditions for the electrochemical deposition of palladium on GC allows control of the morphology of the palladium surface. This is achieved by the choice of the media (pH and type of electrolyte) from which palladium is deposited. Furthermore, the current density in the case of galvanostatic deposition and the applied potential in the case of potentiostatic deposition contribute to the microscopic structure of the Pd surface. A systematic investigation of theses factors has been performed, using SEM and electrochemical methods. The best surface coverage and the highest roughness was achieved using acetate buffer at pH 2 or citrate buffer at pH 3 and a deposition potential of −0.3 V for 60 s or a current density of −5.7 and −7.1 mA/cm^2 for 100 s. Under these conditions, decanethiol and butanethiol SAMs on the electrodeposited palladium substrate shows substantial blocking with methyl viologen redox reaction and suppresses the hydrogen evolution reaction, indicating the suitability of the substrate to support SAMs. Current efforts are focusing on the use of electrodeposition to create a mixed monolayer of metals, which can subsequently

be used to create a mixed SAM of biocomponent and alkanethiol for biosensing applications.

Acknowledgment. This paper partly describes work undertaken in the context of EC IST project Integrated Microsystem for the Magnetic Isolation and Analysis of Single Circulating Tumour Cells for Oncology Diagnostics and Therapy Follow-Up (MASCOT) FP6-2005-IST-027652. The IST programme is partially funded by the European Commission. Financial support by the SAFE Network of Excellence (LSHB-CT-2004-503243) is also acknowledged.

Supporting Information Available: Pd deposition from citrate solution at pH 4 and 5, electrochemistry of methyl viologen, and a photograph of palladinized GC electrodes. This material is available free of charge via the Internet at http://pubs.acs.org.

LA7006777

UNIVERSITAT ROVIRA I VIRGILI
ELECTROCHEMICALLY DEPOSITED METAL NANOSTRUCTURES FOR APPLICATIONS IN GENOSENSORS
Tesfaye Refera Soreta
ISBN:978-84-692-9758-2/DL:T-206-2010

Supplementary Information

Electrochemically deposited palladium as a substrate for self-assembled monolayers

Tesfaye Refera Soreta, Jorg Strutwolf and Ciara K. O'Sullivan
Nanobiotechnology and Bioanalysis Group, Department of Chemical Engineering, Universitat Rovira I

Pd deposition from citrate solution at pH 4 and 5

The SEM images of Pd deposition from citrate solution at pH>3 reveal incomplete coverage (pH 4) or isolated Pd particles (pH 5), as shown in Figure 1.

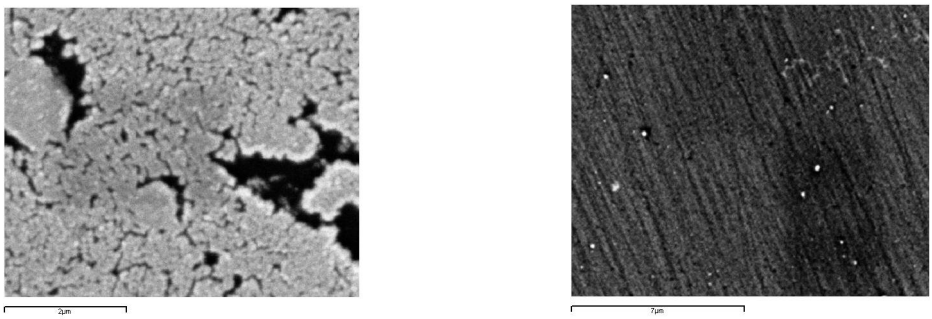

Figure 1: Scanning clectromicroscopy images (magnification 20000×) of palladium deposits on glassy carbon. Electrodes by cyclic voltammetry. Left: Deposition from citrate solution at pH 4. Right: Deposition from citrate solution at pH 5.

Electrochemistry of methylviologen

The CV of methylviologen ion (MV2+) shows two separated redox waves for MV2+ + e $\leftrightarrow$ $MV^{+\cdot}$ and $MV^{+\cdot}$ + e $\leftrightarrow$ MV^0, respectively. The second redox wave at more negative potential is markedly affected by deposition of the neutral methylviologen product, MV^0, as can be seen in Figure 2, unlike the first stage, $MV^{2+}/MV^{+\cdot}$, which shows the typical behaviour of a reversible electron transfer without any evidence of adsorption. For using MV2+ as a probe for the integrity of SAMs on palladium, only this first redox stage was used, since it fells in the accessible potential window. A CV showing the first redox wave is presented in Figure 3, together with the CV of the more familiar $Fe(CN)_6^{3-}/Fe(CN)_6^{2-}$ couple.

ISBN:978-84-692-9758-2/DL:T-206-2010

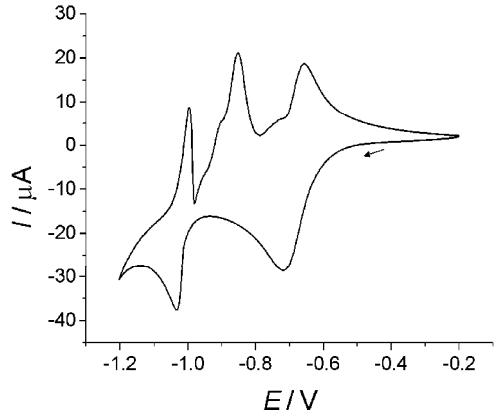

Figure 2: CV of 3mM methylviologen in 0.1M KCl. Scan rate 20mV/s.

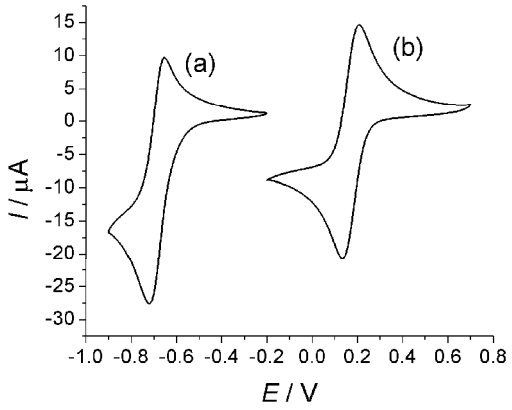

Figure 3: CV of 3mM methylviologen (a) and 3 mM ferrocyanide (b) in 0.1 mM KCl.

Photographs of palladinised glassy carbon electrodes

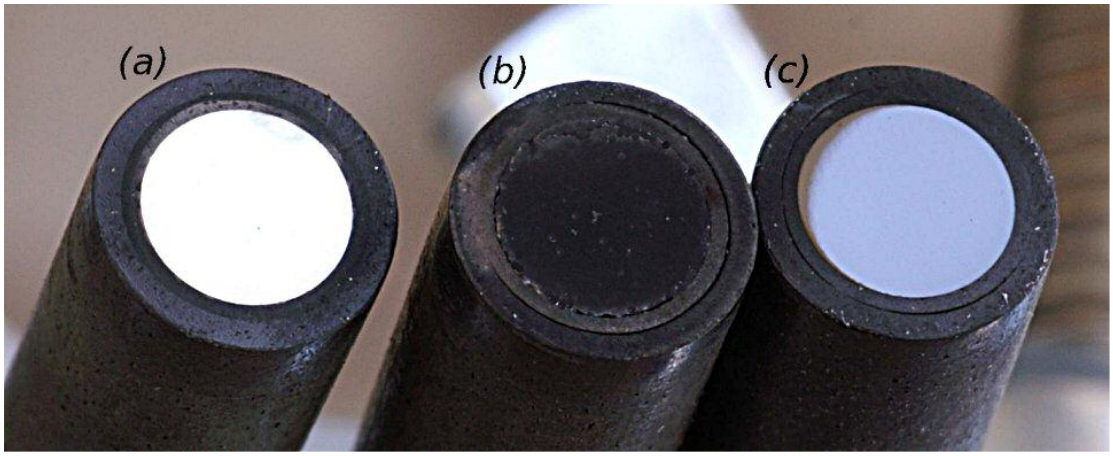

Photographs of the electrodes (diameter 3 mm). (a) shiny Pd layer (current density – 1.4 mA/cm2, 100 s); (b) black Pd layer (-7.1 mA/cm2, 100 s), (c) bare glassy carbon electrode.

UNIVERSITAT ROVIRA I VIRGILI
ELECTROCHEMICALLY DEPOSITED METAL NANOSTRUCTURES FOR APPLICATIONS IN GENOSENSORS
Tesfaye Refera Soreta
ISBN:978-84-692-9758-2/DL:T-206-2010

Chapter 3

Electrochemical Surface Nanopatterning by Selective Reductive Desorption from Mixed Metal Surfaces

UNIVERSITAT ROVIRA I VIRGILI
ELECTROCHEMICALLY DEPOSITED METAL NANOSTRUCTURES FOR APPLICATIONS IN GENOSENSORS
Tesfaye Refera Soreta
ISBN:978-84-692-9758-2/DL:T-206-2010

Electrochimica Acta xxx (2009) xxx–xxx

Contents lists available at ScienceDirect

Electrochimica Acta

journal homepage: www.elsevier.com/locate/electacta

Electrochemical surface nanopatterning by selective reductive desorption from mixed metal surfaces

Tesfaye Refera Soreta[a], Jorg Strutwolf[b], Olivier Y.F. Henry[a,*], Ciara K. O'Sullivan[a,*]

[a] Nanobiotechnology and Bioanalysis Group, Department of Chemical Engineering, Universitat Rovira I Virgiili, Avinguda Paisos Catalans, 26, 43007 Tarragona, Spain
[b] Tyndall National Institute, Lee Maltings, Cork, Ireland

ARTICLE INFO

Article history:
Received 15 October 2008
Received in revised form 12 February 2009
Accepted 28 February 2009
Available online xxx

Keywords:
Mixed metal
Selective desorption
Biosensor
Catalysis
Surface patterning
SAM

ABSTRACT

We report on a novel strategy to the functionalisation of electrode surfaces based on the preparation and patterning of mixed metal electrodes using metal selective electrodesorption of a sacrificial alkanethiol. Plain palladium (Pd) and plain polycrystalline gold (poly-Au) electrodes were used initially to determine metal specific potential windows within which electrodesorption of the short alkanethiol mercaptoethanol could be achieved. We found that stripping of mercaptoethanol from gold was achieved at potentials lower than −0.800 V, whilst stripping from palladium was achieved at more positive potentials i.e. around −0.650 V. Mixed metal electrodes were prepared by electroplating for short period of times palladium onto poly-Au electrodes. The resulting surfaces were characterised electrochemically in 1 M H_2SO_4 and clearly exhibited reduction peaks for both gold and palladium oxide formation. The mixed metal electrodes were coated with mercaptoethanol, which was further selectively removed from Pd by cyclic voltammetry in NaOH in the Pd-specific potential window. The presence of bare Pd domains revealed following electrodesorption was confirmed by subsequently adsorbing the electroactive alkanethiol 6-ferrocenylhexanethiol onto the freshly revealed Pd. Cyclic voltamogramms exhibited sharp redox peaks that could only be attributed to the successful immobilisation of 6-ferrocenylhexanethiol onto fresh Pd domains. Control surfaces, i.e. MCE fully coated Pd/Poly-Au electrode, exposed to 6-ferrocenylhexanethiol did not exhibit significant voltammetric features, attesting to the efficient patterning of the mixed metal electrode by employing metal specific reductive desorption of short alkanethiols. The possibility to pattern electrode surfaces in such way will find application in the field of diagnostics, and also in heterogeneous catalysis where Pd–Au alloys have received an increased interest in the recent years.

1. Introduction

Fine chemical structuring of electrode surfaces is typically achieved by the formation of self-assembled monolayers (SAM) of alkanethiols [1–4] or alkanesilanes [5,6] of varying chemical functionality. Chemical and biochemical diagnostics have largely benefited from the latest advances made in the field and bi-functional surfaces have now become a pre-requisite to favour the recognition of a targeted compound and enhance recognition efficiency [7,8] while excluding a range of undesired interferents from interacting with the surface [9,10]. Chemisorption from a mixture of alkanethiols in solution and the resulting self-assembled monolayer is reported as a practical approach for the realisation of such surfaces where ordering and distribution of the functional chemical head groups at the surface is controlled by the ratio of one component to the other and consequently by the thermodynamic equilibrium existing between the two species at the liquid–solid interface [11,12]. Although practical and facile to implement, such an approach inherently suffers from a lack of control over the surface arrangement, lack of stability and consequently large surface-to-surface irreproducibility [13,14].

On the other hand, direct physical surface patterning of sensor surfaces could remedy issues associated with the tight control required over these processes. By tuning either surface morphology (e.g. polycrystallinity, nanoelectrode bundles [15–18]) or composition during fabrication (e.g. mixed metal, alloy electrodes [19–21]), one can expect to reliably introduce mixed functionality at surfaces based on the inherent characteristics of the base transducer. As such, the quality of functionalisation (i.e. homogeneity of distribution and spacing of functional head groups) and therefore sensor-to-sensor repeatability could be greatly improved.

Of particular interest, the use of mixed metal surface could be employed to disperse functionality on surfaces based on the surface distribution of the metals. By carefully selecting the metals based on their catalytic and electrochemical characteristics, patterning based on the selective reductive desorption of short alkanethiols from one metal preferably than from another can be envisaged.

* Corresponding authors.
E-mail addresses: olivier.henry@urv.cat (O.Y.F. Henry), ciara.osullivan@urv.cat (C.K. O'Sullivan).

0013-4686/$ – see front matter © 2009 Published by Elsevier Ltd.
doi:10.1016/j.electacta.2009.02.101

The developed approach could be exploited for the construction of reproducible biosensor surfaces, particularly DNA sensors, where the state of the art in formation of mixed self-assembled monolayers is based on the chemisorption of alkanethiols. However, this is a thermodynamically driven process where small changes in, for example, length of chemisorption, concentration of alkanethiols used, temperature etc., can have a large effect on the make up of the mixed self-assembled monolayer formed and has a large impact on reproducibility, for example in DNA sensors, where a mixed SAM of DNA probe and short chain alkanethiol is frequently used. The approach reported here details the formation of self-assembled monolayers that can be controlled by the substrate material used. Thus, highly reproducibly patterned surfaces can be produced, and the mixed SAMs formed on these surfaces (for example forming a mixed SAM of a short chain alkanethiol, which could be selectively desorbed from Pd, and a DNA probe adsorbed), would be much more reproducible that those obtained via thermodynamically driven approaches, leading to more reproducible DNA detection using biosensors fabricated using this approach.

Here we report on a novel strategy to the functionalisation of electrode surfaces based on the exploitation of the electrochemical properties of bi-metallic electrode of palladium (Pd) and gold (Au) to prepare mixed-functionality sensor surfaces. After initially finding that we could selectively desorb the short alkanethiol mercaptoethanol (MCE) from Au electrodes and from Pd electrodes via electrochemical reduction using metal specific potential windows, we realised we could use Au/Pd electrodes to control the lateral distribution of chemical functionalities at the surface. Although our prime interest in the development of such surfaces lies in their application in the field of medical diagnostics for DNA sensing, the realisation of functional Pd/Au electrode is also attractive for heterogeneous catalysis where Pd/Au alloys have seen an increased interest in the recent years [20,22–24].

2. Experimental

2.1. Materials

Palladium dichloride ($PdCl_2$, 99.9%, Aldrich), sodium perchlorate ($NaClO_4$, 98%, Sigma), sulphuric acid (H_2SO_4, 95% v/v, Scharlau), sodium hydroxide (NaOH, 98% Scharlau), pH 2 citrate buffer (consisting of 0.03 M citric acid, 0.0082 M HCl, 0.061 M NaCl, Fluka) and ethanol (96% v/v, Scharlau) were used as received. The alkanethiol 2-mercaptoethanol (MCE, 99%) was obtained from Scharlau and 6-ferrocenylhexanethiol from Aldrich.

2.2. Methods

2.2.1. Electrode preparation

Polycrystalline gold (Poly-Au) electrodes from CH Instruments (US) and glassy carbon rods 3 mm in diameter (GCE) from Sigradur® (HTW, Germany) were mechanically polished with varying particle sizes (6 μm to 0.05 μm) of polishing suspensions (BUEHLER Metadi Supreme) on BAS polishing cloth. The electrodes were sonicated in water and further cleaned electrochemically. Poly-Au electrodes were subjected to wide potential scans between 0 V and 1.6 V at 50 mV s^{-1} in 1 M H_2SO_4 until a reproducible gold oxide stripping peak was obtained. GCE were conditioned by potential scanning from 0 V to 1.2 V in 1 M $NaClO_4$ for at least five complete scans at 50 mV s^{-1}. The prepared electrodes were used immediately after mechanical polishing and electrochemical cleaning.

2.2.2. Metal deposition

Palladium electrodes were prepared by potentiostatic deposition of $PdCl_2$ on cleaned GCEs. A constant potential of −0.3 V was applied for 1 min in a Pd deposition bath consisting of 7.5 mM $PdCl_2$ in citrate buffer. To prepare the deposition bath, 133 mg of $PdCl_2$ was added to 100 mL of pH 2 citrate buffer and sonicated for 15 min. The solution was further homogenised by shaking and left overnight in the dark after which period a clear solution was obtained. Finally, the pH of the solution was adjusted to 3 by addition of diluted NaOH. Mixed metal electrodes were prepared by shorter deposition time (1 or 5 s) of Pd on poly-Au electrodes 1.6 mm in diameter from the same Pd deposition bath [25].

2.2.3. Formation of self-assembled monolayers of alkanethiols

Mercaptoethanol (MCE) and 6-ferrocenylhexanethiol were dissolved in ethanol to a final concentration of 2 mM. The electrodes were exposed to 50 μL of the alkanethiol solutions and the formation of self-assembled monolayers allowed proceeding for at least 2 h in the case of mercaptoethanol, and 30 min in the case of 6-ferrocenylhexanethiol.

2.2.4. Electrochemical measurements

Cyclic voltammetry and potential step experiments were carried out using an Autolab model PGSTAT 12 potentiostat/galvanostat controlled with the General Purpose Electrochemical system (GPES) software (EcoChemie B.V., The Netherlands). A three-electrode set-up was adopted comprising of gold electrodes as working electrodes, and a platinum wire (BAS model MW-1032) and an Ag/AgCl (3 M NaCl) electrode as counter and reference electrodes respectively. All potentials were reported with respect to this reference electrode. The reductive desorption of SAM of MCE from poly-Au, Pd and poly-Au/Pd electrodes was realised in 0.5 M NaOH, under argon saturated atmosphere for 10 potential cycles within the studied window (either −0.2 to −1.1 V or −0.2 to −0.675 V) at a scan rate of 20 mV s^{-1}.

3. Results and discussion

3.1. Elucidation of metal specific potential windows for reductive desorption of MCE at Pd and poly-Au electrode

The potential window necessary to desorb MCE from each surface was initially elucidated by working on Au or Pd electrodes separately. Presented in Fig. 1(A), the reductive desorption of MCE from poly-gold surfaces was realised by repeatedly scanning the potential window −0.2 V to −1.1 V.

The first reductive scan exhibits two desorption peaks for the desorption of MCE, present at −0.834 V and −0.947 V (vs. Ag/AgCl), which progressively disappear in subsequent scans. This behaviour is consistent with the selective desorption from a poly-Au surface [15,26–29], where low index crystalline planes exhibit very narrow thiol reductive desorption potential windows.

The same experiment on Pd surface did not produce any clear desorption peaks. Due to the highly active hydrogen reduction taking place at potentials below −0.8 V no defined peaks could be measured. Thus, we determined the reductive desorption in an indirect manner, where the adsorption of the electroactive thiol 6-ferrocenylhexanethiol onto the palladium surface indicated that the alkanethiol previously adsorbed onto this surface had been desorbed. As shown in the voltammograms presented in Fig. 2 (2), the redox peaks attributed to the presence of ferrocene moieties due to the successful immobilisation of a monolayer of 6-ferrocenylhexanethiol on the palladium electrode from which a layer of MCE had been freshly electrochemically desorbed were observed.

The peak-to-peak separation of immobilised ferrocene on the freshly revealed Pd was 12.2 mV suggesting a non-diffusion limited redox process, the consequence of successfully surface immobilised ferrocene moieties [30,31]. Control experiments, where thiolated

Please cite this article in press as: T. Refera Soreta, et al., Electrochemical surface nanopatterning by selective reductive desorption from mixed metal surfaces, Electrochim. Acta (2009), doi:10.1016/j.electacta.2009.02.101

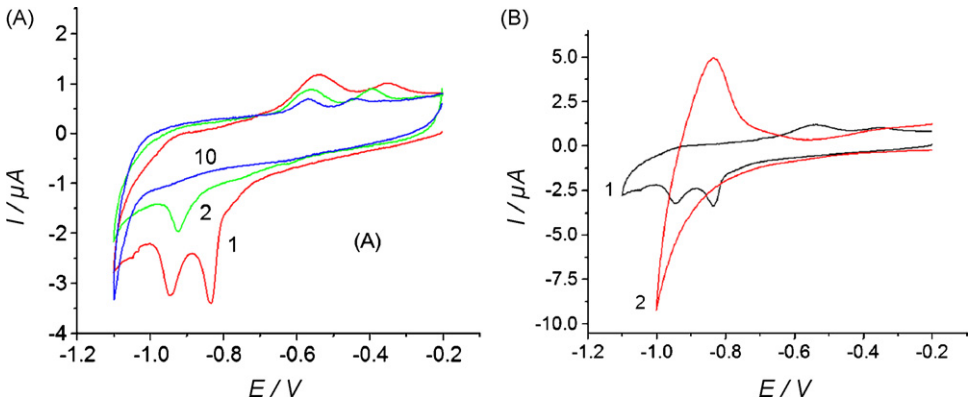

Fig. 1. Reductive desorption of MCE in 0.5 M NaOH from (A) gold surfaces following 1, 2 and 10 scans, and (B) from palladium surfaces (2) and gold (1).

ferrocene was immobilised on MCE coated electrodes and no desorption step was used, did not produce notable current values, although some ferrocene was immobilised following the surface displacement and rearrangement of the monolayer. Rapid exchange near defect points of SAMs and comparatively slow substitution of adsorbates within the crystalline domains are well known and have been widely reported [31–35].

Monitoring the current profile of Pd surface more closely, we found we could efficiently desorb MCE in the potential window −0.2 V to −0.675 V, which corresponds to an area of the polycrystalline Au potential window where no thiol reduction process can occur. These findings facilitated the realisation of metal-selective reductive desorption of short alkanethiols from Au/Pd electrodes and nanostructuring of the spatial distribution of the surface functionality based on the nature of the electrodes and not on a thermodynamically limited process such as chemisorption.

3.2. Electrochemical characterisation of mixed metal electrodes

We prepared Au/Pd electrodes by potentiostatically depositing Pd on plain gold electrodes. Deposition of Pd was realised at 0 V and the time of the deposition varied from 1 to 5 s (Fig. 3).

The resulting surfaces were characterised electrochemically in 1 M H_2SO_4 and the voltammograms are overlayed in Fig. 4. The deposition of Pd on Au is confirmed by the presence of the Pd oxide formation at 0.900 V and subsequent reduction at 0.491 V for 1 s deposition and 0.422 V for 5 s deposition, while the formation and reduction of gold oxide is present at 1.200 V and 0.908 V for 1 s deposition and 0.918 V for 5 s deposition respectively.

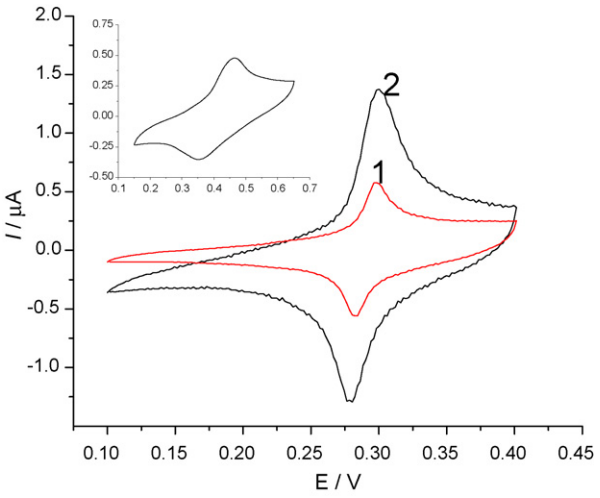

Fig. 3. Cyclic voltammetry in 1 M $NaClO_4$ of 6-ferrocenylhexanethiol immobilised on gold electrode (1) on which palladium deposited for 1 s (2) palladium deposited for 5 s. Inset: on bare gold electrode.

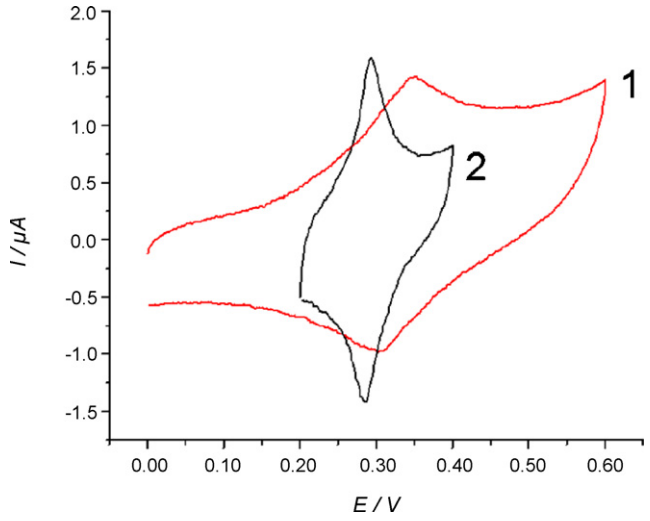

Fig. 2. Cyclic voltammetry in 0.1 M $NaClO_4$ of 6-ferrocenylhexanethiol immobilised on freshly desorbed MCE coated (1) gold and (2) palladium electrodes.

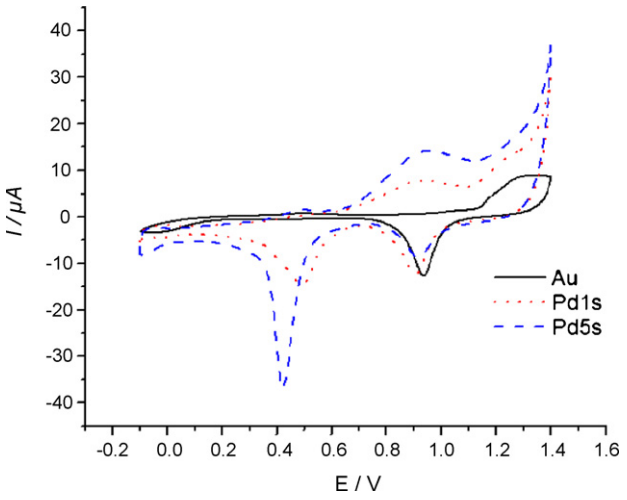

Fig. 4. Cyclic voltammetry of Au, and Au/Pd electrodes following variations in the deposition time of Pd in 1 M H_2SO_4.

Please cite this article in press as: T. Refera Soreta, et al., Electrochemical surface nanopatterning by selective reductive desorption from mixed metal surfaces, Electrochim. Acta (2009), doi:10.1016/j.electacta.2009.02.101

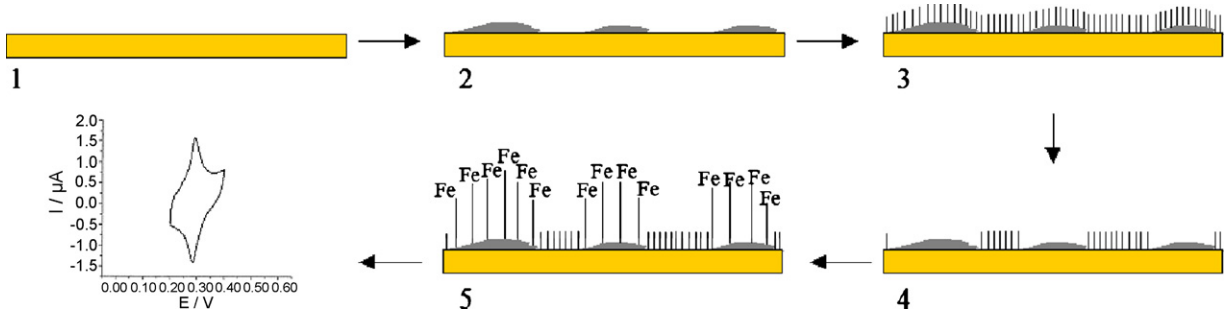

Fig. 5. Schematic of mixed metal electrode functionalisation (1, 2: partial electroplating of Pd on poly-Au electrode; 3: electrode surface blocking with MCE; 4: selective reductive desorption from Pd domains; 5: immobilisation of 6-ferrocenylhexanethiol on the bare Pd and resulting voltammetry).

The measured charges for the reduction of gold and palladium oxide and the corresponding area occupied by each metal are summarised for each electrodes in Table 1.

Interestingly, the amount of gold oxide formed at Au/Pd deposited for 1 s did not vary significantly from non palladium deposited poly-Au electrodes. Longer Pd deposition times did, however, affect the gold oxide formation more noticeably, attributable to the reduced gold active surface area. Finally, the total electrode surface area was considerably increased by factors of 2.18 and 2.83 following the deposition of Pd for 1 and 5 s respectively. As such, using short deposition times, we were able to control the surface ratio of gold to palladium, while avoiding a full coverage of the electrode with Pd. Longer deposition times and lower deposition potential have shown to very rapidly cover entirely gold substrates [24,36]. The deposition process was highly reproducible as was ascertained by monitoring the mass and thickness of palladium deposited on three separate electrodes, for each of 1 s and 5 s deposition times. The mass and thickness obtained was 2.15 μg/cm^2, (RSD = 2.83%, n = 3) and 1.79 nm (RSD = 2.79%, n = 3) for 1 s deposition, and 12.596 μg/cm^2 (RSD = 3.22%, n = 3) and 10.48 nm (RSD = 3.21%, n = 3) for 5 s deposition.

3.3. Metal selective electrochemical patterning of mixed metal electrodes

Finally, in order to assess the functionality of the mixed metal surfaces created, all three electrode types were subjected to the surface derivatisation steps depicted schematically in Fig. 5. The electrodes were coated with a monolayer of MCE (Fig. 5, step 1 to 3) and the selective reductive desorption from Pd domains only was attempted by cycling repeatedly in the potential window −0.2 V to −0.675 V previously elucidated (Fig. 5, step 4). Following this treatment, the mixed metal surface, with the MCE now desorbed selectively from the palladium domains only, was additionally exposed to a solution of 6-ferrocenylhexanethiol, expected to preferably anchor at free Pd regions, rather than MCE-occupied poly-Au (Fig. 5, step 5).

The successful immobilisation of 6-ferrocenylhexanethiol on Pd domains was assessed by cyclic voltammetry. The resulting voltamogramms are presented in Fig. 6. The presence of ferrocene

Table 1
Current intensity recorded for the reduction of gold and palladium oxide and estimated surface area for a polycrystalline gold electrode (poly-Au) and for polycrystalline gold electrodes partially covered with Pd deposited for 1 s or for 5 s.

Electrodes	Oxide reduction peak (μC)		Surface area (cm^2)	
	Au	Pd	Au	Pd
Poly-Au	30.74	–	0.077	–
Poly-Au/Pd 1 s	27.22	42.54	0.068	0.10
Poly-Au/Pd 5 s	18.92	72.59	0.047	0.171

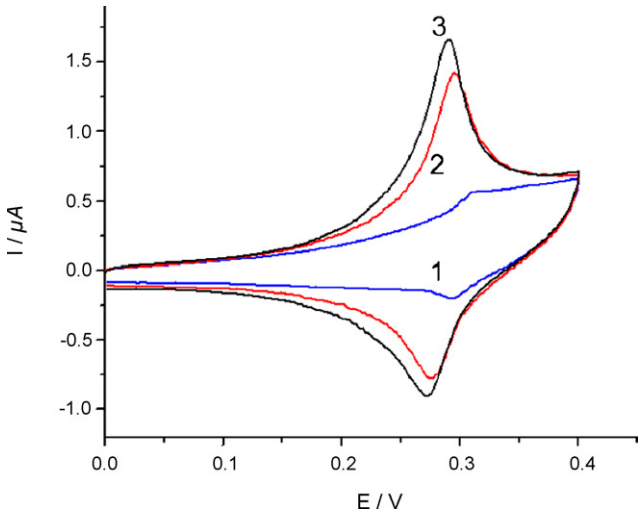

Fig. 6. Voltammetric responses for electrode initially coated with a monolayer of MCE, later subjected to selective reductive desorption, and finally exposed to ferrocene alkanethiols: (1) gold electrode, (2) Au/Pd deposited for 1 s and (3) Au/Pd deposited for 5 s.

moieties on Pd coated electrodes can be clearly seen from the pronounced ferrocene redox peaks, while very little signal can be recorded at the plain poly-Au electrode which followed the same treatment. Peak-to-peak separations were 26.3 mV, 19.1 mV and 19.7 mV for plain Au electrode, poly-Au/Pd 1 s and poly-Au/Pd 5 s electrode respectively. The plain poly-Au electrode served as a control to confirm that the peaks we observed could truly be attributed to the selective desorption of the MCE from palladium followed by immobilisation of 6-ferrocenylhexanethiol.

During the reductive desorption step performed in the potential window −0.2 V/−0.675 V, no peaks that could be attributed to the reductive desorption of MCE from the gold surface were observed, thus confirming that no MCE had been stripped from the gold surface. Following immersion in 6-ferrocenylhexanethiol, a small redox peak could be observed, most likely due to a small degree of displacement of the adsorbed mercaptoethanol at the boundary of defect points as previously explained in Section 3.1. The insignificance of the signals in comparison to those observed for both poly-Au/Pd 1 s and 5 s surfaces demonstrated the feasibility to employ such scheme to rationally design the chemical functionality of a solid–liquid interface.

4. Conclusions

In conclusion, we presented a rational approach to the formation of bi-functional surfaces via a metal-selective reductive process employing an initial sacrificial SAM layer of MCE. The spatial

Please cite this article in press as: T. Refera Soreta, et al., Electrochemical surface nanopatterning by selective reductive desorption from mixed metal surfaces, Electrochim. Acta (2009), doi:10.1016/j.electacta.2009.02.101

distribution of the surface functionality is therefore not controlled by a thermodynamically limited process such as chemisorption of alkanethiols, but rather takes advantage of the metal distribution at the surface. Such distribution is inherent to the material used and could be controlled during the fabrication process. The approach presented here may find particular application in the field of biosensors where surface-to-surface reproducibility is crucial to ensure a reliable performance and repeatability of the measurements, but also in heterogeneous catalysis.

Acknowledgements

This work has been carried out as part of the Commission of the European communities ICT project Integrated Microsystem for the magnetic isolation and Analysis of Single circulating tumour Cells for Oncology diagnostics and Therapy follow-up, MASCOT, FP6-2004-IST-026752.

References

[1] R.G. Nuzzo, D.L. Allara, J. Am. Chem. Soc. 105 (1983) 4481.
[2] H. O. Finklea (Ed.), Electrochemistry of organized monolayers of thiols and related molecules on electrodes (Electroanalytical Chemistry: a Series of Advances), 1996, p. 109.
[3] J.C. Love, L.A. Estroff, J.K. Kriebel, R.G. Nuzzo, G.M. Whitesides, Chem. Rev. 105 (2005) 1103.
[4] A. Ulman, Chem. Rev. 96 (1996) 1533.
[5] Z.H. Jin, D.V. Vezenov, Y.W. Lee, J.E. Zull, C.N. Sukenik, R.F. Savinell, Langmuir 10 (1994) 2662.
[6] H.O. Finklea, L.R. Robinson, A. Blackburn, B. Richter, D. Allara, T. Bright, Langmuir 2 (1986) 239.
[7] R.J. White, N. Phares, A.A. Lubin, Y. Xiao, K.W. Plaxco, Langmuir 24 (2008) 10513.
[8] M. Satjapipat, R. Sanedrin, F. Zhou, Langmuir 17 (2001) 7637.
[9] T.M. Herne, M.J. Tarlov, J. Am. Chem. Soc. 119 (1997) 8916.
[10] D.D. Schlereth, R.P.H. Kooyman, J. Electroanal. Chem. 444 (1998) 231.
[11] S. Peeters, T. Stakenborg, G. Reekmans, W. Laureyn, L. Lagae, A. Van Aerschot, M. Van Ranst, Biosens. Bioelectronics 24 (2008) 72.
[12] C. Boozer, S.F. Chen, S.Y. Jiang, Langmuir 22 (2006) 4694.
[13] K. Shimazu, Y. Hashimoto, T. Kawaguchi, K. Tada, J. Electroanal. Chem. 534 (2002) 163.
[14] M. Nishizawa, T. Sunagawa, H. Yoneyama, J. Electroanal. Chem. 436 (1997) 213.
[15] J. Strutwolf, C.K. O'Sullivan, Electroanalysis 19 (2007) 1467.
[16] I. Vlassiouk, P. Takmakov, S. Smirnov, Langmuir 21 (2005) 4776.
[17] V.P. Menon, C.R. Martin, Anal. Chem. 67 (1995) 1920.
[18] H. Masuda, K. Fukuda, Science 268 (1995) 1466.
[19] Y. Gimeno, A. HernandezCreus, P. Carro, S. Gonzalez, R.C. Salvarezza, A.J. Arvia, J. Phys. Chem. B 106 (2002) 4232.
[20] G.J. Hutchings, Chem. Commun. (2008) 1148.
[21] J.S. Mayell, W.A. Barber, J. Electrochem. Soc. 116 (1969) 1333.
[22] P. Han, S. Axnanda, I. Lyubinetsky, D.W. Goodman, J. Am. Chem. Soc. 129 (2007) 14355.
[23] C.W. Yi, K. Luo, T. Wei, D.W. Goodman, J. Phys. Chem. B 109 (2005) 18535.
[24] F. Maroun, F. Ozanam, O.M. Magnussen, R.J. Behm, Science 293 (2001) 1811.
[25] T.R. Soreta, J. Strutwolf, C.K. O'Sullivan, Langmuir 23 (2007) 10823.
[26] T. Oyama, T. Okajima, T. Ohsaka, J. Electrochem. Soc. 154 (2007) D322.
[27] R. Madueno, J.M. Sevilla, T. Pineda, A.J. Roman, M. Blazquez, J. Electroanal. Chem. 506 (2001) 92.
[28] R.T. Carvalhal, R.S. Freire, L.T. Kubota, Electroanalysis 17 (2005) 1251.
[29] K. Arihara, T. Ariga, N. Takashima, T. Okajima, F. Kitamura, K. Tokuda, T. Ohsaka, Phys. Chem. Chem. Phys. 5 (2003) 3758.
[30] T.R. Soreta, J. Strutwolf, C.K. O'Sullivan, ChemPhysChem 9 (2008) 920.
[31] C.E.D. Chidsey, C.R. Bertozzi, T.M. Putvinski, A.M. Mujsce, J. Am. Chem. Soc. 112 (1990) 4301.
[32] D.M. Collard, M.A. Fox, Langmuir 7 (1991) 1192.
[33] E. Cooper, G.J. Leggett, Langmuir 15 (1999) 1024.
[34] T. Kakiuchi, K. Sato, M. Iida, D. Hobara, S. Imabayashi, K. Niki, Langmuir 16 (2000) 7238.
[35] G.G. Baralia, A.S. Duwez, B. Nysten, A.M. Jonas, Langmuir 21 (2005) 6825.
[36] J. Tang, M. Petri, L.A. Kibler, D.M. Kolb, Electrochimica Acta 51 (2005) 125.

Please cite this article in press as: T. Refera Soreta, et al., Electrochemical surface nanopatterning by selective reductive desorption from mixed metal surfaces, Electrochim. Acta (2009), doi:10.1016/j.electacta.2009.02.101

UNIVERSITAT ROVIRA I VIRGILI
ELECTROCHEMICALLY DEPOSITED METAL NANOSTRUCTURES FOR APPLICATIONS IN GENOSENSORS
Tesfaye Refera Soreta
ISBN:978-84-692-9758-2/DL:T-206-2010

UNIVERSITAT ROVIRA I VIRGILI
ELECTROCHEMICALLY DEPOSITED METAL NANOSTRUCTURES FOR APPLICATIONS IN GENOSENSORS
Tesfaye Refera Soreta
ISBN:978-84-692-9758-2/DL:T-206-2010

Chapter 4

Electrochemical Fabrication of Nanostructured Surfaces for Enhanced Response

UNIVERSITAT ROVIRA I VIRGILI
ELECTROCHEMICALLY DEPOSITED METAL NANOSTRUCTURES FOR APPLICATIONS IN GENOSENSORS
Tesfaye Refera Soreta
ISBN:978-84-692-9758-2/DL:T-206-2010

CHEMPHYSCHEM

DOI: 10.1002/cphc.200700793

Electrochemical Fabrication of Nanostructured Surfaces for Enhanced Response

Tesfaye Refera Soreta,[a] Jörg Strutwolf,*[a] and Ciara K. O'Sullivan*[a, b]

The objective of this work is to explore approaches to enhance electrochemical signals through sequential deposition and capping of gold particles. Gold nanoparticles are electrodeposited from $KAuCl_4$ solution under potentiostatic conditions on glassy carbon substrates. The number density of the nanoparticles is increased by multiple deposition steps. To prevent secondary nucleation processes, the nanoparticles are isolated after each potentiostatic deposition step by self-assembled monolayers (SAMs) of decanethiol or mercaptoethanol. The increasing number of particles during five deposition/protection rounds is monitored by assembling electroactive SAMs using a ferrocene-labeled alkanethiol. A precise estimation of the surface area of the gold nanoparticles by formation of an oxide layer on gold is difficult due to oxidation of the glassy carbon surface. As an alternative approach, the charge flow of the electroactive SAM is used for surface measurement of the gold surface area. A sixfold increase in the redox signal in comparison to a bulk gold surface is observed, and this increase in redox signal is particularly notable given that the surface area of the deposited nanoparticles is only a fraction of the bulk gold surface. After five rounds of deposition there is a gold loading of 1.94 $\mu g\,cm^{-2}$ of the deposited nanoparticles as compared to 23.68 $\mu g\,cm^{-2}$ for the bulk gold surface. Remarkably, however, the surface coverage of the ferrocene alkanethiol on the bulk material is only 10% of that achieved on the deposited nanoparticles. This enhancement in signal of the nanoparticle-modified surface in comparison to bulk gold is thus demonstrated not to be attributable to an increase in surface area, but rather to the inherent properties of the surface atoms of the nanoparticles, which are more reactive than the surface atoms of the bulk material.

Introduction

A major influence on electrode development over the last decade has been the progress in nanotechnology. The application of metal nanoparticles in electroanalytical and bioanalytical science has been a subject of continuously growing interest, as documented in recent reviews.[1–6] Nanoparticles have also had an important impact on electrocatalysis research,[1,7–11] for example, gold nanoparticles show excellent catalytic properties towards the electrochemical reduction of molecular oxygen[12–14] and towards the low-temperature oxidation of CO.[11,15] The electrocatalytic effect of gold nanoparticles on ascorbic acid oxidation allows the selective electrochemical analysis of dopamine and ascorbic acid[16,17] coexisting in biological liquids, whereas using conventional (bulk) Au electrodes, the oxidation waves of ascorbic acid have almost the same potential, which results in poor selectivity and reproducibility. The use of gold nanoparticles as labels has also been reported for electrochemical genosensors.[18,19] The technological prospects of the application of gold nanoparticle-based materials are a major motivation for the development and fabrication of nanoparticles with predetermined dimensions. Thus, substantial effort has been devoted to the preparation of size- and shape-controlled nanoparticles, particularly of metal nanoparticles for electroanalytical applications.[6,20]

One of the main reasons that nanomaterials show properties different from those of the bulk material is the size effect: atoms at the surface have lower coordination numbers and are therefore less stable than bulk atoms. The smaller a particle, the larger the fraction of atoms at the surface, and thus the more reactive is the surface, which makes nanosized materials of immense interest as substrates for biosensor applications.

Electrochemical deposition is a rapid and easy procedure for the production of nanoparticles on conducting surfaces, and many reports have been devoted to the electrodeposition of Au onto glassy carbon (GC).[17,21–26] The composite surface of GC modified with gold nanoparticles offers the possibility of further site-selective modification, as GC has no affinity towards thiol or disulfide groups in contrast to gold, on which thiol-based self-assembled monolayers (SAMs) are readily formed. Thus, it is possible to protect or selectively functionalize spots on an overall conducting surface. Finot et al.[24] used a SAM of octadecanethiol (ODT) to protect deposited Au nanocrystallites after the deposition step on GC electrodes. New gold nanoparticles were then electrodeposited from an aqueous $KAuCl_4$ solution without causing crystal growth of the par-

[a] *T. Refera Soreta, Dr. J. Strutwolf,[+] Dr. C. K. O'Sullivan*
Nanobiotechnology & Bioanalysis Group
Departament d'Enginyeria Quimica
Universitat Rovira i Virgili, 43007 Tarragona (Spain)
Fax: (+34) 977 559621
E-mail: ciara.osullivan@urv.cat

[b] *Dr. C. K. O'Sullivan*
Institució Catalana de Recerca i Estudis Avançats
Passeig Lluis Campanys 23, 08010 Barcelona (Spain)

[+] *Current address: Tyndall National Institute*
Lee Maltings, Cork (Ireland)
Fax: (+353) 21427-0271
E-mail: jorg.strutwolf@tyndall.ie

ticles deposited in the previous steps, which were protected by an ODT film. The deposition–protection sequence was repeated and, to prove that during each deposition step new Au crystallites were formed, the authors used the electron transfer (ET) of catechol at the GC surface, which is relatively slow in comparison to the ET rate at a gold substrate. After each Au deposition step, the peak potential separation of the cyclic voltammogram had the typical value of a reversible ET, while after blocking the Au crystallites with ODT, an increase of the peak separation indicated the nonreversible ET taking place at the GC surface.[24] The electrodeposition/SAM formation process was also used by El-Deab et al. to produce ternary SAMs on gold nanoparticles deposited on GC by domain-selective chemisorption/desorption of thiol compounds at three different domains of the Au crystallites.[27]

Herein, we report the exploitation of a multiple gold deposition/SAM formation sequence similar to the procedure used by Finot et al.,[24] but improving on the method by employing coadsorption of ferrocene-terminated and unsubstituted thiols on the gold nanoparticles to create electroactive SAMs[28,29] during each deposition/SAM formation step. This enables monitoring of the Au particle formation after each deposition/formation sequence by measuring the redox current of the attached ferrocene entity.

An extraordinary increase in the redox signal of the electroactive SAM of ferrocene-$C_{11}SH$ ($FcC_{11}SH$) is observed which cannot be attributed solely to the increase of gold surface area during each deposition step. A higher number of chemisorbed electroactive molecules per area is observed for nanoparticle-modified electrodes than for bulk gold, which is attributed to the inherent properties of the deposited nanoparticles.

Results and Discussion

The main interest of this work is to demonstrate a new scheme of nanostructured electrode preparation by the sequential deposition of gold nanoparticles as a strategy for signal amplification of redox-active labels for application in biosensors. Control over the size and distribution of electrodeposited gold nanoparticles is also demonstrated by combining previously reported approaches with the scheme reported here, and an electroactive labeled thiol was used to distinguish the GC electroactive surfaces from the gold nanoparticle deposits.

The sequential deposition/protection procedure is illustrated in Scheme 1. After electrochemical deposition, the gold nanoparticles on the GC surface are protected by the self-assembly of a thiol monolayer to prevent them from being used as seeds in the subsequent gold deposition step. In the next deposition step, new particles are mainly formed on the GC surface due to the insulating action of the SAM on the gold particles deposited in the previous step. By repeating this procedure, a higher density of isolated nanoparticles can be achieved with each cycle of deposition.

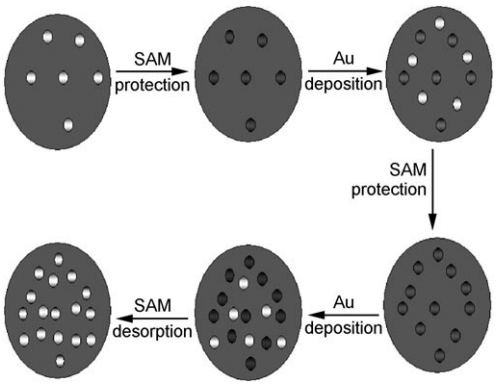

Scheme 1. The sequential electrodeposition/protection procedure for nanoparticle deposition on GC. White circles: unprotected particles; black circles: gold particles protected by a SAM. Three rounds of the deposition/protection sequence are shown.

Gold Nanoparticle Electrodeposition

A wide-potential cyclic voltammetric scan (Figure 1) of 1 mM $KAuCl_4$ in 0.5 M aqueous H_2SO_4 probes the most suitable potential for deposition of the gold particles. The voltammogram

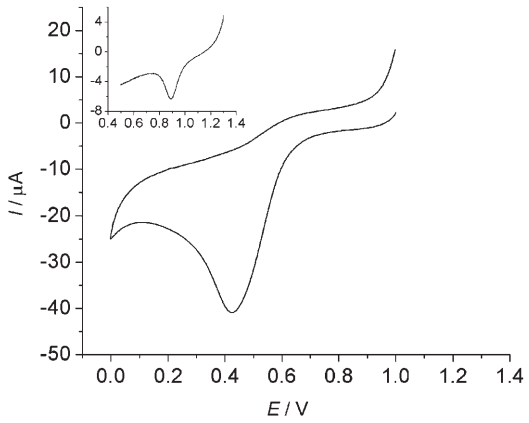

Figure 1. Cyclic voltammogram of 0.1 mM K_4AuCl_4 in 0.5 M H_2SO_4 using a GC electrode. Inset: reduction of a gold oxide layer formed on the deposited gold particles. Scan rate: 50 mV s^{-1}.

is very similar to that reported by Finot et al.,[23] with gold starting to deposit at a potential of +0.8 V with a peak potential at +0.51 V. The process is irreversible within the potential window studied. The presence of gold deposits is confirmed by the formation of a gold oxide layer followed by its reduction in the reverse scan, where the peak potential for reduction of gold oxide is +0.90 V (Figure 1, inset).

Gold nanoparticles are deposited from $KAuCl_4$ at concentrations of 1 mM and 0.1 mM. The deposition potential is varied between 0 and 600 mV and the deposition time of 1–25 s. Optimal conditions regarding particle size, distribution, and number density occur at an applied potential of 0 V for 5 s from a 0.1 mM $KAuCl_4$ solution, which is in agreement with the conditions reported by Finot et al.[23] The nanoparticles deposited using these parameters also show optimal characteristics

towards the formation of SAMs of ferrocene-labeled alkanethiols.

The nucleation mechanism of a metal is influenced by several factors,[34] such as the presence of organic additives,[35] the applied overpotential, and notably the nature of the substrate, as nucleation is proposed to initiate at the step edges and kink sites of the substrate. A rapid nucleation growth rate is observed, in agreement with Finot et al.,[23] due to the fast growth of the Au particles in the initial state. We were not able to experimentally access the rising portion of the transient under our conditions (transient time resolution 1 ms). However, an instantaneous nucleation process for gold on GC was reported.[36] In a progressive nucleation process particles are formed continuously during the application of the potential pulse, while instantaneous nucleation refers to a scenario where the timescale during which nucleation occurs is much shorter than the subsequent growth phase, which results in a more uniform particle-size dispersion. Therefore, to form uniform structures by metal deposition, instantaneous nucleation is desirable, in particular with the multiple-deposition experiments presented here.

Characterization of the Au Particles by SEM

Figure 2 presents typical scanning electron microscopy (SEM) images for the deposition of gold crystallites from 0.1 mM $KAuCl_4$ solution at a deposition potential of 0.0 V on GC. Figure 2A shows gold particles formed after a single 5 s potential step from 1.1 to 0 V. Figure 2B shows gold particles formed during three consecutive deposition steps (5 s each, step potential from 1.1 to 0 V), with a mercaptoethanol (ME) layer assembled on the particles after each deposition. Figure 2C is similar to Figure 2B, but decanethiol (DT) is used instead of ME for protecting the gold nanoparticles after each deposition step. For comparison, Figure 2D shows particles formed during three 5 s deposition steps without the use of a SAM as a protecting layer. The number of particles *n* for the single-step deposition (Figure 2A) is 187 μm^{-2}, measured over an area of 48 μm^2, while for the three deposition rounds with ME and DT SAMs (Figures 2B and C) *n* has values of 314 and 386 μm^{-2}, respectively. Three deposition rounds without SAM formation result in a particle density of 41 μm^{-2} (Figure 2D).

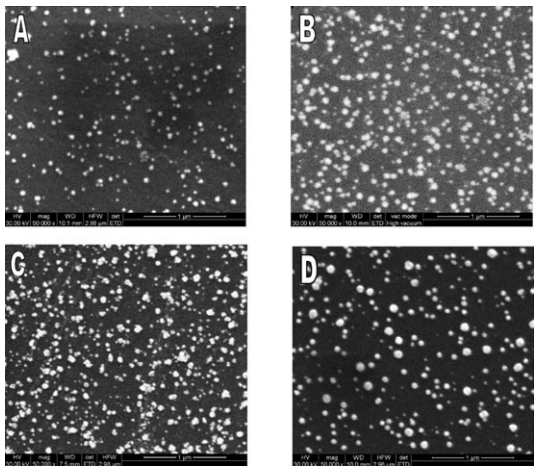

Figure 2. SEM images of electrochemically deposited gold nanoparticles on GC. Deposition potential: 0 V from 0.1 mM K_4AuCl_4 in 0.5 M aq. H_2SO_4. A) One 5 s deposition step. B) Three deposition rounds of 5 s each. After each deposition step the particles were protected by ME SAMs. C) The same as (B) but DT SAMs are used for protection. D) As (B), but without SAM protection.

From these results it can be concluded that both the DT and ME SAMs give good protection of the gold nanoparticles and prevent secondary nucleation during subsequent deposition rounds, with DT SAMs being slightly more protecting than ME SAMs. This result is not surprising, as it is known that thiols with longer *n*-alkane chains form dense layers on gold surfaces.[37] The high number of particles (187 μm^{-2}) created in the first deposition step is not repeated in subsequent deposition steps, despite protection with ME or DT. This finding indicates major consumption of active nucleation sites on the GC surface during the first deposition step. These nucleation sites are then not available in subsequent deposition experiments, and the number of particles formed in the first round cannot be reached in the following deposition rounds, despite protection of the gold particles. However, the protection mechanism to increase the number density of nanoparticles by sequential deposition is successful, as a comparison with a three-step deposition without protection, where the number density *n* is 41 μm^{-2}, reveals a substantially lower value of *n* than with protection of the nanoparticles. Coalescences of particles might be responsible for the low *n* value, which is also manifested by the increased particle size, as revealed by comparing the SEM images in Figure 2.

Although a DT monolayer offers slightly better insulation of the Au particles than ME, a SAM of DT has the disadvantage of being impossible to remove completely from the particles by reductive desorption within a negative potential limit at which the carbon surface or the particles themselves are not damaged, whereas ME can be reductively removed by repeatedly cycling the potential between −0.2 and −1.2 V. The possibility of removing the protective layer is important for potential analytical application of the nanoparticle-modified surface, where reductive desorption can be exploited for creating mixed monolayers.

Gold Surface Area Estimation by Oxide Layer Stripping

To understand if the achieved signal enhancement is simply due to an increase in surface area or to the properties of the deposited nanoparticles, a reliable method for estimation of the area is needed, and the electrochemical reduction of Au surface oxides to estimate the area of exposed gold[32] is used. Following the deposition of Au nanocrystals, the surface is oxidized by a potential step to 1.5 V for 5 s. Although both the Au and GC surfaces are likely to be oxidized during this applied positive potential, the oxide film on Au is selectively reduced during the reduction scan.[23,32]

A direct estimation of the gold surface area after each deposition/DT assembling process is not possible, because the DT used to protect the already-created Au nanocrystals substan-

tially suppresses the formation of an oxide layer on gold. By comparing the surface area calculated from the oxide layer reduction before and after assembling of a DT layer on nanocrystals, a 50% decrease is detected, in agreement with the trend observed by Finot et al.,[24] who reported 15 and 70% for hexanethiol and dodecanethiol, respectively. Attempts to remove DT from the nanocrystals by reductive desorption either by repeatedly cycling the potential to −1.4 V or applying a potential of −1.4 V for 10 s was not successful, since it was not possible to recover the full surface area estimated from the oxide reduction before DT assembling, which may be attributed to two sources. First, it is well established that the longer the alkyl chain length of the thiol, the more negative the peak potential required for reductive desorption, which reflects the stronger hydrophobic intermolecular interaction of the alkyl chains,[38,39] and therefore the reductive desorption attempts might have led to only partial removal of DT. Alternatively, the source of error could be damaging of the gold particles on the GC surface, due to the high applied potential.

To overcome this problem a SAM that blocks growth of already-formed gold nanoparticles during the sequential deposition procedure but does not prevent gold oxide formation could be used. Figures 2B and C reveal that the insulating effect of a ME SAM to suppress further growth of previous generations of particles during electrochemically induced nucleation is comparable to the protection by a DT SAM. In addition, the area of the oxide reduction peak of bare gold particles and of the same gold particles modified with ME differs by less than 2%, which indicates a very minor degree of blocking of the formation of an oxide layer on gold; using this ME SAM, a more accurate estimate of the surface area of deposited gold nanoparticles is achieved. Therefore, a reductive desorption step to remove the ME SAM prior to the oxide formation/reduction process is not necessary, and ME is used for protection of the gold nanoparticles during sequential deposition rounds. It is also likely that ME is oxidatively removed during the oxide layer formation step at 1.5 V, as is observed in the case of mercaptopropionic acid.[40]

The stepwise procedure of gold nanoparticle deposition, protection, and area estimation involved the following steps: 1) deposition of gold nanoparticles, 2) estimation of Au surface area by oxide layer formation and reduction, 3) protection of deposited particles by formation of a ME SAM, and 4) deposition of gold nanoparticles. Steps 1–4 are repeated (cf. Scheme 1).

The amount of gold deposited during each of the deposition/protection steps is roughly constant at a value of about 0.3 to 0.4 $\mu g\,cm^{-2}$, with the exception of the gold loading in the first deposition round, which is larger due to the higher number of nucleation sites available on a "fresh" GC surface. The gold loading is calculated from the flow of charge during the potential step, with the deposition transients corrected by background subtraction (Table 1, column 3).

Table 1. Characterization of stepwise gold nanoparticle deposition at 0 V on a GC surface.

Deposition step	Deposition time [s]	Au loading [$\mu g\,cm^2$] per deposition step[a]	Au surface area [cm^2][b]	Au surface area [cm^2][c]
1	5	0.56	0.023	0.025
2	5	0.27	0.044	0.054
3	5	0.41	0.063	0.081
4	5	0.39	0.072	0.125
5	5	0.31	0.082	–
1	25	23.68	0.124	–

[a] Calculated from background-corrected current transients during electrodeposition. [b] Estimated from the charge related to the reduction peak of the surface oxide monolayer on Au (see Figure 2) using a reported value[32] of 400 $\mu C\,cm^{-2}$. [c] Estimated from the charge of a self-assembled $FcC_{11}SH$ layer, assuming a theoretical maximal coverage[43,44] of 4.5×10^{-10} $mol\,cm^{-2}$.

A complete gold layer is plated on the GC substrate using a single potential step of 0 V for 25 s and the surface appears shiny gold with a roughness factor of 1.4, which indicates a relatively smooth gold surface. Application of a single 25 s potential step results in a 23.7 $\mu g\,cm^{-2}$ gold loading on the GC substrate, with a calculated thickness of 12 nm assuming a uniform deposition on the GC surface.

Cyclic voltammograms for the reduction of gold surface oxides of three deposition/protection cycles are presented in Figure 3. The gold surface areas can be calculated by integration of the peak areas, and the results are listed in the fourth column of Table 1. The increase of surface area during each deposition/protection round is roughly constant, thus indicating a principally surface-controlled nucleation process for each deposition step.

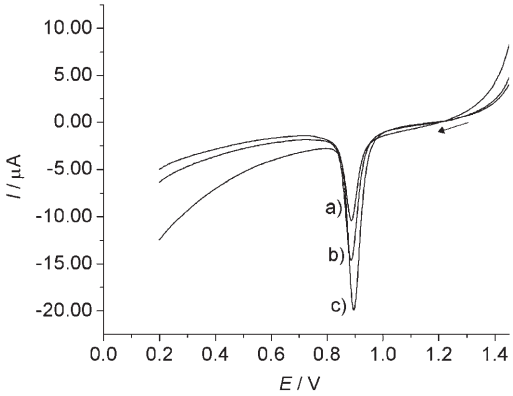

Figure 3. Voltammogram for the reduction of gold surface oxides from electrochemically deposited gold nanoparticles on GC. a) Single deposition step; b) two rounds of deposition and protection with ME; c) three rounds of deposition and protection with ME. Scan rate: 50 $mV\,s^{-1}$. The deposition potential for the gold nanoparticles was 0 V from 0.1 mM aq. $KAuCl_4$ and the length of each deposition step was 5 s.

Self-Assembling of Electroactive Monolayers

The interfacial properties of the gold nanoparticles are further investigated with a SAM of $FcC_{11}SH$, a ferrocene-terminated alkanethiol, backfilled with DT. The electroactive $FcC_{11}SH$/DT monolayer not only protects the gold nanoparticles during the sequential deposition/assembling procedure, but also allows monitoring of thiol immobilization after each deposition/protection step by measuring the diffusionless current of the covalently bound ferrocene moiety. Cyclic voltammograms for five deposition/assembling rounds from 0.1 mM $KAuCl_4$ solution, each recorded after formation of the $FcC_{11}SH$/DT SAM on the freshly deposited gold nanoparticles, are shown in Figure 4. As expected, the current increases with each deposition round, since additional ferrocene-labeled alkanethiol can be assembled on the newly created gold nanoparticles. Repeated rounds of deposition ultimately result in the saturation of nucleation centers. Consequently, additional steps of gold deposition do not lead to new nucleation centers, but instead the already-formed gold crystals grow, finally leading to a complete gold layer on the GC substrate. In this situation, additional gold deposition steps do not affect the overall gold area. For deposition from 1 mM $KAuCl_4$ the current peak levels off after the fourth deposition/SAM formation round, while for deposition from 0.1 mM $KAuCl_4$ a slight increase is still observed after the sixth deposition/SAM formation round because of a slower growth of the particles due to the lower concentration of gold ions.

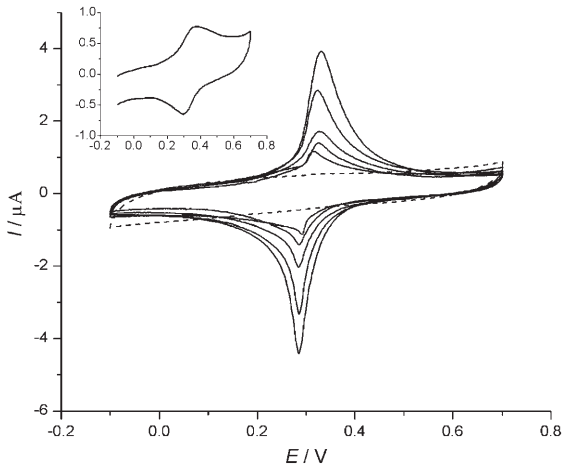

Figure 4. Cyclic voltammograms of an $FcC_{11}SH$ monolayer self-assembled on gold nanoparticles. The number of deposition rounds of the nanoparticles is one to five (with increasing peak currents). The dashed line is for a bare GC electrode and defines the background current. Inset: voltammogram of an $FcC_{11}SH$ monolayer assembled on a gold-plated GC electrode.

The performances of a GC surface completely plated with gold and of a GC surface modified with stepwise deposition of gold nanoparticles were compared in terms of formation of the $FcC_{11}SH$ electroactive SAM. The GC substrate was completely covered with gold as previously described, and the electroactive SAM prepared using the same conditions as for a five-round nanoparticle deposition, with the surface being exposed five times to solutions of $FcC_{11}SH$ and DT for backfilling to form the electroactive layer, with washing after each SAM deposition step (see Experimental Section). This procedure enables the refilling of defect sites in the monolayer with thiols and allows the bulk electrode surface and the nanoparticle surface to be directly compared.

The inset in Figure 4 shows the redox behavior of the gold-plated electrode. The charges related to the oxidation and reduction of the ferrocene end groups are $Q_A = 1.20$ and $Q_C = 1.34$ μC, respectively. The charge due to the redox reaction is increased with increasing rounds of nanoparticle deposition (see Figure 4). After five rounds the measured oxidation and reduction charges are $Q_A = 7.20$ and $Q_C = 7.26$ μC, which is a sixfold increase compared to the charge measured for a fully gold-covered GC (inset of Figure 4). The active gold area estimated by oxide layer reduction for a complete gold layer formed on the GC electrode during a single 25 s potential step to 0 V is 0.124 cm^2, while the active surface for the gold nanoparticles deposited during five 5 s potential step/SAM protection rounds is 0.082 cm^2. The increase of the redox signal and therefore of the amount of immobilized $FcC_{11}SH$ cannot be explained simply by an increase in the gold surface available for SAM formation, since the measured gold area of the nanoparticles is even slightly smaller than that of the gold-plated GC electrode. It has been established that nanometer-sized gold particles can exhibit excellent catalytic activity[41,42] due to their relatively high surface-to-volume ratio and their interface-dominated properties, which significantly differ from those of their bulk counterparts.[11,41,42] The unfavorable energetic state of surface atoms of the gold nanoparticles results in an enhanced reactivity of the metal atoms at the surface towards binding processes, in this case towards the formation of sulfur bonds, and is the likely explanation for the significant enhancement in signal, which is ninefold when normalized to the area.

The gold surface area was calculated from the charge of the self-assembled $FcC_{11}SH$ layer, assuming a theoretical maximum coverage[43,44] of 4.5×10^{-10} mol cm^{-2}, with the charge being estimated by integration of the anodic peak with correction for the charging current contribution. The theoretical maximum coverage is based on the assumption of hexagonal packing of the ferrocene moiety, with a sphere of diameter 6.6 Å.[44] The theoretical maximum coverage is in good agreement with an experimental value of 4.6×10^{-10} mol cm^{-2}, estimated by cyclic voltammetry (CV) for $FcC_{12}SH$ by Lee et al.,[43] although a value for the surface coverage of 5.9×10^{-10} mol cm^{-2} for (hydroxymethyl)ferrocene on polycrystalline gold has been reported.[45]

The gold surface areas estimated from the $FcC_{11}SH$ charge and from oxide layer formation for the first deposition round are in good agreement. However, with increasing number of deposition rounds, the difference between the areas estimated by the two methods increases, with the surface area estimated by oxide formation being smaller.

Both methods of surface area estimation have their own limitations. Gold surface area measurements by gold oxide layer formation and reduction is a simple and frequently used technique, although oxygen adsorption measurement appears to be a somewhat arbitrary procedure to determine the real sur-

face area,[46] due to the assumption of complete monolayer formation with a gold/oxygen ratio of 1:1 and to the uncertainty of the exact value of the corresponding charge required for the reduction of this monolayer, which depends on the composition of the exposed crystalline planes. However, gold surface estimation by oxide monolayer formation is widely used.[32,47] The oxide coverage on a gold-plated GC electrode as a function of potential is evaluated and is in agreement with published data.[48] For a complete gold layer, a roughness factor of 1.8 is estimated by surface oxide reduction, which is in agreement with the value reported for polished polycrystalline gold electrodes.[49] However, in the case of the deposited gold nanoparticles, the surface compromises a large part of the GC and the high anodic potential necessary for oxide layer formation on gold might introduce oxidation processes at the GC surface.[50] The interference of both oxidation processes leads to an underestimation of the surface of the gold nanoparticles arranged on the GC electrode.

Estimation of the surface area from the charge of the redox-active SAM, on the other hand, has the disadvantage that an assumption regarding the surface coverage with $FcC_{11}SH$ molecules has to be made. As the maximum theoretical value of surface coverage of 4.5×10^{-10} mol cm^{-2} is used, the values presented in Table 1 give lower limits of the real surface areas.

To summarize, although both of these methods for surface area determination result in an underestimation of the real surface area of electrodeposited nanoparticles, the area estimated by the charge of the electroactive $FcC_{11}SH$ SAM is likely to be closer to the real surface area of the gold nanoparticles than the area measured by gold oxide formation, since the area estimation by the former method gives bigger values. However, because of a lack of reliability in the accuracy of surface area measurements, we cannot correctly attribute what portion of the signal enhancement achieved is due to the area of the nanoparticles' surface as compared to the bulk gold electrode, or to the inherently improved catalytic efficiencies and favorability to form SAMs as a result of the enhanced reactivity of the surface atoms of the deposited nanoparticles.

Despite this, the large difference in the electrochemical signal of the electroactive SAM on bulk gold and on the gold nanoparticles (Figure 4) cannot be attributed to the surface area alone. The deposited area is 0.124 cm^2 for the bulk gold electrode and 0.082 cm^2 (estimated after five rounds of deposition by oxide layer formation) and 0.125 cm^2 (estimated from the charge of the electroactive SAM after four rounds of deposition) for the gold nanoparticles. Even the assumption of 100% underestimation of the surface area of the gold nanoparticles cannot explain the enhancement of the redox signal solely by the increase in surface area. The ferrocene signal of the bulk gold electrode is approximately the same only for the first round of nanoparticle deposition, despite the fact that the gold surface of the nanoparticles, as evidenced by the SEM images as well as the oxide estimation, is only a fraction of the bulk gold surface. It is therefore clear that the signal enhancement is principally due to the unique properties of nanoparticles, which makes the self-assembly processes of thiol-based monolayers more effective compared to bulk gold. This is clearly demonstrated when comparing the signal obtained from the chemisorbed electroactive SAM, where the signal obtained with the bulk gold surface is 90% less than that obtained with the deposited gold nanoparticle surface. Additionally, as the deposited nanoparticles are highly reactive, there is no need for the lengthy cleaning and activation procedures, such as chemical (e.g. piranha solution), electrochemical, and physical (e.g. polishing, UV–ozone) methods, routinely used to prepare gold surfaces prior to SAM formation.

Conclusions

Enhancement of electrochemical signals has been demonstrated using an approach of sequential electrodeposition and capping of gold nanoparticles. The electrodeposition of gold nanoparticles on GC has been optimized with regard to size and number density. The nucleation of the gold particles is fast and instantaneous, not progressive. This is a prerequisite for the successful application of the sequence of deposition/SAM protection rounds presented here, to impede secondary nucleation and increase the particle number density on the GC surface. SEM images show that the isolation of deposited nanoparticles by a SAM to prevent them from further growth in subsequent gold electrodeposition steps is successful.

The estimation of the surface area of the gold nanoparticles by oxygen adsorption is likely to be complicated by the interference of anodic processes at the GC surface at the negative potentials necessary for oxygen adsorption. This leads to an underestimation of the active gold area. Area estimation was also performed by self-assembling an electroactive layer ($FcC_{11}SH$) on the gold particles and measuring the charge. This method requires knowledge of the surface coverage of the electroactive molecules, and the theoretical maximum value has been assumed. Therefore, this method gives a lower limit of the active gold area. Both methods are consistent in showing an increase in surface area with subsequent deposition/protection steps.

In comparison to bulk gold, nanoparticles of gold immobilized on a GC surface show an increased affinity towards SAM formation and this can be used for signal amplification. This property is especially relevant in the context of electrochemical biosensors, where gold nanoparticles can be used as a transducer element for the anchoring of the probe biomolecule. An added advantage of the reported method is that no cleaning or activation of the gold surface, such as the use of piranha solution or UV–ozone, is required, and the alkanethiol/thiolated biomolecule can be chemisorbed immediately following the sequential rounds of deposition. The reported approach for signal enhancement that exploits highly reactive nanoparticulate surfaces will find considerable application in electrochemical biosensing, particularly DNA sensors for protein/nucleic acid detection by exploiting redox-tagged stem-loop structures,[30,31] where considerable improvement in detection limits would be expected.

Experimental Section

Materials: Potassium tetrachloroaurate(III) ($KAuCl_4$, 99.995%, Aldrich), sulfuric acid (95% v/v, Scharlau), sodium perchlorate (98%, Sigma), 2-ME (99%, Scharlau), 3-mercaptopropionic acid (99%, Acros Organics), DT (96% v/v, Aldrich), and ethanol (96% v/v, Scharlau) were used as received. 11-Ferrocenyl-1-undecanethiol ($HSC_{11}Fc$) was obtained from Prochimia (Poland). Aqueous solutions were prepared using MilliQ water (18.2 MΩ cm).

Electrochemistry: CV and potential-step experiments were carried out using an Autolab model PGSTAT 12 potentiostat/galvanostat controlled with the General Purpose Electrochemical System (GPES) software (Eco Chemie B.V., The Netherlands). A conventional three-electrode setup was used with the GC electrode as working electrode and a platinum wire counter electrode. All potentials were reported with respect to an Ag/AgCl reference electrode.

GC rods (Sigradur, HTW Hochtemperatur Werkstoffe, Germany) with a length of 7 cm and a diameter of 3 mm were pressed into two layers of heat-shrinking polyolefin tubes. One end of the rod, which served as the electrode surface, was polished using an electrode polishing pad (BAS) and further smoothed with 0.3-μm alumina slurry (Buehler) in MilliQ water. After polishing, the electrodes were carefully rinsed with water and sonicated for about 15 min. The electrodes were then washed with ethanol and water and conditioned by potential scanning from 0 to 1.2 V in 1 M $NaClO_4$ for at least five complete scans at 50 mV s^{-1}, at which the high background current due to GC oxidation diminished and a reproducible cyclic voltammogram was obtained. Afterwards, the background current of the bare electrode was measured by CV within the potential window used for probing the ferrocene redox reaction. Electrodes that showed a high background current above some arbitrarily selected reference were excluded. The electrodes were used immediately following the cleaning and conditioning steps.

Gold nanoparticles were electrodeposited on GC electrodes from a 0.5 M H_2SO_4 solution containing 0.1 mM $KAuCl_4$ by applying a potential step of 0 or 0.4 V for 5 s. For self-assembling monolayers of alkanethiols on gold nanoparticle deposits, the electrodes were maintained in a 2 mM ethanolic solution of the thiol (50 μL) for at least 2 h at room temperature (22 °C). The SAM of $HSC_{11}Fc$ was formed on freshly deposited gold nanoparticles by covering the electrode surface with 2 mM $HSC_{11}Fc$ (50 μL) in ethanol. The electrodes were subsequently carefully and thoroughly washed with ethanol and later with water, followed by air drying. Before gold nanoparticle deposition, SAMs of $HSC_{11}Fc$ were placed in contact for 1 h with 2 mM ethanolic solutions of ME or DT for backfilling. Following this backfilling step, a slight decrease of the ferrocene peaks was observed due to reorganization of ferrocene-terminated alkanethiols. To exclude the possibility of immobilization/adsorption of $HSC_{11}Fc$ on GC, a bare GC electrode was immersed overnight in a 2 mM $FcC_{11}SH$ ethanolic solution. The voltammogram with this electrode did not show any peaks related to the redox reactions of the ferrocene terminal entities.

The amount of gold deposited on GC (gold loading) was estimated from the charge consumed during the deposition process, which was obtained by integrating the area under the current transient curve and subtracting the charging current for a bare electrode.

The area of the deposited gold nanoparticles was estimated from the charge consumed for reduction of a formed gold oxide monolayer. For the formation of these oxide layers on the electrodeposited Au particle surfaces, a potential step of 1.5 V was applied for 5 s. The formed oxide layer was reduced by scanning the potential from 1.5 to 0 V in 0.5 M H_2SO_4 solution with a scan rate of 50 mV s^{-1}, and the surface area was estimated from the charge consumed during reduction of the oxide monolayer of Au using a reported[32] value of 400 μC cm^{-2}.

SEM for characterization of gold nanoparticles on a GC electrode was carried out using a Fei Quanta 600 environmental scanning electron microscope at an acceleration voltage of 20 kV and a working distance of 10 mm in a high-vacuum mode. Image analysis was performed with the ImageJ software (ver. 1.37v).[33]

Acknowledgements

This paper partly describes work undertaken in the context of the EC IST project Integrated Microsystem for the Magnetic Isolation and Analysis of Single Circulating Tumor Cells for Oncology Diagnostics and Therapy Follow-up (MASCOT) FP6-2005-IST-027652. The IST program is partially funded by the European Commission. Financial support by the SAFE Network of Excellence (LSHB-CT-2004-503243) is also acknowledged.

Keywords: electrochemistry · gold · monolayers · nanoparticles · self-assembly

[1] D. Hernández-Santos, M. B. Gonzalez-Garcia, A. C. Garcia, *Electroanalysis* **2002**, *14*, 1225–1235.
[2] S. G. Penn, L. He, M. J. Natan, *Curr. Opin. Chem. Biol.* **2003**, *7*, 609–615.
[3] A. N. Shipway, E. Katz, I. Willner, *ChemPhysChem* **2000**, *1*, 18–52.
[4] E. Katz, I. Willner, J. Wang, *Electroanalysis* **2004**, *16*, 19–44.
[5] X. L. Luo, A. Morrin, A. J. Killard, M. R. Smyth, *Electroanalysis* **2006**, *18*, 319–326.
[6] C. W. Welch, R. G. Compton, *Anal. Bioanal. Chem.* **2006**, *384*, 601–619.
[7] R. Narayanan, M. A. El-Sayed, *J. Phys. Chem. B* **2005**, *109*, 12663–12676.
[8] *Nanoparticles made in Mesoporous Solids*, L. M. Bronstein in *Colloid Chemistry 1, Top. Curr. Chem., Vol. 226*, Springer, Heidelberg, **2003**, pp. 55–89.
[9] J. D. Aiken, R. G. Finke, *J. Mol. Catal. A* **1999**, *145*, 1–44.
[10] B. F. G. Johnson, *Coord. Chem. Rev.* **1999**, *190–192*, 1269–1285.
[11] M. Haruta, *Catal. Today* **1997**, *36*, 153–166.
[12] M. S. El-Deab, T. Ohsaka, *Electrochem. Commun.* **2002**, *4*, 288–292.
[13] M. S. El-Deab, T. Ohsaka, *J. Electroanal. Chem.* **2003**, *553*, 107–115.
[14] C. R. Raj, A. I. Abdelrahman, T. Ohsaka, *Electrochem. Commun.* **2005**, *7*, 888–893.
[15] C. X. Xu, J. X. Su, X. H. Xu, P. P. Liu, H. J. Zhao, F. Tian, Y. Ding, *J. Am. Chem. Soc.* **2007**, *129*, 42–43.
[16] C. R. Raj, T. Okajima, T. Ohsaka, *J. Electroanal. Chem.* **2003**, *543*, 127–133.
[17] L. Zhang, X. Jiang, *J. Electroanal. Chem.* **2005**, *583*, 292–299.
[18] M. T. Castaneda, S. Alegret, A. Merkoci, *Electroanalysis* **2007**, *19*, 743–753.
[19] M. T. Castaneda, A. Merkoci, M. Pumera, S. Alegret, *Biosens. Bioelectron.* **2007**, *22*, 1961–1967.
[20] M. Brust, C. J. Kiely, *Colloids Surf. A* **2002**, *202*, 175–186.
[21] M. S. El-Deab, T. Sotomura, T. Ohsaka, *J. Electrochem. Soc.* **2005**, *152*, C730–C737.
[22] M. S. El-Deab, T. Sotomura, T. Ohsaka, *J. Electrochem. Soc.* **2005**, *152*, C1–C6.
[23] M. O. Finot, G. D. Braybrook, M. T. McDermott, *J. Electroanal. Chem.* **1999**, *466*, 234–241.
[24] M. O. Finot, M. T. McDermott, *J. Electroanal. Chem.* **2000**, *488*, 125–132.
[25] F. F. Gao, M. S. El-Deab, T. Okajima, T. Ohsaka, *J. Electrochem. Soc.* **2005**, *152*, A1226–A1232.
[26] L. Zhang, X. U. Jiang, E. K. Wang, S. J. Dong, *Biosens. Bioelectron.* **2005**, *21*, 337–345.
[27] M. S. El-Deab, T. Okajima, T. Ohsaka, *J. Electrochem. Soc.* **2006**, *153*, E201–E206.
[28] C. E. D. Chidsey, C. R. Bertozzi, T. M. Putvinski, A. M. Mujsce, *J. Am. Chem. Soc.* **1990**, *112*, 4301–4306.
[29] H. X. Ju, D. Leech, *Phys. Chem. Chem. Phys.* **1999**, *1*, 1549–1554.

[30] C. H. Fan, K. W. Plaxco, A. J. Heeger, *Proc. Natl. Acad. Sci. USA* **2003**, *100*, 9134–9137.
[31] A. E. Radi, J. L. A. Sanchez, E. Baldrich, C. K. O'Sullivan, *J. Am. Chem. Soc.* **2006**, *128*, 117–124.
[32] S. Trasatti, O. A. Petrii, *Pure Appl. Chem.* **1991**, *63*, 711–734.
[33] http://rsb.info.nih.gov/ij.
[34] G. Staikov, W. J. Lorenz, E. Budevski, *Electrochemical Phase Formation and Growth*, Wiley-VCH, Weinheim, **1996**.
[35] J. Strutwolf, M. Wunsche, H. Meyer, R. Schumacher, *Z. Phys. Chem.* **1999**, *208*, 239–251.
[36] H. Yang, T. H. Lu, K. H. Xue, S. G. Sun, S. P. Chen, *J. Appl. Electrochem.* **1997**, *27*, 428–433.
[37] H. O. Finklea, S. Avery, M. Lynch, T. Furtsch, *Langmuir* **1987**, *3*, 409–413.
[38] T. Kondo, T. Sumi, K. Uosaki, *J. Electroanal. Chem.* **2002**, *538*, 59–63.
[39] C. J. Zhong, M. D. Porter, *J. Electroanal. Chem*. **1997**, *425*, 147–153.
[40] C. A. Canaria, J. So, J. R. Maloney, C. J. Yu, J. O. Smith, M. L. Roukes, S. E. Fraser, R. Lansford, *Lab Chip* **2006**, *6*, 289–295.
[41] A. N. Shipway, M. Lahav, I. Willner, *Adv. Mater.* **2000**, *12*, 993–998.
[42] M. Králik, A. Biffis, *J. Mol. Catal. A* **2001**, *177*, 113–138.
[43] L. Y. S. Lee, T. C. Sutherland, S. Rucareanu, R. B. Lennox, *Langmuir* **2006**, *22*, 4438–4444.
[44] P. Seller, J. D. Dunitz, *Acta Crystallogr. Sect. B* **1979**, *35*, 2020–2032.
[45] S. E. Creager, L. A. Hockett, G. K. Rowe, *Langmuir* **1992**, *8*, 854–861.
[46] J. C. Hoogvliet, M. Dijksma, B. Kamp, W. P. van Bennekom, *Anal. Chem.* **2000**, *72*, 2016–2021.
[47] J. S. Gordon, D. C. Johnson, *J. Electroanal. Chem*. **1994**, *365*, 267–274.
[48] B. Piela, P. K. Wrona, *J. Electroanal. Chem.* **1995**, *388*, 69–79.
[49] R. T. Carvalhal, R. S. Freire, L. T. Kubota, *Electroanalysis* **2005**, *17*, 1251–1259.
[50] X. G. Zhang, Y. Murakami, K. Yahikozawa, Y. Takasu, *Electrochim. Acta* **1997**, *42*, 223–227.

Received: November 27, 2007
Published online on March 25, 2008

UNIVERSITAT ROVIRA I VIRGILI
ELECTROCHEMICALLY DEPOSITED METAL NANOSTRUCTURES FOR APPLICATIONS IN GENOSENSORS
Tesfaye Refera Soreta
ISBN:978-84-692-9758-2/DL:T-206-2010

Chapter 5

Electrochemical Surface Structuring with Palladium Nanoparticles for Signal Enhancement

UNIVERSITAT ROVIRA I VIRGILI
ELECTROCHEMICALLY DEPOSITED METAL NANOSTRUCTURES FOR APPLICATIONS IN GENOSENSORS
Tesfaye Refera Soreta
ISBN:978-84-692-9758-2/DL:T-206-2010

UNIVERSITAT ROVIRA I VIRGILI
ELECTROCHEMICALLY DEPOSITED METAL NANOSTRUCTURES FOR APPLICATIONS IN GENOSENSORS
Tesfaye Refera Soreta
ISBN:978-84-692-9758-2/DL:T-206-2010

Electrochemical Surface Structuring with Palladium Nanoparticles for Signal Enhancement

Tesfaye Refera Soreta, Jörg Strutwolf[+], Olivier Henry, Ciara K. O'Sullivan[,++]*

Nanobiotechnology & Bioanalysis Group, Department of Chemical Engineering, Universitat Rovira I Virgili, Avinguda Països Catalans, 26, 43007, Tarragona, Spain

ciara.osullivan@urv.cat

RECEIVED DATE (to be automatically inserted after your manuscript is accepted if required according to the journal that you are submitting your paper to)

[+] Current address: Tyndall National Institute, Lee Maltings, Cork, Ireland

[++] Institucio´Catalana de Recerca I Estudis Avançats, Passeig Lluis Companys 23, 08010 Barcelona, Spain

UNIVERSITAT ROVIRA I VIRGILI
ELECTROCHEMICALLY DEPOSITED METAL NANOSTRUCTURES FOR APPLICATIONS IN GENOSENSORS
Tesfaye Refera Soreta
ISBN:978-84-692-9758-2/DL:T-206-2010

Abstract

Surface nanostructuring with metal nanoparticles has gained importance due to the unique physicochemical properties of the nanoparticles. More particularly, the fields of heterogeneous catalysis and chemical and biochemical sensing have benefited of recent developments in surface nanostructuring with nanoparticles. We have fabricated nanostructured surfaces based on the sequential electrochemical deposition of palladium nanoparticles (Pd-NPs) onto glassy carbon electrodes (GCEs). In order to increase the number density of the Pd-NPs at the GC electrode surface, successive rounds of deposition/protection cycles were realised. Freshly deposited Pd-NPs were immediately capped with 6-ferrocenylhexanethiol (Fc-C_6SH) to prevent secondary nucleation processes to occur during subsequent deposition rounds. This approach allowed maintaining a narrow size distribution and as such the inherent properties of the deposited Pd-NPs. Scanning electron microscopy (SEM) was used to confirm the successful deposition as well as to measure the size and spatial distribution of the deposited Pd-NPs. SEM image analysis results showed that the number density of Pd-NPs increased in each sequential deposition stage. The anodic peak current signal recorded for the electroactive SAM of Fc-C_6SH following six consecutive deposition/protection cycles was found to be 50 times higher than that formed on a bulk palladium electrode. The signal enhancement recorded was explained by the high surface reactivity behaviour of the deposited palladium NPs. Finally, for comparison, gold NP were deposited on GCEs following the same approach, and exhibited considerably reduced signal enhancement properties as compared to the Pd-NPs. The work presented here should find wide applicability in the field of electrochemical and

ISBN:978-84-692-9758-2/DL:T-206-2010

biochemical sensing for enhancing biosensor signals by specifically designing and structuring transducer surfaces at the nano-scale.

KEYWORDS Palladium, nanoparticles, surface nanonostructuring, electrocactive SAM, ferrocene, glassy carbon, metal deposition

Introduction

Nanostructured materials possess large surface areas and usually exhibit high surface concentrations of edges, corners, defect sites or other unusual structural features [1] and great attention has thus been given to the fabrication and characterisation of metal nanoparticles (NP) for applications in catalysis [2-5] and as a support for self-assembled monolayers (SAM) of alkanethiols of diverse chemical functionality [6, 7]. Enhanced catalytic activity of metallic nanoparticles can be attributed to the high surface-area to-volume ratio that results in an increase of surface atom distribution, coupled with the property that these surface atoms have the highest reactivity due to the lower number of atom neighbours [8].

Electrochemical deposition approaches are often reported as methods of choice for the simple and low cost nanostructuring and nanopatterning of electrode surfaces. The deposition of metal onto metal electrodes occurs via an atomic layer-by-layer process beginning with under-potentially deposited monolayers. At some critical thickness of the electrodeposited layer, islands that are more than one atomic layer in height begin to form a continuous metal multi-layer [9, 10]. The electrodeposition of metals on carbonaceous

ISBN:978-84-692-9758-2/DL:T-206-2010

surfaces, on the other hand, proceeds differently as the wetting of coordinative saturated surfaces by electrodeposited metal is energetically unfavourable [10]. In effect, metal NPs can be electrochemically deposited onto carbon supports such as glassy carbon electrodes (GCEs) by applying short potential pulses to initiate the creation of metal nucleation centres, the size of which can be controlled by adjusting the length, number and amplitude of the potential pulses. Glassy carbon supports are often the preferred material due to their electrochemical inertness in a wide potential window and their amorphous structure with a random distribution of active sites for nucleation [11]. The size and density of the deposited metal nanoparticles on GCEs is dependent on the over-potential applied for deposition as well as the length of deposition time. Longer deposition time causes inter-particle coupling, where the growth of two particles located in close proximity become coupled after sufficient growth time [10] and result in particle size dispersion. Zoval et.al, [12-14] have demonstrated deposition of different metal nanoparticles on carbon electrodes by applying a short over potential to initiate nucleation followed by longer growth potential that can be exploited to minimize non uniform size distribution of the nucleated metal particles. However, very few approaches for increasing the number density of electrochemically deposited metal nanoparticles in order to maximally increase reactivity and catalytic activity have been reported and an optimum compromise between density, size and spatial arrangement needs to be found in order to achieve the highest signal enhancement.

Electrophoretic deposition is one of the methods that have been employed for deposition of metal nanoparticles and offers good particle size monodispersity [15-17]. The metal nanoparticles are preformed in a suspension and their surface stabilized by a thick layer of

ISBN:978-84-692-9758-2/DL:T-206-2010

polymer or a thiol monolayer to prevent aggregation of the particles. Due to the surface stabilizer that effectively shield the particles, however, the electrocatalytic property of the nanoparticles is affected and there is additional undesirable electrical resistance results between the particle and the electrode surface [12]; moreover any attributed signal enhancement is purely due to an increase in surface area and not due to the unique catalytic properties observed on a nanoscale.

Metal nanoparticles have gained strong interest in chemical and biochemical sensing where the considerable enhancement in the measured activity could be beneficially applied to the design of ultrasensitive transducer surfaces [18-20]. There are several reports on the deposition of various metals such as gold (Au) [21, 22], platinum [23, 24] , and palladium (Pd) [25-38], but these are mainly applied to the field of heterogeneous catalysis. The morphology of the deposits is known to vary from a few tens of nanometers up to several micrometers in diameter depending on the deposition conditions as revealed by scanning electron microscopy (SEM) and atomic force microscopy.

In a previous work we reported on an approach to increase the number density of electrodeposited gold nanoparticles, whilst maintaining their unique properties, and as an extension of this work the developed technique could be exploited using alternative metals of higher catalytic and reactivity. Palladium is a well known catalyst for many reactions such as electrocatalytic oxidation of formaldehyde [39, 40], hydrazine [33], hydrogenation of unsaturated hydrocarbons [41-43], for reduction of oxygen [44], oxidation of alcohols [45, 46], oxidation of hydrogen to hydrogen peroxide [47], and is routinely used in the automobile

UNIVERSITAT ROVIRA I VIRGILI
ELECTROCHEMICALLY DEPOSITED METAL NANOSTRUCTURES FOR APPLICATIONS IN GENOSENSORS
Tesfaye Refera Soreta
ISBN:978-84-692-9758-2/DL:T-206-2010

industry in catalytic converters to reduce the amounts of nitrogen oxides, carbon monoxide, unburned hydrocarbons [48]. In parallel, palladium nanoparticles have also found application in the development of biosensors and have been exploited as a component in an enzymatic glucose biosensor [49] as well as for detection of catecholamine [50] and DNA [51].

The catalytic activity of a metal can often be correlated with the energy of the centre of the d band and with its density of states [52]. In palladium, the density of states rises sharply in the vicinity of the Fermi level, where it is high and consists mainly of contributions from d electrons. In contrast, the d band in gold lies much lower, and the density of states at the Fermi level is low. It could be anticipated that palladium nanoparticles should thus show a higher surface reactivity and catalytic activity than gold nanoparticles, and result in a further signal enhancement [53]. The suitability of electrodeposited palladium as a substrate for the immobilisation of alkanethiols SAM has been demonstrated [27, 54]. In addition, SAMs formed on Pd are often found to be of superior quality to those formed onto Au [55, 56].

In the work we report herein, we combined sequential electrochemical deposition of Pd NPs on GCEs to increase number density, maintaining a narrow NP size distribution whilst avoiding aggregation via the formation of insulating SAMs on the electrodeposited Pd NPs. After each step of electrochemical deposition, the Pd NPs were capped with an alkanethiol SAM in order to form an electrically insulating layer preventing their participation as seeds during the subsequent electrodeposition rounds [57]. By insulating the deposited NPs, new nucleation centres at the exposed carbon surface were created which promoted the controlled growth of new Pd NPs. This approach facilitated control of size, density and

ISBN:978-84-692-9758-2/DL:T-206-2010

distribution of the deposited particles. Using an alkanethiol labelled with an electroactive redox marker as the "capping agent", the surface area of the deposited nanoparticles could be measured and an estimate of the enhancement of electrochemical signal obtained. In addition, it was observed that Pd NPs exhibited better SAM coverage than the corresponding planar metallic substrate, and a combination of this coupled with the nanoparticle reactivity resulted in significant enhancement of signal.

2. Experimental Section

2.1 Reagents

Palladium dichloride ($PdCl_2$, 99.9%, Aldrich) was used for electrochemical deposition in citrate buffer solution pH 2 (consisting of 0.03 M citric acid, 0.0082 M HCl, 0.061 M NaCl, pH 2, Fluka). The pH was adjusted to 3 by addition of diluted sodium hydroxide (2 M, Scharlau). The supporting electrolytes used were 1 M sulfuric acid (95% v/v, Schalau), and 1 M sodium perchlorate (98%, Sigma). For the formation of alkanethiols SAMs, 2-mercaptoethanol (ME, 99% Scharlau), 6-ferrocenylhexanethiol (Fc-C6SH, Aldrich), or n-dodecanethiol (DDT, 96% v/v, Aldrich) were used. Aqueous solutions were prepared using Milli-Q water (18.2 MΩ.cm). Ethanol (96% v/v, Scharlau) was used for preparation of thiol solutions and for washing the electrodes. All chemicals were provided by Sigma (Madrid, Spain) and used as received.

ISBN:978-84-692-9758-2/DL:T-206-2010

2.2 Instrumentation

2.2.1 Electrochemical Measurements

Cyclic voltammetry and potentiostatic experiments were carried out using an Autolab model PGSTAT 12 potentiostat/galvanostat controlled with the General Purpose Electrochemical System (GPES) software (Eco Chemie B.V., The Netherlands). A conventional three-electrode set-up was used with a glassy carbon electrode (GCE) as working electrode and a platinum wire counter electrode. An Ag/AgCl electrode (CHI 111) served as a reference electrode. All potentials were reported with respect to this reference electrode. The solution of $PdCl_2$ was stirred by a magnetic stirrer (p-Selecta 88E) during palladium deposition.

2.2.2 Scanning electron microscopy

Scanning electron microscopy for characterization of Pd nanoparticles on glassy carbon electrode was carried out using a Fei Quanta 600 environmental scanning electron microscope at an acceleration voltage of 20 kV and a working distance of 10 mm in a high vacuum mode. Image analysis was performed with the ImageJ software (National Institute of Health (NIH) v. 1.38x).[58]

2.3 Methods

2.3.1 Electrode preparation

Glassy carbon rods (Sigradur®, HTW Hochtemperatur Werkstoffe, Germany) with a length of 7 cm and a diameter of 3 mm were pressed into two layers of heat shrinking

ISBN:978-84-692-9758-2/DL:T-206-2010

polyolefine tubes. One end of the rod, which serves as the electrode surface was polished with 0.3 μm alumina slurry (BUEHLER). Upon polishing, the electrodes were carefully rinsed with Milli-Q water and sonicated for about 15 minutes. After sonication, the electrodes were washed with ethanol and water and conditioned by potential scanning from 0V to 1.4 V in 1M $NaClO_4$ for at least five complete scans at 50 mV/s, where the high background current due to glassy carbon oxidation diminishes and a reproducible cyclic voltammogram was obtained. The background current of the bare electrode was measured by cyclic voltammetry within the potential window of 0 to 0.7 V. Electrodes with high background current above a selected reference were excluded. The electrodes were used immediately following the cleaning and conditioning steps

2.3.2 Electrochemical deposition of palladium nanoparticles on glassy carbon electrode and formation of SAM

The sequential deposition of metal nanoparticles was performed as follows; for the first stage of the palladium nanoparticles deposition, the potential was stepped from 1.10V for 5 seconds to 0 V for 1 second in a stirred 7.5 mM $PdCl_2$ solution of pH 3. The formed palladium nanoparticles were protected by capping them with a SAM of either DDT or Fc-C_6SH. A 2mM ethanolic solution of DDT was used to form a SAM of DDT. A solution of Fc-C_6SH was prepared by dissolving 1μL of the stock Fc-C_6SH provided by Aldrich in 1mL of ethanol (96% v/v). A 50μL of the thiol solution was immobilized for 2 hours on electrodes immediately after deposition of palladium nanoparticles. The electrodes were carefully washed in stirred ethanol for 5 minutes to remove any Fc-C_6SH that was not chemisorbed on the electrode surface. The washing step was repeated until a reproducible

ISBN:978-84-692-9758-2/DL:T-206-2010

cyclic voltammogram for the surface attached ferrocene was observed. Subsequently, a 50μL of 2mM of ME solution was applied and the electrode placed in a humidity chamber to avoid evaporation for 30 minutes. Mercaptoethanol was used to fill any defects of the SAM of Fc-C_6SH formed on the palladium nanoparticles. For any subsequent deposition stages, a step potential of 0 V was applied for 1 second in stirred $PdCl_2$ solution and the protection of the new NP using DDT or Fc-C_6SH as capping layer realized prior to any further deposition step.

3. Results and discussion

We previously reported the electrochemical deposition of palladium from $PdCl_2$ in pH 3 citrate buffer on glassy carbon electrodes (GCE) [27]. From the CV of $PdCl_2$ obtained from that work, we selected suitable deposition potentials for the electrochemical deposition of palladium nanoparticles (Pd-NP). The conditions for the deposition of Pd-NPs were further optimised by varying the deposition potential and deposition time as these parameters are critical for controlling the nucleation and growth of the palladium particles on the glassy carbon surface. A short deposition time was required to initiate nucleation centres as well as to suppress further growth of the particles, while the deposition over potential was important to control the number density of the nucleation centres. We have selected a deposition potential of 0V for 1 second was selected as an optimal condition to deposit a higher number of isolated palladium nanoparticles. Under these deposition conditions, the adsorption of hydrogen on the deposited Pd-NP is minimized [27] as it is more positive than the hydrogen ion reduction peak.

UNIVERSITAT ROVIRA I VIRGILI
ELECTROCHEMICALLY DEPOSITED METAL NANOSTRUCTURES FOR APPLICATIONS IN GENOSENSORS
Tesfaye Refera Soreta
ISBN:978-84-692-9758-2/DL:T-206-2010

Sequential deposition of palladium nanoparticles and formation of electroactive SAM

By taking advantage of a conducting carbon support known not to be able to support self assembled monolayers (SAMs) of alkanethiols, palladium nanoparticles can be deposited electrochemically via sequential deposition technique as depicted in Scheme 1.

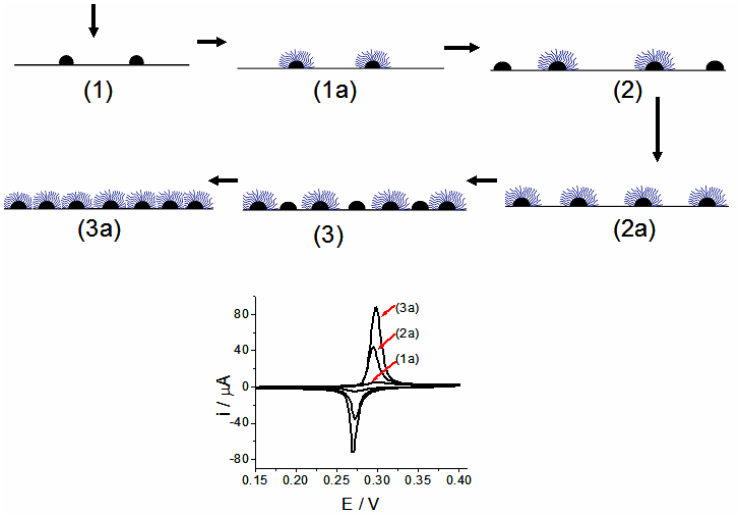

Scheme 1. An illustration of the first three sequential deposition/protection procedure for palladium nanoparticles on GC: (1, 2 , 3 refers the first, second and third palladium nanoparticles deposition stages respectively; 1a, 2a and 3a represent the protection stage with SAM of Fc-C_6SH following the Pd-NPs deposition stages).

For the first stage of palladium nanoparticle deposition, the potential was stepped from 1.10 V for 5 seconds to 0 V for 1 second in the stirred $PdCl_2$ solution. The electrode was washed with water, air dried and a SAM of Fc-C_6SH formed by application of 50 μL of the

ISBN:978-84-692-9758-2/DL:T-206-2010

ethanolic solution of the Fc-C_6SH. This step was important to protect the particles electrodeposited by capping them with the alkanethiol SAM whilst at the same time facilitating the characterization of the particles from the CV of the ferrocene moiety. The electrodes were washed in stirred ethanol for 5 minutes and a cyclic voltamogram of Fc-C_6SH measured in 1 M $NaClO_4$. The washing step was repeated until a reproducible CV was obtained that is believed to mark removal of any non-specifically adsorbed Fc-C_6SH on the electrode surface. In order to fill any defect in the Fc-C_6SH SAM, 50 μL of 2 mM ME was applied as a "backfilling" SAM. In subsequent deposition stages, nucleation should be formed on the exposed glassy carbon surface, as the previously deposited particles were insulated with organic capping layer. With this approach it was possible to increase palladium nanoparticles number density on the electrode surface.

Characterization of Pd-NPs by scanning electron microscopy

Scanning electron microscopy (SEM) was used to confirm the deposition as well as to measure the size and spatial distribution of the deposited NPs. For the analysis of the number of deposited Pd-NP, a surface area of 2.98 μm × 2.55 μm at a magnification scale of 50 000 was taken into account. Figure 1a shows SEM images for the first stage deposition of palladium nanoparticles. At this deposition stage, there are 42 particles per μm^2 area of the electrode with the average diameter of the deposited palladium nanoparticles about 50 nm, covering only 8% of the total electrode area [58]. For comparison, SEM images of GCEs surfaces following three rounds of Pd-NP deposition with Fc-C_6SH SAM protection (Figure 1b) and without SAM protection (Figure 1c) are also shown.For three rounds of deposition of palladium nanoparticles without SAM protection, an average

ISBN:978-84-692-9758-2/DL:T-206-2010

of 31 nanoparticles per μm^2, with particle size of 77.4 nm in diameter was obtained. In this case, the total area occupied by the deposited nanoparticles represented 14.7% of the electrode area. Surfaces subjected to three consecutive rounds of Pd-NP deposition without SAM protection (Figure 1c) were very similar to that observed in the case of first round deposition (Figure 1a) with the exception that the average particle size measured was larger and that the number of particles was reduced due to the merging of proximal particles as a consequence of repeated deposition, as the particles deposited in the initial stage were used as nucleation centers during subsequent depositions (Figure 1c). SEM images of GCEs following three rounds of deposition of Pd-NP with a SAM of Fc-C_6SH protection (Figure 1b) were very different from that of first round (Figure 1a) and three rounds without SAM protection (Figure 1c) as a higher number of Pd-NP was deposited. The increase in particle number is due to the effect of the SAM protection that prevents further particle growth on initially deposited particles and as such, creates new nucleation centers on the exposed glassy carbon surfaces during subsequent deposition rounds. As previously mentioned, the formation of the electroactive SAM of Fc-C_6SH was selected for two reasons; the SAM layer provides protection layer to avoid growth of deposited particles in sequential deposition and also facilitates monitoring the deposition process from the CV of the Fc-C_6SH SAM in each deposition stage.

Estimation of the area of deposited palladium nanoparticles in each deposition stage

UNIVERSITAT ROVIRA I VIRGILI
ELECTROCHEMICALLY DEPOSITED METAL NANOSTRUCTURES FOR APPLICATIONS IN GENOSENSORS
Tesfaye Refera Soreta
ISBN:978-84-692-9758-2/DL:T-206-2010

Estimation of electrode area based on diffusion controlled electrochemical methods, i.e., chronocoulometry and cyclic voltammetry [59] of redox labels in solution, were not suitable for this system as, the measurements of redox species in solution cannot provide

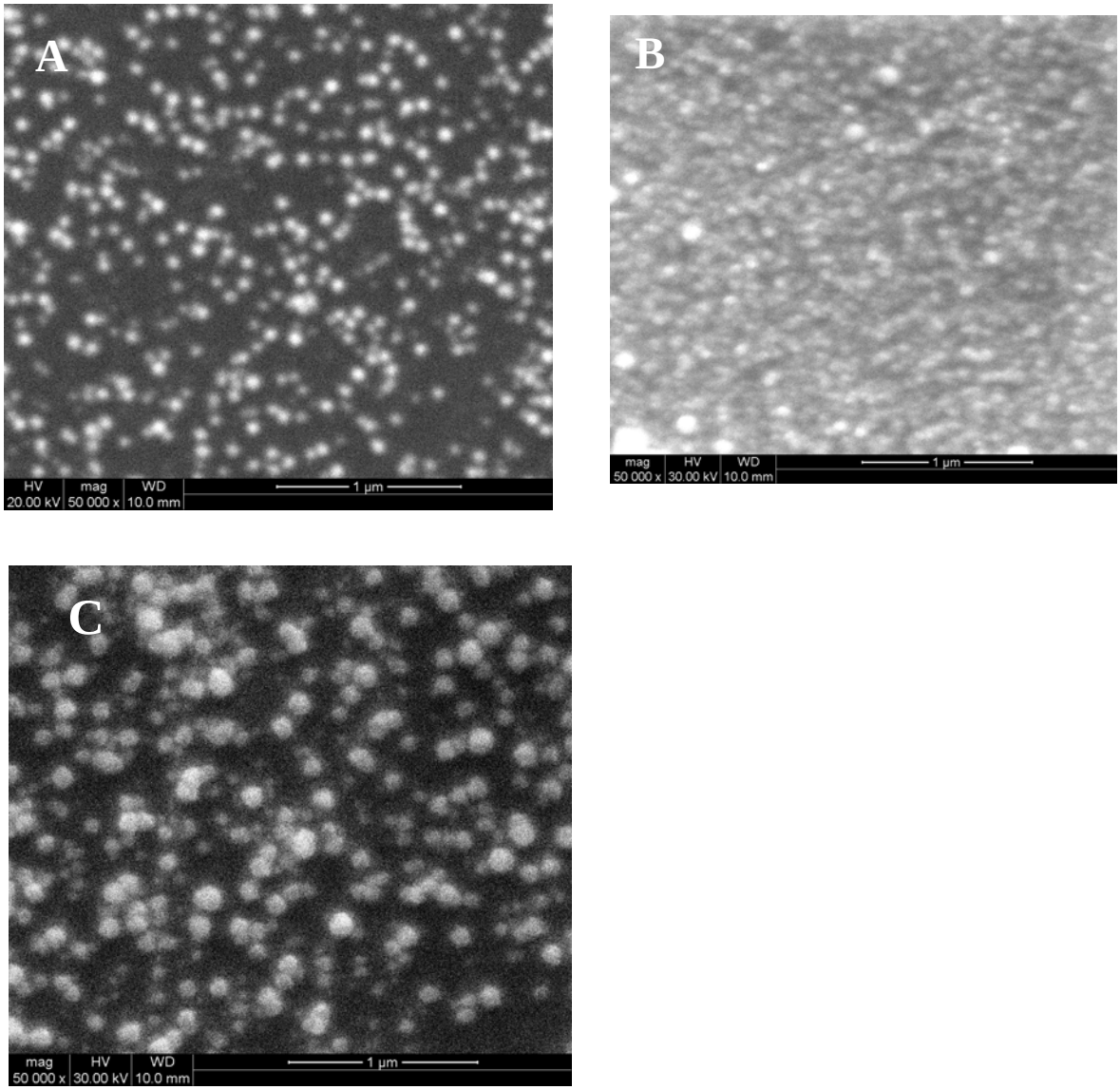

Figure 1. Scanning electron microscope (SEM) image of electrochemically deposited palladium nanoparticles on a glassy carbon electrode from a stirred 7.5mM $PdCl_2$ deposition bath (pH 3). A) first deposition stage at 0V for 1s, B) three deposition/protection

ISBN:978-84-692-9758-2/DL:T-206-2010

stages where the deposited particles are protected with a SAM of 6-ferrocenylhexanethiol in each deposition stage, (C) Three round deposition without protection of the the nanoparticles with an alkanethiol SAM.

sufficient experimental information on the electrode surface composition in order to differentiate between the free GCE area (i.e. area where Pd-Nps are not deposited) and the electrodeposited Pd-NPs. Consequently, diffusionless approaches capable of quantifying the area of the palladium particles excluding the glassy carbon surface were preferred, and a diffusionless method based on formation and stripping of a palladium oxide monolayer was employed for estimating the area of the deposited Pd-NP at each stage of deposition.

The area of palladium deposited can be quantified by formation of a palladium oxide layer in 1 M H_2SO_4 and measuring the charge required to strip the oxide layer. It has been reported that 424 $\mu C.cm^{-2}$ is required to strip a complete palladium oxide monolayer [60, 61]. The electrochemical conditions for the formation of palladium oxide was optimised by taking into account the limit of oxidation potential required to create a monolayer of palladium oxide whilst avoiding partial removal of palladium from the electrode surface. The measurement was performed using linear scan voltammetry where oxide formation was achieved by maintaining the potential of the electrode at 1.1 V for 5 s and scanning in a negative direction until –0.2 V with a scan rate of 50 mV/s. Under these conditions a reproducible palladium oxide reduction peak was obtained. Even though both the glassy carbon electrode and the deposited palladium could be oxidized at this potential, the

UNIVERSITAT ROVIRA I VIRGILI
ELECTROCHEMICALLY DEPOSITED METAL NANOSTRUCTURES FOR APPLICATIONS IN GENOSENSORS
Tesfaye Refera Soreta
ISBN:978-84-692-9758-2/DL:T-206-2010

oxidized palladium layer can be selectively quantified from the reduction peak at 0.46V by taking into account the electrode charging current contribution (Figure 2).

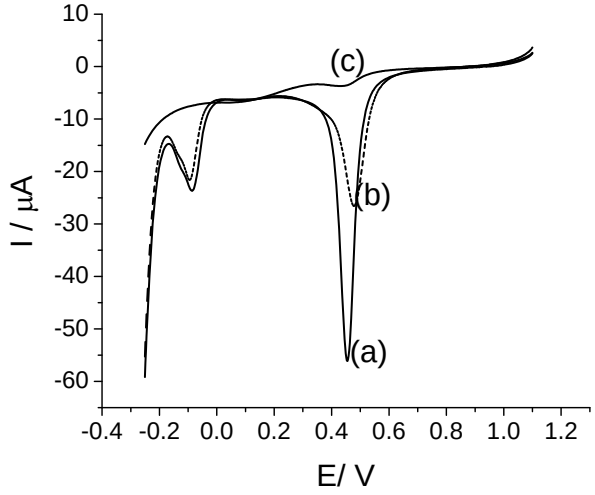

Figure 2. Linear scan voltammetry of palladium oxide formation, followed by reduction for estimation of the area of the deposited palladium particles on glassy carbon electrode. A constant potential of 1.1V is applied for 5s and scanned in a negative direction at 50mV/s in 1M H_2SO_4. The palladium particles were deposited by application of three 1s potential steps of 0V. (a) freshly deposited palladium nanoparticles, (b) palladium particles insulated by a SAM of ME, (C) palladium nanoparticles insulated by a SAM of DDT

In sequential deposition of Pd-NPs, as the particles were protected with a SAM of alkanethiols, a significant reduction of palladium oxide formation was expected. For example, when the short alkanethiol, 2 - mercaptoethanol was used as a protection layer, the palladium oxide stripping peak decreased by 40% (Figure 2b), whereas a longer alkanethiol dodecanethiol (DDT) more effectively prevented the formation of palladium oxide layer (Figure 2c). In these experiments for estimation of surface area of deposited

ISBN:978-84-692-9758-2/DL:T-206-2010

nanoparticles, DDT was used to insulate the deposited palladium nanoparticles in sequential deposition to exclude any palladium oxide reduction current contribution from previous deposition stages. The Pd-NPs area for each deposition step was measured following the deposition stage before capping with a SAM of DDT. Table 1, Column 4 shows the area of the Pd-NPs measured in each deposition step as estimated by this method. On average 0.056 ±0.015 cm^2 of new palladium area is created in each deposition stage and for six deposition / protection stages a total area of 0.33 cm^2 was obtained.

Comparison of Pd-NPs coverage with planar Pd electrode

Palladium was deposited on GC for a longer deposition time to form an electrode surface coated with a planar palladium thin film. A step potential of 0 V was applied for 100 s in the stirred solution of $PdCl_2$ and a shiny palladium layer was deposited with a calculated film thickness of 100nm and this electrode is furthermore referred to as "planar palladium electrode". The area of the planar palladium electrode was estimated by the formation of a PdO layer, and the area of this planar palladium electrode was measured to be about 6 times higher than the total area of the Pd-NPs prepared by six deposition / protection stages (Table 1).

Signal enhancement by sequential deposition of Pd NPs using electroactive protective SAMs

Figure 3 shows the CV of Fc-C_6SH SAM formed on the sequentially deposited Pd-Nano at each deposition / protection process. As previously stated, the Fc-C_6SH was used for

ISBN:978-84-692-9758-2/DL:T-206-2010

protection of the deposited palladium nanoparticles in each deposition stage and backfilled with ME. The ferrocene peaks increased with increasing deposition and protection stages, providing additional information to indicate the creation of new palladium surface in sequential deposition of Pd NPs. Figure 3B shows the increase of the anodic peak current as a function of the deposition stages. The inset in Figure 3A depicts the typical CV of SAM of Fc-C_6SH on the planar palladium electrode.

In order to estimate the contribution of repeated immobilization of Fc-C_6SH on the ferrocene signal, immobilization of a solution of Fc-C_6SH followed by backfilling with 2-mercaptoethanol (ME) and CV measurement of the ferrocenyl signal was repeated four times. Due to repeated exposure of the electrode to Fc-C_6SH, a slight increase was observed in second immobilization which was maintained constant in further immobilization steps. The contribution of repeated immobilization on the overall signal enhancement was thus demonstrated to be minimal. The effect of repeated immobilization of Fc-C_6SH solution on the planar palladium electrode was also studied and no signal increase was observed. The anodic peak current of the CV of SAM of Fc-C_6SH formed on Pd-NPs deposited for six deposition/protection rounds was about 50 times higher than that measured on the planar palladium electrode (Table 1), and this signal enhancement was deemed to be attributable to the unique reactivity and catalytic activity of the Pd-NPs to improve surface adsorption of alkanethiols as well as to enhance the electrochemical signal

.

UNIVERSITAT ROVIRA I VIRGILI
ELECTROCHEMICALLY DEPOSITED METAL NANOSTRUCTURES FOR APPLICATIONS IN GENOSENSORS
Tesfaye Refera Soreta
ISBN:978-84-692-9758-2/DL:T-206-2010

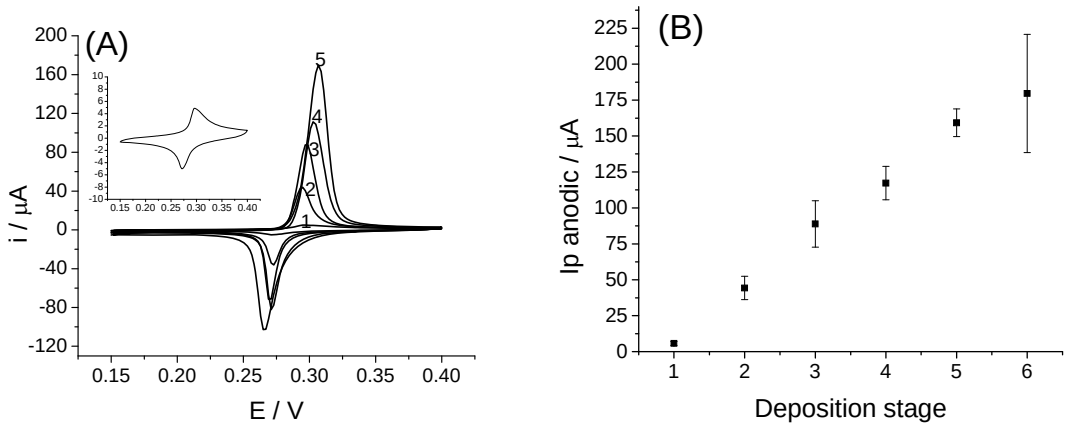

Figure 3. (A) Cyclic voltammogram of SAM of Fc-C_6SH formed on sequentially deposited palladium nanoparticles electrodeposited on glassy carbon electrode. The numbers indicate the deposition stages at which the monolayer of Fc-C_6SH is formed on palladium. The inset is a cyclic voltammogram of SAM of Fc-C_6SH on the planar palladium electrode. (B) Plot of anodic peak current of SAM of Fc-C_6SH versus palladium nanoparticles deposition/protection stages. Error bar: standard deviation of the anodic peak current for three electrodes prepared with the same procedure.

The surface coverage of the Fc-C_6SH SAM (Γ) formed on Pd-NPs and planar palladium electrode was calculated using the area (A) estimated by PdO stripping and the charge (Q) from anodic peak signal (after subtracting the background current) using the relation, $\Gamma = Q/nFA$. For second step and higher deposition steps, the area of the Pd-NPs was taken as the sum of areas until the deposition stage for which the calculation was required. For the ferrocene-ferrocenium conversion, n *is*1. The values for surface coverage as shown in Table 1 clearly showed that there was higher surface coverage of Fc-C_6SH on Pd-NPs than

ISBN:978-84-692-9758-2/DL:T-206-2010

the planar palladium electrode and this is postulated to be related to the enhanced surface reactivity of Pd NPs towards formation of SAM.

Table 1. Estimation of palladium loading and real area of deposited palladium nanoparticles

Deposition stage	Deposition time / s	Pd loading / ($\mu g.cm^{-2}$)	Area* / cm^2	Anodic ferrocenyl peak** / μA	Calculated surface coverage of Fc-C_6SH/ 10^{-10} $mol.cm^{-2}$
1	1	1.56	0.051	5.7	8.1
2	1	1.48	0.064	44.3	15.6
3	1	1.43	0.062	88.9	19.6
4	1	1.22	0.040	117.2	20.1
5	1	1.29	0.077	159.2	20.2
6	1	0.92	0.039	179.6	26.2
1	3***	6.79	0.109	10.4	5.7
1	100s	122.77	2.185	3.8	0.3

* Area of Pd-NPs deposited in each deposition stage before capping with DDT estimated from the charge for reduction of palladium oxide monolayer based on the conversion factor of 424 $\mu C/cm^2$. A SAM protection layer of DDT was used in sequential deposition of palladium

** SAM of Fc-C_6SH used for protection in all stages of deposition stages. The anodic peak current of the ferrocenyl by subtraction baseline current

*** Three consecutive pulses of 0V, each for duration of 1s without protection with SAM of alkanethiol

To demonstrate the specific catalytic activity and reactivity of palladium, the signal enhancement obtained was compared to that observed with gold nanoparticles deposited in

ISBN:978-84-692-9758-2/DL:T-206-2010

a similar manner of sequential protected deposition, and the CV of the SAM of Fc-C_6SH used as a protective layer in sequential deposition of Pd nanoparticles resulted in a markedly higher signal enhancement [57]. For five deposition/protection steps of gold nanoparticles, a maximum of 8 μC of anodic peak was observed, whilst for the palladium nanoparticles, a ferrocene oxidation charge as high as 57 μC for five rounds deposition / protection steps and about 100 μC for six rounds was recorded demonstrating the enhanced reactivity and catalytic activity of palladium nanoparticles electrodeposited using the approach reported here as compared to gold nanoparticles electrodeposited in the same manner. The maximum signal obtained with gold nanoparticles was about 15% of the signal observed with palladium nanoparticles electrodeposited in the same manner.

4. Conclusions

A method for electrodeposition of palladium nanoparticles was reported, which involves sequential deposition and protection of the nanoparticles with alkanethiols SAM to increase their number density on the electrode surface. A higher number of palladium nanoparticles can be deposited with this method via prevention of particle coalescence and creation of new nucleation centres, which has confirmed using SEM image analysis and estimation of the area of deposits. The area of electrodeposited palladium nanoparticles in each deposition stage was estimated using the method of palladium oxide formation and stripping. The electrode area measurement indicated the creation of new palladium nanoparticles with each deposition stage. The surface coverage of the SAM of Fc-C_6SH was calculated from the charge of anodic peak of CV of Fc-C_6SH SAM by excluding the

ISBN:978-84-692-9758-2/DL:T-206-2010

charging current contribution, and it is clearly observed that palladium nanoparticles have a higher surface coverage of alkanethiols SAM than planar palladium electrodes. The use of a Fc-C_6SH SAM as a protection layer in the vsequential deposition of metal nanoparticles also revealed the electrochemical signal amplification as a result of the creation of new nanoparticles in each deposition stage The signal enhancement obtained by Pd-NP by sequential deposition was much higher than that of Au-NP which correlates with the higher surface catalytic property of palladium. Having immense potential application in areas such as biosensing and catalysis, we are currently exploring routes to exploit this signal enhancement in electrochemical DNA sensors.

Acknowledgements This paper partly describes work undertaken in the context of the EC IST project MASCOT FP6-2005-IST-027652. OYF thanks Marie Curie Intra European Fellowship European Community FP7-IEF-221198. Financial support by URV BRDI fellowship is also acknowledged.

References

1. Kenneth J. Klabunde, R. S. M., Chemical and catalytic aspects of nanocrystals. In *Nanoscale Materials in Chemistry*, Klabunde, K. J., Ed. John Wiley: New York, 2001; pp 238-239.
2. Durand, J.; Teuma, E.; Gomez, M., An overview of palladium nanocatalysts: Surface and molecular reactivity. *European Journal of Inorganic Chemistry* **2008**, (23), 3577-3586.
3. Roduner, E., Size matters: why nanomaterials are different. *Chemical Society Reviews* **2006,** 35, (7), 583-592.
4. Arvia, A. J.; Salvarezza, R. C.; Triaca, W. E., Noble metal surfaces and electrocatalysis. Review and perspectives. *Journal of New Materials for Electrochemical Systems* **2004,** 7, (2), 133-143.

ISBN:978-84-692-9758-2/DL:T-206-2010

5. Aiken, J. D.; Finke, R. G., A review of modern transition-metal nanoclusters: their synthesis, characterization, and applications in catalysis. *Journal of Molecular Catalysis a-Chemical* **1999,** 145, (1-2), 1-44.
6. El-Deab, M. S.; Okajima, T.; Ohsaka, T., Fabrication of phase-separated multicomponent self-assembled monolayers at gold nanoparticles electrodeposited on glassy carbon electrodes. *Journal of the Electrochemical Society* **2006,** 153, (12), E201-E206.
7. Su, L.; Mao, L., Gold nanoparticle/alkanedithiol conductive films self-assembled onto gold electrode: Electrochemistry and electroanalytical application for voltammetric determination of trace amount of catechol. *Talanta* **2006,** 70, (1), 68-74.
8. Klabunde, K. J., Introduction to Nanotechnology. In *Nanoscale Materials in Chemistry*, Klabunde, K. J., Ed. John Wiley and Sons Inc.: New York, 2001; p 7.
9. Paunovic, M.; Schlesinger, M., *Fundamentals of electrochemical deposition*. 2nd ed.; Hoboken, NJ : John Wiley & Sons, cop.: 2006.
10. Sasha Gorer, H. L., Rebeca M. Stiger, Michael P. Zach, James V. Zoval, and Reginald M. Penner, *Electrodeposition of Metal Nanoparticles on Graphite and Silicon*. Marcel Dekker, Inc.: New York, 2002; p 237-259.
11. Milchev, A.; Zapryanova, T., Nucleation and growth of copper under combined charge transfer and diffusion limitations - Part II. *Electrochimica Acta* **2006,** 51, (23), 4916-4921.
12. Zoval, J. V.; Lee, J.; Gorer, S.; Penner, R. M., Electrochemical Preparation of Platinum Nanocrystallites with Size Selectivity on Basal Plane Oriented Graphite Surfaces. *J. Phys. Chem. B* **1998,** 102, (7), 1166-1175.
13. Gorer, S.; Liu, H. T.; Stiger, R. M.; Zach, M. P.; Zoval, J. V.; Penner, R. M., Electrodeposition of metal nanoparticles on graphite and silicon. *Metal Nanoparticles: Synthesis, Characterization, and Applications* **2002**, 237-259.
14. Penner, R. M., *Metal Deposition*. First edition ed.; New Mexico, 2007; p 661-709.
15. Giersig, M.; Mulvaney, P., Preparation of ordered colloid monolayers by electrophoretic deposition. *Langmuir* **1993,** 9, (12), 3408-3413.

ISBN:978-84-692-9758-2/DL:T-206-2010

16. Teranishi, T.; Hosoe, M.; Miyake, M., Formation of monodispersed ultrafine platinum particles and their electrophoretic deposition on electrodes. *Advanced Materials* **1997,** 9, (1), 65-&.
17. Rozenberg, B. A.; Tenne, R., Polymer-assisted fabrication of nanoparticles and nanocomposites. *Progress in Polymer Science* **2008,** 33, (1), 40-112.
18. Eugenii Katz, I. W. J. W., Electroanalytical and Bioelectroanalytical Systems Based on Metal and Semiconductor Nanoparticles. *Electroanalysis* **2004,** 16, (1-2), 19-44.
19. Sadik, O. A.; Aluoch, A. O.; Zhou, A., Status of biomolecular recognition using electrochemical techniques. *Biosensors and Bioelectronics* **2009,** 24, (9), 2749-2765.
20. Xiliang Luo, A. M. Anthony J. K. Malcolm R. S., Application of Nanoparticles in Electrochemical Sensors and Biosensors. *Electroanalysis* **2006,** 18, (4), 319-326.
21. El-Deab, M. S.; Sotomura, T.; Ohsaka, T., Oxygen reduction at Au nanoparticles electrodeposited on different carbon substrates. *Electrochimica Acta* **2006,** 52, (4), 1792-1798.
22. Zhang, Y.; Asahina, S.; Yoshihara, S.; Shirakashi, T., Oxygen reduction on Au nanoparticle deposited boron-doped diamond films. *Electrochimica Acta* **2003,** 48, (6), 741-747.
23. Rajalakshmi, N.; Dhathathreyan, K. S., Nanostructured platinum catalyst layer prepared by pulsed electrodeposition for use in PEM fuel cells. *International Journal of Hydrogen Energy* **2008,** 33, (20), 5672-5677.
24. Wei, Z. D.; Chan, S. H.; Li, L. L.; Cai, H. F.; Xia, Z. T.; Sun, C. X., Electrodepositing Pt on a Nafion-bonded carbon electrode as a catalyzed electrode for oxygen reduction reaction. *Electrochimica Acta* **2005,** 50, (11), 2279-2287.
25. Diculescu, V. C.; Chiorcea-Paquim, A. M.; Corduneanu, O.; Oliveira-Brett, A. M., Palladium nanoparticles and nanowires deposited electrochemically: AFM and electrochemical characterization. *Journal of Solid State Electrochemistry* **2007,** 11, (7), 887-898.
26. Gimeno, Y.; Creus, A. H.; Carro, P.; Gonzalez, S.; Salvarezza, R. C.; Arvia, A. J., Electrochemical formation of palladium islands on HOPG: Kinetics, morphology, and growth mechanisms. *Journal of Physical Chemistry B* **2002,** 106, (16), 4232-4244.

ISBN:978-84-692-9758-2/DL:T-206-2010

27. Soreta, T. R.; Strutwolf, J.; O'Sullivan, C. K., Electrochemically deposited palladium as a substrate for self-assembled monolayers. *Langmuir* **2007,** 23, (21), 10823-10830.
28. Liu, H.; Favier, F.; Ng, K.; Zach, M. P.; Penner, R. M., Size-selective electrodeposition of meso-scale metal particles: a general method. *Electrochimica Acta* **2001,** 47, (5), 671-677.
29. Penner, R. M., Mesoscopic Metal Particles and Wires by Electrodeposition. *J. Phys. Chem. B* **2002,** 106, (13), 3339-3353.
30. Walter, E. C.; Murray, B. J.; Favier, F.; Kaltenpoth, G.; Grunze, M.; Penner, R. M., Noble and Coinage Metal Nanowires by Electrochemical Step Edge Decoration. *J. Phys. Chem. B* **2002,** 106, (44), 11407-11411.
31. Lubert, K.-H.; Guttmann, M.; Beyer, L., Electrode reactions and accumulation of hydrogen at carbon paste electrodes in the presence of tetrachloropalladate. *Journal of Electroanalytical Chemistry* **1999,** 462, (2), 174-180.
32. Lubert, K.-H.; Guttmann, M.; Beyer, L.; Kalcher, K., Experimental indications for the existence of different states of palladium(0) at the surface of carbon paste electrodes. *Electrochemistry Communications* **2001,** 3, (2), 102-106.
33. Li, F.; Zhang, B.; Dong, S.; Wang, E., A novel method of electrodepositing highly dispersed nano palladium particles on glassy carbon electrode. *Electrochimica Acta* **1997,** 42, (16), 2563-2568.
34. Christopher Batchelor-McAuley, C. E. B. A. O. S. T. G. J. J. R. G. C., Nano-Electrochemical Detection of Hydrogen or Protons Using Palladium Nanoparticles: Distinguishing Surface and Bulk Hydrogen. *ChemPhysChem* **2006,** 7, (5), 1081-1085.
35. Fournée, V.; Barrow, J. A.; Shimoda, M.; Ross, A. R.; Lograsso, T. A.; Thiel, P. A.; Tsai, A. P., Palladium clusters formed on the complex pseudo-10-fold surface of the [xi]'-Al77.5Pd19Mn3.5 approximant crystal. *Surface Science* **2003,** 541, (1-3), 147-159.
36. Ji, X.; Banks, C. E.; Xi, W.; Wilkins, S. J.; Compton, R. G., Edge Plane Sites on Highly Ordered Pyrolytic Graphite as Templates for Making Palladium Nanowires via Electrochemical Decoration. *J. Phys. Chem. B* **2006,** 110, (45), 22306-22309.

ISBN:978-84-692-9758-2/DL:T-206-2010

37. Atashbar, M. Z.; Banerji, D.; Singamaneni, S.; Bliznyuk, V., Deposition of parallel arrays of palladium nanowires and electrical characterization using microelectrode contacts. *Nanotechnology* **2004,** 15, (3), 374-378.
38. Gimeno, Y.; Hernandez Creus, A.; Gonzalez, S.; Salvarezza, R. C.; Arvia, A. J., Preparation of 100−160-nm-Sized Branched Palladium Islands with Enhanced Electrocatalytic Properties on HOPG. *Chemistry of Materials* **2001,** 13, (5), 1857-1864.
39. Gao, G.-Y.; Guo, D.-J.; Li, H.-L., Electrocatalytic oxidation of formaldehyde on palladium nanoparticles supported on multi-walled carbon nanotubes. *Journal of Power Sources* **2006,** 162, (2), 1094-1098.
40. Safavi, A.; Maleki, N.; Farjami, F.; Farjami, E., Electrocatalytic oxidation of formaldehyde on palladium nanoparticles electrodeposited on carbon ionic liquid composite electrode. *Journal of Electroanalytical Chemistry* **2009,** 626, (1-2), 75-79.
41. Teschner, D.; Vass, E.; Hävecker, M.; Zafeiratos, S.; Schnörch, P.; Sauer, H.; Knop-Gericke, A.; Schlögl, R.; Chamam, M.; Wootsch, A.; Canning, A. S.; Gamman, J. J.; Jackson, S. D.; McGregor, J.; Gladden, L. F., Alkyne hydrogenation over Pd catalysts: A new paradigm. *Journal of Catalysis* **2006,** 242, (1), 26-37.
42. Trapp, O.; Weber, S. K.; Bauch, S.; Backer, T.; Hofstadt, W.; Spliethoff, B., High-throughput kinetic study of hydrogenation over palladium nanoparticles: Combination of reaction and analysis. *Chemistry-a European Journal* **2008,** 14, (15), 4657-4666.
43. Mukherjee, D., Potential application of palladium nanoparticles as selective recyclable hydrogenation catalysts. *Journal of Nanoparticle Research* **2008,** 10, (3), 429-436.
44. Chih-Chio Yang, Annamalai S. K. J.-M. Z., Electrocatalytic Reduction and Determination of Dissolved Oxygen at a Preanodized Screen-Printed Carbon Electrode Modified with Palladium Nanoparticles. *Electroanalysis* **2006,** 18, (1), 64-69.
45. Jing Chen, Q. Z. Y. W. H. W., Size-Dependent Catalytic Activity of Supported Palladium Nanoparticles for Aerobic Oxidation of Alcohols. *Advanced Synthesis & Catalysis* **2008,** 350, (3), 453-464.

ISBN:978-84-692-9758-2/DL:T-206-2010

46. Bianchi, C. L.; Canton, P.; Dimitratos, N.; Porta, F.; Prati, L., Selective oxidation of glycerol with oxygen using mono and bimetallic catalysts based on Au, Pd and Pt metals. *Catalysis Today* **2005,** 102-103, 203-212.
47. Choudhary, V. R.; Samanta, C., Role of chloride or bromide anions and protons for promoting the selective oxidation of H2 by O2 to H2O2 over supported Pd catalysts in an aqueous medium. *Journal of Catalysis* **2006,** 238, (1), 28-38.
48. Nishihata, Y.; Mizuki, J.; Akao, T.; Tanaka, H.; Uenishi, M.; Kimura, M.; Okamoto, T.; Hamada, N., Self-regeneration of a Pd-perovskite catalyst for automotive emissions control. *Nature* **2002,** 418, (6894), 164-167.
49. Santhosh, P.; Manesh, K. M.; Uthayakumar, S.; Komathi, S.; Gopalan, A. I.; Lee, K. P., Fabrication of enzymatic glucose biosensor based on palladium nanoparticles dispersed onto poly(3,4-ethylenedioxythiophene) nanofibers. *Bioelectrochemistry* **2009,** 75, (1), 61-66.
50. Thiagarajan, S.; Yang, R.-F.; Chen, S.-M., Palladium nanoparticles modified electrode for the selective detection of catecholamine neurotransmitters in presence of ascorbic acid. *Bioelectrochemistry* **2009,** 75, (2), 163-169.
51. Chang, Z.; Pan, H.; Zhao, K.; Chen, M.; He, P. G.; Fang, Y. Z., Electrochemical DNA biosensors based on palladium nanoparticles combined with carbon nanotubes. *Electroanalysis* **2008,** 20, (2), 131-136.
52. Hammer, B.; Nørskov, J. K.; Bruce, C. G. a. H. K., Theoretical surface science and catalysis--calculations and concepts. In *Advances in Catalysis*, Academic Press: 2000; Vol. Volume 45, pp 71-129.
53. Sánchez, C. G.; Leiva, E. P. M.; Schmickler, W., On the catalytic activity of palladium clusters generated with the electrochemical scanning tunnelling microscope. *Electrochemistry Communications* **2003,** 5, (7), 584-586.
54. Corthey, G. n.; Rubert, A. A.; Benitez, G. A.; Fonticelli, M. H.; Salvarezza, R. C., Electrochemical and X-ray Photoelectron Spectroscopy Characterization of Alkanethiols Adsorbed on Palladium Surfaces. *The Journal of Physical Chemistry C* **2009,** 113, (16), 6735-6742.

ISBN:978-84-692-9758-2/DL:T-206-2010

55. Carvalho, A.; Geissler, M.; Schmid, H.; Michel, B.; Delamarche, E., Self-Assembled Monolayers of Eicosanethiol on Palladium and Their Use in Microcontact Printing. *Langmuir* **2002,** 18, (6), 2406-2412.
56. Love, J. C.; Wolfe, D. B.; Chabinyc, M. L.; Paul, K. E.; Whitesides, G. M., Self-Assembled Monolayers of Alkanethiolates on Palladium Are Good Etch Resists. *J. Am. Chem. Soc.* **2002,** 124, (8), 1576-1577.
57. Soreta, T. R.; Strutwolf, J.; O'Sullivan, C. K., Eectrochemical fabrication of nanostructured surfaces for enhanced response. *Chemphyschem* **2008,** 9, (6), 920-927.
58. Rasband, W. S. ImageJ. http://rsb.info.nih.gov/ij/
59. A.J. Bard, L. R. F., *Electrochemical Methods: Fundamentals and Applications*. 2nd ed.; John Wiely& Sons: 2001.
60. Rand, D. A. J.; Woods, R., Determination of Surface Composition of Smooth Noble-Metal Alloys by Cyclic Voltammetry. *Journal of Electroanalytical Chemistry* **1972,** 36, (1), 57-&.
61. Bartlett, P. N.; Gollas, B.; Guerin, S.; Marwan, J., The preparation and characterisation of H-1-e palladium films with a regular hexagonal nanostructure formed by electrochemical deposition from lyotropic liquid crystalline phases. *Physical Chemistry Chemical Physics* **2002,** 4, (15), 3835-3842.

UNIVERSITAT ROVIRA I VIRGILI
ELECTROCHEMICALLY DEPOSITED METAL NANOSTRUCTURES FOR APPLICATIONS IN GENOSENSORS
Tesfaye Refera Soreta
ISBN:978-84-692-9758-2/DL:T-206-2010

Chapter 6

Electrochemical Surface Nanostructuring for Enhancement of Signal of DNA Biosensors

UNIVERSITAT ROVIRA I VIRGILI
ELECTROCHEMICALLY DEPOSITED METAL NANOSTRUCTURES FOR APPLICATIONS IN GENOSENSORS
Tesfaye Refera Soreta
ISBN:978-84-692-9758-2/DL:T-206-2010

UNIVERSITAT ROVIRA I VIRGILI
ELECTROCHEMICALLY DEPOSITED METAL NANOSTRUCTURES FOR APPLICATIONS IN GENOSENSORS
Tesfaye Refera Soreta
ISBN:978-84-692-9758-2/DL:T-206-2010

Electrochemical Surface Nanostructuring for Enhancement of Signal of DNA Biosensors

Tesfaye Refera Soreta[1], Olivier Henry[1], Jörg Strutwolf, Ciara K. O´Sullivan[1,2]

[1] *Nanobiotechnology and Bioanalysis Group, Department of Chemical Engineering, Univeritat Rovira I Virgili, 26 Paisos Catalans, 43007, Tarragona, Spain*

[2] *Institució Catalana de Recerca i Estudis Avançats, Passeig Lluís Companys 23, 08010 Barcelona, Spain*

Corresponding author: olivier.henry@urv.cat, ciara.osullivan@urv.cat

UNIVERSITAT ROVIRA I VIRGILI
ELECTROCHEMICALLY DEPOSITED METAL NANOSTRUCTURES FOR APPLICATIONS IN GENOSENSORS
Tesfaye Refera Soreta
ISBN:978-84-692-9758-2/DL:T-206-2010

Abstract

Biosensor signals can be enhanced by specifically designing transducer surfaces for an optimal interaction between biorecognizing probes with the target. This is particularly evident in the case of genosensors, where spacing and orientation of immobilized DNA capture probes need to be controlled to maximize subsequent surface hybridization with the target sequence and achieve high binding signals. To that end, we present a novel approach to the surface nanostructuring of glassy carbon electrodes (GCEs) towards the development of highly sensitive electrochemical genosensors. Gold nanoparticles are sequentially electrochemically nucleated on GCEs to form a dense array of randomly distributed gold nanodomains. The number density of the electronucleated nanoparticles can be increased with sequential electronucleation strategy reported in here and nanoparticles aggregation can be prevented by insulating the nucleated nanoparticles following each round of deposition. The gold nanodomains protected with thiolated probe DNA had an average diameter of 77.07 ± 2.03 nm with density number of 14 $NP.\mu m^{-2}$, 80.86±4.16 nm, with a density number of 23 $NP.\mu m^{-2}$ following 1^{st} and 3rd rounds of deposition respectively. The performances of planar gold electrodes and that of the nanopatterned surfaces prepared following several rounds of deposition were compared for the amperometric detection of DNA. Of all surfaces, that prepared following 3 rounds of deposition exhibited the highest sensitivity 44.89 (nA/nM), with a dynamic detection range spanning from 0.53 nM to 25 nM of the targeted sequence, as compared to 13.67 nA/nM and a linear range of 5.22 to 25 nM for the planar gold electrodes. The use of the nanostructured surface we report here may find application in DNA biosensor for multiplexing on a single electrode surface.

UNIVERSITAT ROVIRA I VIRGILI
ELECTROCHEMICALLY DEPOSITED METAL NANOSTRUCTURES FOR APPLICATIONS IN GENOSENSORS
Tesfaye Refera Soreta
ISBN:978-84-692-9758-2/DL:T-206-2010

1. Introduction

Electrochemical DNA biosensors have been intensively investigated due to their potential for rapid and low cost DNA testing. Some of the applications of these sensors include gene expression monitoring[1], diagnosis of genetic disorders [2, 3], investigation of DNA damage[4], bio-analysis of environmental pollution[5], food quality control and traceability [6, 7]. Electrochemical DNA biosensors exploit electrode surfaces functionalised with short single stranded DNA sequences approximately 15 to 25 bases long and usually referred to as DNA probes.

The performance of DNA biosensors is dependent on the overall efficiency of the surface hybridization event. DNA probes are typically immobilized onto metal electrode substrates via the introduction of a thiol moiety at the 5'-end of the probe sequence to enable the formation of highly packed DNA self-assembled monolayers (SAMs). In order to optimize the hybridization process, parameters such as the surface density and orientation of the immobilized DNA probes require accurate control. Several reports have demonstrated that the rate of surface hybridization decreases with increasing DNA probe density [8-11]. A DNA SAM with a high packing density is not suitable for effective hybridization with the targeted sequence, due to steric hindrance and electrostatic repulsion [12-13]. On the other hand, although a low DNA probe density could solve steric problems as long as the probe orientation can be kept optimum, the electrochemical signal that will be generated might be too low to allow for sensitive measurements.

Controlling the surface density of the probes while maintaining their correct orientation is a challenge that needs to be addressed. Both top-down and bottom-up fabrication

ISBN:978-84-692-9758-2/DL:T-206-2010

approaches have been reported for the preparation of DNA modified substrates of controlled surface probe density. For DNA biosensors where the thiolated probes are attached to the electrode surface by chemisorption, the high probe density on the surface can be diluted using a back-filling approach [14, 15]. After formation of a thiolated single stranded probe DNA SAM on gold surface, a diluter thiol like 6-mercaptohexanol is immobilized to displace non-specifically attached probes and orientate the chemisorbed probes. Even though, this the most commonly used approach in electrochemical DNA sensor application using thiolated DNA probes [16], the main problem is surface reproducibility [17]. Another approach exploits the co-immobilisation of thiolated DNA and short alkanethiols, which is particularly advantageous due to the simplicity of the preparation steps involved, and the improved sensor-to-sensor reproducibility [13, 18, 19]. Other reported strategies to address problem of high surface density consist of the selective electrochemical desorption of DNA or sacrificial alkanethiol SAMs [12, 20, 21], the initial immobilization of DNA probe-target sequence duplexes followed by thermal denaturation[11], the dendron-controlled spacing of probes [22, 23] or the direct grafting of probe sequences at surfaces [24, 25]. For example, the reductive desorption approach was reported for improving the hybridization efficiency resulted in a quartz crystal microbalance signal amplification by one order of magnitude over SAMs containing only the thiolated single stranded DNA [20].

Transducer surface nano-structuring presents the greatest potential for the optimal spacing of the DNA probes at the transducer surface whilst enhancing transducer sensitivity by providing defined nanoscaled immobilization domains as well as the unique catalytic properties of metallic nanoparticles. Nanoelectrochemistry is a branch of electrochemistry that investigates the electrical and electrochemical properties of

ISBN:978-84-692-9758-2/DL:T-206-2010

materials at the nanometer size regime. Surface nanostructures be realized in a verity of manners, including the random electrochemical nucleation and deposition of metal NP on an electrode substrate or the controlled positioning of metallic NPs using scanning probe microscopy (SPM) techniques [26, 27].

The work reported here presents a novel approach to the fabrication of electrochemical DNA biosensors based on the formation of DNA SAMs on electrochemically nucleated gold NP at the surface of glassy carbon electrodes (GCEs). We found that electrochemical nucleation of gold lead to the formation of highly active 77 nm diameter gold NPs. Performing sequential nucleation rounds the NP density number could be tightly controlled, and after each round of deposition, the deposited nanoparticles were capped with thiolated DNA probe and backfilled with mercaptoethanol. Using a model system for the detection of the lymphotoxin alpha gene (LTA) sandwich format with enzyme labeled reporter probe, the sensitivity of these biosensors prepared after each round of deposition was compared. Although three rounds provided the highest sensitivity, biosensors prepared following one, two or four rounds exhibited considerably higher sensitivity when compared to plain gold electrodes, and offered markedly lower detection limits. This novel approach offers great prospects towards the development of highly sensitive, reproducible electrochemical DNA biosensors.

UNIVERSITAT ROVIRA I VIRGILI
ELECTROCHEMICALLY DEPOSITED METAL NANOSTRUCTURES FOR APPLICATIONS IN GENOSENSORS
Tesfaye Refera Soreta
ISBN:978-84-692-9758-2/DL:T-206-2010

2. Materials and methods

2.1. Reagents

Potassium tetrachloro aurate (III) ($KAuCl_4$, 99.995%, Aldrich), sulfuric acid (H_2SO_4, 95%, Scharlau), potassium nitrate (KNO_3, 99%, Sigma), sodium perchlorate ($NaClO_4$, 98%, Sigma), sodium chloride (NaCl, synthesis grade, Scharlau), potassium di hydrogenphosphate (KH_2PO_4, Fluka), hydroquinone ($C_6H_4(OH)_2$, 99%,Sigma), hydrogen peroxide (H_2O_2, 30 %, Scharlau), PBS-Tween (containing 0.05% Tween 20, Sigma), 6-mercapto-hexanol (MCH, 97%, Fluka), 2-mercaptoethanol (ME, 99%, Acros organics), absolute ethanol (Scharlau) were used without any purification. The solutions were prepared in high purity deionized water obtained with a Milli-Q RG system (Millipore Ibérica, Madrid, Spain).

Synthetic oligonucleotides of the following sequences were purchased as lyophilized powder from Biomers (Germany):

- Target amplicon (**TA**) (63-mer sequence: 5′-GGG TTC CCT AAG GGT TGG ACT TCT CCC CAT GAC ACC ACC TGA ACG TCT CTT CCT CCC AAG GGT -3′
- Thiolated DNA probe: 5′-SH-$(CH_2)_6$-ACC CTT GGG AGG AAG AGA CG-3′
- Non.complementary target (**NTA**) (62-mer sequence: 5′- GGG TTC CCT AAG GGT TGG ACC CTT ACC TGG AAT CTG GAA TCA GCC TCT TCT CTG ATG ACC CT
- horseradish peroxidase (HRP) conjugated marker probe (**MP**) at 5′of the sequence: 5′-HRP-TCC AAC CCT TAG GGA ACC C-3’

ISBN:978-84-692-9758-2/DL:T-206-2010

Aliquots of 100 μM of stock solution of these oligonucleotides were prepared in water according to the supplier's instruction and stored frozen until needed. Working oligonucleotide solutions were prepared by appropriate dilution in hybridisation buffer.

2.2. Instrumentation

Electrochemical Measurements. Cyclic voltammetry, potential step deposition of gold nanoparticles and chronoamperometric determination of target were carried out using an Autolab model PGSTAT 12 potentiostat/galvanostat controlled with the General Purpose Electrochemical System (GPES) software (Eco Chemie B.V., The Netherlands). A conventional three-electrode setup was used with the GC electrode modified with gold nanoparticles as the working electrode and a platinum wire as a counter electrode. An Ag/AgCl electrode (CHI 111) served as reference electrode. All potentials were reported with respect to this reference electrode. A magnetic stirrer (p-Selecta 88E) provided the convective transport during potential step deposition and chronoamperometric experiments.

Scanning electron microscopy. Scanning electron microscopy for characterization of the electronucleated gold nanoparticles on glassy carbon electrode was carried out using a Fei Quanta 600 environmental scanning electron microscope at an acceleration voltage of 20 kV in a high vacuum mode and at a working distance of 5 to 10 mm.

2.3. Electrode cleaning and conditioning

Glassy carbon rods (Sigradur®, HTW Hochtemperatur Werkstoffe, Germany) with a length of 7 cm and a diameter of 3 mm were pressed into two layers of heat shrinking

ISBN:978-84-692-9758-2/DL:T-206-2010

polyolefine tubes. One end of the rod, which serves as the electrode surface was polished with 0.3 μm alumina slurry (BUEHLER). The electrodes were washed in water and sonicated in 50:50 (V/V) water:ethanol solution for about 15 minutes. After sonication, the electrodes were washed with water and electrochemically conditioned by potential scanning from 0 V to 1.4 V in 1M $NaClO_4$ for at least five complete scans at $50mV.s^{-1}$ where the high background current due to glassy carbon oxidation diminishes and a reproducible cyclic voltammogram was obtained. Afterwards the background current of the bare electrode was measured by cyclic voltammetry within the potential window of 0 to 0.7 V. Electrodes that showed high background current above a selected reference were excluded. The electrodes were used immediately following the cleaning and conditioning steps.

2.4. Electrochemical deposition of gold nanoparticles

Gold nanoparticles were deposited on polished and cleaned glassy carbon electrode by electrochemical reduction of potassium tetrachloroaurate (III) ($KAuCl_4$, Aldrich) on glassy carbon electrode. A gold deposition bath was prepared by injecting 10 μL of 0.05 M $KAuCl_4$ (in 0.5 M H_2SO_4) into 5 mL of 0.5 M sulphuric acid (H_2SO_4). In cases where the electrode was functionalized with DNA probes, 10 μL of the 0.05 M $KAuCl_4$ was injected into 5 mL of 0.2 M potassium nitrate (KNO_3) so as to prevent the exposure of the DNA probes to low pH conditions. The gold nanoparticles were deposited by chronoamperometry where a pre-treatment potential of 1.1 V was applied for 5 s and followed by a reduction potential of 0 V applied for 5 s in a stirred gold deposition bath using p-Selecta 88-E magnetic stirrer. The electrodes were removed immediately after the deposition step, rinsed with water and exposed to thiolated probe (20 μL, 1 μM).

ISBN:978-84-692-9758-2/DL:T-206-2010

Plain gold electrodes were also prepared by electrochemical deposition of gold on GCEs by extending the deposition time to 30 s in 2 mM $KAuCl_4$ prepared in 0.5 M H_2SO_4.

2.5. Formation of SAM of capture probe DNA and backfilling

Working DNA probe solution was prepared at a concentration of 1 μM in 1M KH_2PO_4, pH 3.8. For immobilisation, 20 μL of the solution was deposited onto the electrodes immediately after the gold electrodeposition step for at least 3 hours. A thorough washing was required in order to remove any weakly bound thiolated probes and minimize non-specific adsorption problems. The electrodes were washed in a stirred solution of PBS-Tween 0.05% for 20min and Milli-Q water for 10 min. For backfilling, 1mM solution of 2-mecarptoethanol prepared in water was immobilized for 30min at room temperature. We have observed that, the use of 2-mercaptoethanol for backfilling on plane gold could not block non-specific adsorption of HRP effectively. As a result, it was substituted with 6-mecarptohexanol. The electrodes were then washed in stirred solution of PBS-Tween 0.05% for 20min and Milli-Q water for 10 min.

2.6. Hybridization

For hybridization of the targets to the surface immobilized probes, 10 mM PBS buffer containing 0.6 M NaCl, pH 7.4 (PBS-600) was used (hybridization buffer). Working oligonucleotide solutions in the concentration range 0.1 – 25 nM were prepared by appropriate dilution of the 100 μM stock solution in hybridization buffer. Following hybridization, the electrodes were washed in stirred PBS-Tween for 10 minutes and 20 μL of 10 nM marker probe prepared in hybridization buffer was deposited on the electrodes and left to interact with the surface duplex for 20 minutes. The electrodes

UNIVERSITAT ROVIRA I VIRGILI
ELECTROCHEMICALLY DEPOSITED METAL NANOSTRUCTURES FOR APPLICATIONS IN GENOSENSORS
Tesfaye Refera Soreta
ISBN:978-84-692-9758-2/DL:T-206-2010

were finally washed in stirred PBS-Tween for 10 minutes and rinsed thoroughly in hybridization buffer before being transferred to the electrochemical cell.

2.7. Chronoamperometric detection of the hybridised target

Chronoamperometric detection[28] was performed in 4.6 mL of stirred hybridization buffer, at an applied potential of -0.1 V. After the signal stabilised (typically within 25 seconds), 200 µL of 0.5 M hydroquinone was injected followed by the injection of 200 µL of 0.5 M H_2O_2. The current required to reduce the hydroquinone oxidized during the regeneration of the HRP label (Figure 1) was measured and used for the realization of calibration curves. Following chronoamperometric measurement, the electrodes were regenerated for repeated use by washing them in stirred hot water (~ 90ºC) for 3 minutes.

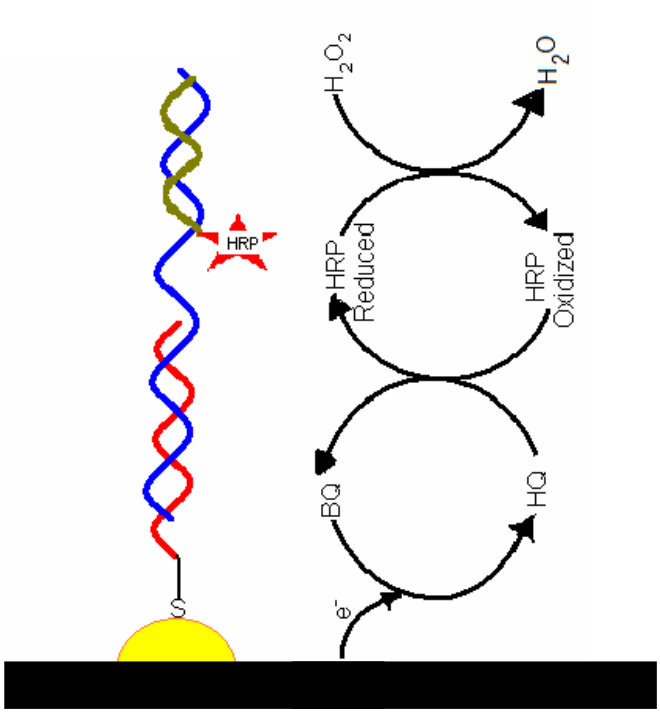

Figure 1 - The electrochemical sandwich assay employed for the detection of LTA and the corresponding electron-relay for generation of chronoamperometric signal. (HQ

ISBN:978-84-692-9758-2/DL:T-206-2010

hydroquinone, BQ benzoquinone, HRP Horseradish peroxidase, H_2O_2 hydrogen peroxide, O_2 oxygen)

3. Results and discussion

3.1. Sequential deposition of gold nanoparticles for DNA biosensor applications

Gold nanoparticles were electrochemically deposited by reduction of the $KAuCl_4$ solution at the electrode surface. As we previously reported, the sequential deposition approach can be used to increase the particle number density of electronucleated gold NP [29]. In order to control the growth of the gold NP and ensure that new NP are formed during each nucleation round, the fresh gold NP should be insulated with a capping agent. Efficient insulation will guarantee that the growth of new NP, during the next nucleation round, will only occur on the glassy carbon substrate ensuring the first deposited NP could not be nucleation centers in subsequent deposition stages. Blocking was achieved by immediately exposing the freshly prepared NP to a solution of thiolated DNA probes, followed by backfilling of the possibly remaining uncovered gold with a short alkanethiol such as ME or MCH [30]. Figure 2.A. illustrate the strategy employed.

UNIVERSITAT ROVIRA I VIRGILI
ELECTROCHEMICALLY DEPOSITED METAL NANOSTRUCTURES FOR APPLICATIONS IN GENOSENSORS
Tesfaye Refera Soreta
ISBN:978-84-692-9758-2/DL:T-206-2010

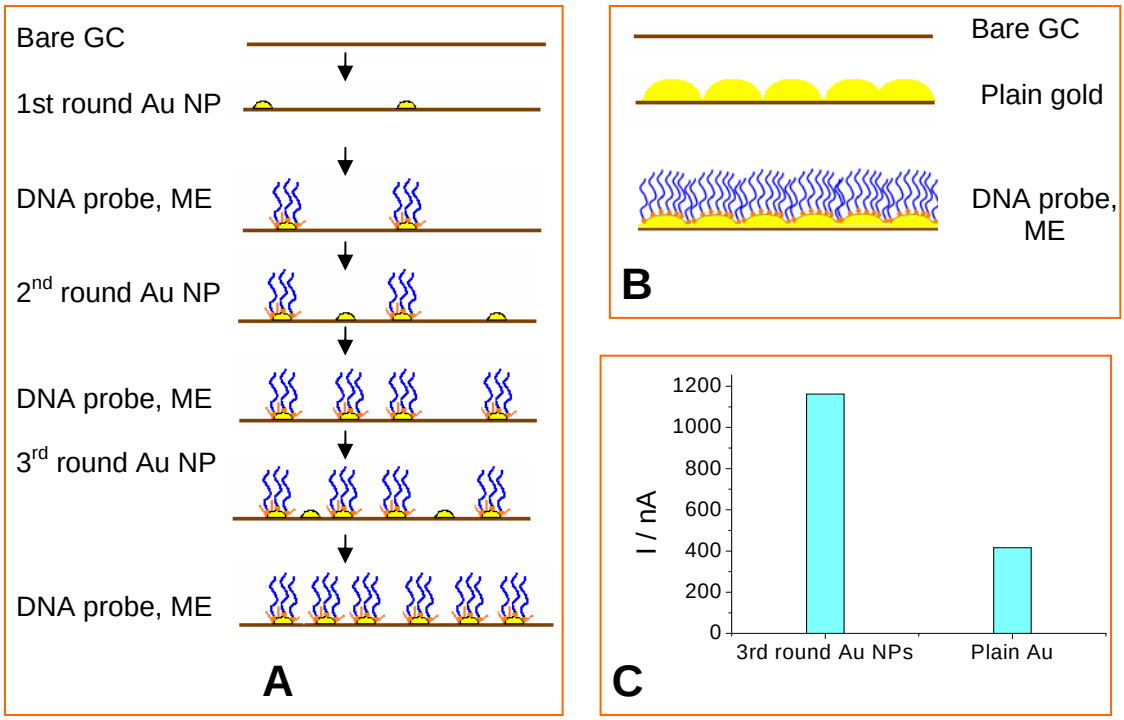

Figure 2 – (A) Illustration of the sequential electronucleation process for the detection of target DNA at electrochemically deposited gold NP using 1, 2, and 3 rounds of electronucleation as compared to (B) plain gold electrode; (C) Amperometric signal comparison for detection 25 nM concentration of the target using three stage gold NPs and plain gold

For the first deposition stage, the deposition bath consisted of 0.1 mM $KAuCl_4$ in 0.5 M H_2SO_4 which is a well established procedure for electronucleation of gold NP on glassy carbon surface [29, 31]. In subsequent deposition stages, the gold bath was changed to KNO_3 so that the immobilized DNA was not damaged by the low pH condition. We therefore used 0.1 mM $KAuCl_4$ in 0.2 M KNO_3 in all subsequent electronucleation rounds

UNIVERSITAT ROVIRA I VIRGILI
ELECTROCHEMICALLY DEPOSITED METAL NANOSTRUCTURES FOR APPLICATIONS IN GENOSENSORS
Tesfaye Refera Soreta
ISBN:978-84-692-9758-2/DL:T-206-2010

The prepared electrodes where inspected using SEM (Figure 3), confirming that the aggregation of gold NP did not occur during deposition. These observations lead us to believe that the mixed SAMs of DNA and short chain alkanethiol provided sufficient insulation to initiate the creation of new nucleation sites at the GCE surface. SEM imaging also allowed us to estimate the density number of the NP to be approximately 14 NP.μm^{-2}, and 23 NP.μm^{-2} following 1 and 3 rounds of deposition/protection stages respectively.

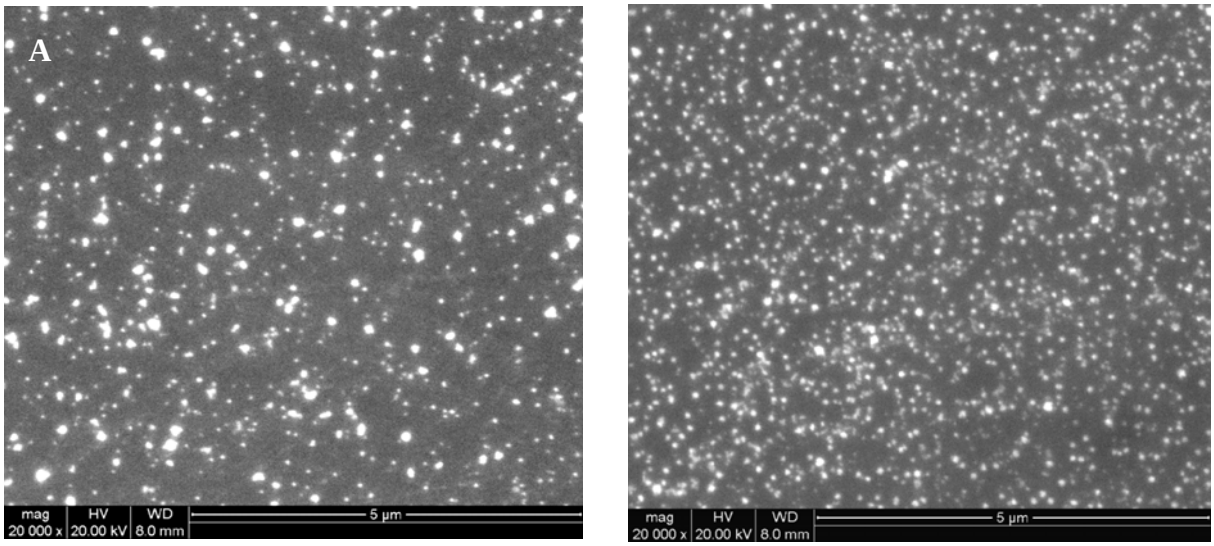

Figure 3 - Scanning electron microscopy images of gold NP modified GCEs. A- The first round electrochemical deposition (B) three rounds of electrochemical deposition with protecting SAM of capture probe (scale bars represent 5 µm).

3.2. Thermal regeneration of the electrodes

We investigated the influence of thermal regeneration on the stability of the gold NP using linear scan voltammetry. A gold oxide monolayer on freshly electrodeposited gold nanoparticles was formed by applying a constant potential of 1.5 V for 5 s, and immediately stripping the oxide layer [29] by scanning from 1.5 V to 0 V at a scan rate of 50 mV.s^{-1}.

ISBN:978-84-692-9758-2/DL:T-206-2010

The electrodes were subsequently placed into a water bath set at 90 ºC for 5 minutes and allowed to be cooled down at room temperature. The gold oxide formation and stripping experiment was repeated using these electrodes and a reproducible gold oxide stripping peak was observed (gold oxide monolayer reduction charge of 1.74 μC before thermal treatment and 1.81 μC after thermal treatment), demonstrating that there was no appreciable change in the gold surface area due to particle dislocation or merging of the nearby particles as a result of the thermal treatment. Consequently, heat treatment was carried out to regenerate the GCEs exposed to the complementary and non-complementary sequences, for developmental work, although the authors are aware that in a final application of the genosensor there would be no requirement for regeneration of the electrode surface,

3.3. DNA Detection on sequential electronucleated gold NP modified GCEs.

For the realization of the DNA biosensor presented here, we used the DNA probe was exploited not only as the bio-sensing element but also for the creation of a protective SAM layer for protection of the electrodeposited nanoparticles during subsequent electronucleation stages. As illustrated in Figure 2.B., we compared the chronomaperometric response recorded at GCEs prepared after 1, 2, 3 and 4 rounds of electronucleation as well as the response at a plain gold electrode following exposure to 25 nM of the target amplicon (Table 1).

ISBN:978-84-692-9758-2/DL:T-206-2010

Table 1. Determination of P1-LTA amplicons on gold nanostructured substrates

Electro nucleation round	Chronoamperometric signal for 25 nM target amplicon / nA	Slope [a] / ($A.mol.L^{-1}$)	Detection limit [b] / nM
1	748	28.27 ± 1.53	0.752
3	1138	44.89 ± 0.49	0.53
4	687	25.35 ± 2.13	1.88
plain gold	416	13.67 ± 1.74	5.22

[a] from linear-fitting of the calibration curve as obtained from Origin 6.0 software

[b] calculated from concentration equivalent to 3 times the standard deviation of triplicate determination in the absence of target amplicon.

For the purpose of comparison, the chronoamperometric signal for 25 nM target, the slope of the calibration curve and the lower concentrations of the target that could be detected were considered. We observed that the chronoamperometric signal of three rounds sequentially deposition of gold NPs was the highest studied. Further deposition deteriorates the electrode performance as demonstrated for Round 4 deposition.

3.4. Calibration curves: Nanostructured vs planar gold surfaces

On a freshly electrochemically deposited gold thin film on glassy carbon electrode, as well as on electrodes following one, two and three rounds of sequential deposition, the sandwich assay for quantification of the LTA target amplicon was assembled. Different concentrations of P1-LTA that range from 25 nM to 0.1 nM were measured. As depicted in Figure 4, for a plain gold electrode, a variation in signal with change in concentration was observed for concentrations 5 nM to 25 nM. Lower concentrations

ISBN:978-84-692-9758-2/DL:T-206-2010

could not be discriminated that could be due to substantial signal contribution of non-specific adsorption of Y-HRP, whereas for the nanostructured electrode, after three round of deposition, could detect concentrations as low as 0.53 nM.

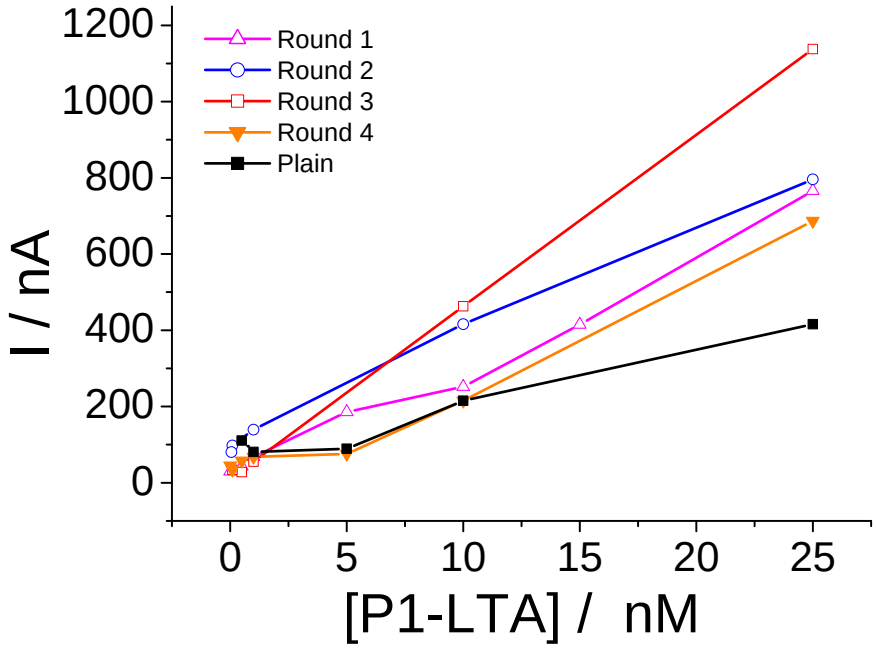

Figure 4 - Calibration curves for detection of P1-LTA on electrochemically nano-structured surface

Conclusion

Nanostructured surfaces exploiting sequential deposition of gold nanoparticles were prepared as substrates for a DNA biosensor, and showed better analytical performance than a planar gold electrode, with the highest signal enhancement observed after three rounds of nanoparticle deposition, with a 3 fold enhancement as compared to plane gold electrode. The enhancement in signal was attributed to the improved condition for effective hybridization between the capture probe and the target as a result of surface nanostructuring, the enhanced reactivity of the nanoparticles allowing a higher level of DNA probe immobilization, as well as to the unique catalytic properties of the

ISBN:978-84-692-9758-2/DL:T-206-2010

deposited nanoparticles. Ongoing work is looking at the applicability of the approach to multiplexing on a single electrode surface.

References

1. Berney, H.; West, J.; Haefele, E.; Alderman, J.; Lane, W.; Collins, J. K., A DNA diagnostic biosensor: development, characterisation and performance. *Sensors and Actuators B-Chemical* **2000,** 68, (1-3), 100-108.
2. Patolsky, F.; Lichtenstein, A.; Willner, I., Highly sensitive amplified electronic detection of DNA by biocatalyzed precipitation of an insoluble product onto electrodes. *Chemistry-a European Journal* **2003,** 9, (5), 1137-1145.
3. Alfonta, L.; Bardea, A.; Khersonsky, O.; Katz, E.; Willner, I., Chronopotentiometry and Faradaic impedance spectroscopy as signal transduction methods for the biocatalytic precipitation of an insoluble product on electrode supports: routes for enzyme sensors, immunosensors and DNA sensors. *Biosensors & Bioelectronics* **2001,** 16, (9-12), 675-687.
4. Oliveira Brett, A. M.; Diculescu, V. C.; Chiorcea-Paquim, A. M.; Serrano, S. H. P.; Merkoçi, S. A. a. A., Chapter 20 DNA-electrochemical biosensors for investigating DNA damage. In *Comprehensive Analytical Chemistry*, Elsevier: 2007; Vol. Volume 49, pp 413-437.
5. Bagni, G.; Osella, D.; Sturchio, E.; Mascini, M., Deoxyribonucleic acid (DNA) biosensors for environmental risk assessment and drug studies. *Analytica Chimica Acta* **2006,** 573, 81-89.
6. Bettazzi, F.; Lucarelli, F.; Palchetti, I.; Berti, F.; Marrazza, G.; Mascini, M., Disposable electrochemical DNA-array for PCR amplified detection of hazelnut allergens in foodstuffs. *Analytica Chimica Acta* **2008,** 614, (1), 93-102.
7. Marmiroli, N.; Maestri, E.; Gulli, M.; Malcevschi, A.; Peano, C.; Bordoni, R.; De Bellis, G., Methods for detection of GMOs in food and feed. *Analytical and Bioanalytical Chemistry* **2008,** 392, (3), 369-384.
8. Yguerabide, J.; Ceballos, A., Quantitative Fluorescence Method for Continuous Measurement of DNA Hybridization Kinetics Using a Fluorescent Intercalator. *Analytical Biochemistry* **1995,** 228, (2), 208-220.
9. Wilkins Stevens, P.; Henry, M. R.; Kelso, D. M., DNA hybridization on microparticles: determining capture-probe density and equilibrium dissociation constants. *Nucl. Acids Res.* **1999,** 27, (7), 1719-1727.
10. Henry, M. R.; Wilkins Stevens, P.; Sun, J.; Kelso, D. M., Real-Time Measurements of DNA Hybridization on Microparticles with Fluorescence Resonance Energy Transfer. *Analytical Biochemistry* **1999,** 276, (2), 204-214.
11. Peterson, A. W.; Heaton, R. J.; Georgiadis, R. M., The effect of surface probe density on DNA hybridization. *Nucl. Acids Res.* **2001,** 29, (24), 5163-5168.
12. Sanchez-Pomales, G.; Santiago-Rodriguez, L.; Rivera-Velez, N. E.; Cabrera, C. R., Control of DNA self-assembled monolayers surface coverage by electrochemical desorption. *Journal of Electroanalytical Chemistry* **2007,** 611, (1-2), 80-86.
13. Tokuhisa, H.; Liu, J. A.; Omori, K.; Kanesato, M.; Hiratani, K.; Baker, L. A., Efficient Biosensor Interfaces Based on Space-Controlled Self-Assembled Monolayers. *Langmuir* **2009,** 25, (3), 1633-1637.

ISBN:978-84-692-9758-2/DL:T-206-2010

14. Levicky, R.; Herne, T. M.; Tarlov, M. J.; Satija, S. K., Using Self-Assembly To Control the Structure of DNA Monolayers on Gold: A Neutron Reflectivity Study. *Journal of the American Chemical Society* **1998,** 120, (38), 9787-9792.
15. Berganza, J.; Olabarria, G.; García, R.; Verdoy, D.; Rebollo, A.; Arana, S., DNA microdevice for electrochemical detection of Escherichia coli 0157:H7 molecular markers. *Biosensors and Bioelectronics* **2007,** 22, (9-10), 2132-2137.
16. Herne, T. M.; Tarlov, M. J., Characterization of DNA Probes Immobilized on Gold Surfaces. *J. Am. Chem. Soc.* **1997,** 119, (38), 8916-8920.
17. Berggren, C.; Bjarnason, B.; Johansson, G., Capacitive biosensors. *Electroanalysis* **2001,** 13, (3), 173-180.
18. Steel, A. B.; Levicky, R. L.; Herne, T. M.; Tarlov, M. J., Immobilization of nucleic acids at solid surfaces: Effect of oligonucleotide length on layer assembly. *Biophysical Journal* **2000,** 79, (2), 975-981.
19. Henry, O. Y. F.; Perez, J. G.; Sanchez, J. L. A.; O'Sullivan, C. K., Electrochemcial characterisation and hybridisation efficiency of co-assembled monolayers of PEGylated ssDNA and mercaptohexanol on planar gold electrodes. *Biosensors and Bioelectronics* In Press, Corrected Proof.
20. Satjapipat, M.; Sanedrin, R.; Zhou, F. M., Selective desorption of alkanethiols in mixed self-assembled monolayers for subsequent oligonucleotide attachment and DNA hybridization. *Langmuir* **2001,** 17, (24), 7637-7644.
21. Henry, O. Y. F.; Maliszewska, A.; O'Sullivan, C. K., DNA surface nanopatterning by selective reductive desorption from polycrystalline gold electrode. *Electrochemistry Communications* **2009,** 11, (3), 664-667.
22. Oh, S. J.; Ju, J.; Kim, B. C.; Ko, E.; Hong, B. J.; Park, J.-G.; Park, J. W.; Choi, K. Y., DNA microarrays on a dendron-modified surface improve significantly the detection of single nucleotide variations in the p53 gene. *Nucl. Acids Res.* **2005,** 33, (10), e90-.
23. Choi, Y. S.; Yoon, C. W.; Lee, H. D.; Park, M.; Park, J. W., Efficient protein-ligand interaction by guaranteeing mesospacing between immobilized biotins. *Chemical Communications* **2004**, (11), 1316-1317.
24. Liu, G. Y.; Xu, S., Nanografting: A new fabrication method using simultaneous nanoshaving and molecular self-assembly. *Abstracts of Papers of the American Chemical Society* **1997,** 214, 29-IEC.
25. Liu, M. Z.; Liu, G. Y., Hybridization with nanostructures of single-stranded DNA. *Langmuir* **2005,** 21, (5), 1972-1978.
26. Leiva, E., *Nanoelectrochemistry*. Second ed.; John Wiley & Sons, Inc.: New Jersey, 2006; p 679 - 691.
27. Hugelmann, M.; Hugelmann, P.; Lorenz, W. J.; Schindler, W., Nanoelectrochemistry and nanophysics at electrochemical interfaces. *Surface Science* **2005,** 597, (1-3), 156-172.
28. Ryoo, H.; Kim, Y.; Lee, J.; Shin, W.; Myung, N.; Hong, H. G., Immobilization of horseradish peroxidase to electrochemically deposited gold-nanoparticles on glassy carbon electrode for determination of H2O2. *Bulletin of the Korean Chemical Society* **2006,** 27, (5), 672-678.
29. Soreta, T. R.; Strutwolf, J.; O'Sullivan, C. K., Eectrochemical fabrication of nanostructured surfaces for enhanced response. *Chemphyschem* **2008,** 9, (6), 920-927.
30. Herne, T. M.; Tarlov, M. J., Characterization of DNA Probes Immobilized on Gold Surfaces. *Journal of the American Chemical Society* **1997,** 119, (38), 8916-8920.

ISBN:978-84-692-9758-2/DL:T-206-2010

31. Finot, M. O.; Braybrook, G. D.; McDermott, M. T., Characterization of electrochemically deposited gold nanocrystals on glassy carbon electrodes. *Journal of Electroanalytical Chemistry* **1999,** 466, (2), 234-241.

UNIVERSITAT ROVIRA I VIRGILI
ELECTROCHEMICALLY DEPOSITED METAL NANOSTRUCTURES FOR APPLICATIONS IN GENOSENSORS
Tesfaye Refera Soreta
ISBN:978-84-692-9758-2/DL:T-206-2010

ISBN:978-84-692-9758-2/DL:T-206-2010

Chapter 7

General Conclusions and Future Work

UNIVERSITAT ROVIRA I VIRGILI
ELECTROCHEMICALLY DEPOSITED METAL NANOSTRUCTURES FOR APPLICATIONS IN GENOSENSORS
Tesfaye Refera Soreta
ISBN:978-84-692-9758-2/DL:T-206-2010

UNIVERSITAT ROVIRA I VIRGILI
ELECTROCHEMICALLY DEPOSITED METAL NANOSTRUCTURES FOR APPLICATIONS IN GENOSENSORS
Tesfaye Refera Soreta
ISBN:978-84-692-9758-2/DL:T-206-2010

Chapter 7. General conclusions and future work

7.1. Conclusions

Biosensor signals can be enhanced by specifically designing transducer surfaces with the objective of providing the best environment to the recognition molecules. This is particularly evident in the case of genosensors, where spacing and orientation of immobilised DNA capture probes need to be carefully controlled to maximise subsequent surface hybridisation with the target sequence and achieve high binding signals. To address the spacing and orientation requirements, nanostructured electrode surface preparation methods can be exploited for the development of electrochemical genosensors to alleviate problems related to surface crowding of capture probes and the creation of a suitable environment for enhancement of the biorecognition events. To this end, several surface nanostructuring approaches have been investigated.

The first surface nanostructuring approach studied was based on the initial formation of self-assembled monolayers of alkanethiols (SAM) on bi-metallic substrates, followed by the selective desorption of the SAM from one of the metals by applying metal-specific alkanethiol reduction potentials. In order to realise this objective, two metals should be identified and their ability to form SAMs of alkanethiols investigated.

In line with the first objective of this PhD thesis, we explored metals other than the classically used gold (like palladium, platinum, rhodium and ruthenium) for developing procedures for electrochemical deposition of these metals on glassy carbon electrode to provide functional surface for the formation alkanethiol based SAMs. The first element of interest was palladium which was reported to form stable alkanethiol SAM. There was no report on electrochemical characterisation of alkanethiol SAMs on palladium, and therefore full study on electrochemical deposition of palladium and electrochemical characterisation of alkanethiols SAM formed on this substrate was studied.

Electrochemical deposition parameters for palladium were optimised. Different palladium deposition baths (metal ion source, pH and supporting electrolyte),

ISBN:978-84-692-9758-2/DL:T-206-2010

electrochemical deposition conditions (cyclic voltammetry, galvanostatic and potentiostatic conditions) were studied. The deposited palladium thin films were characterised by microscopic methods such as scanning electron microscopy (surface morphology) and electrochemical methods (metal loading, thickness of the deposited palladium layer). Two sets of electrodes on which palladium thin film electrodeposited were prepared for SAM formation. The first set consisted of electrodes with a mirror-like palladium surface, produced under lower galvanostatic and potentiostatic conditions. The palladium surface of the second set of electrodes had a black and non-reflecting appearance, again produced by constant potential and galvanostatic conditions. Only very minor blocking of methylviologen as a redox probe was observed for the SAMs on shiny palladium surfaces generated both potentiostatically and galvanostatically and explained by the presence of microcracks and smoothness of the deposit. In contrast, monolayers assembled on the black palladium surfaces form a substantial barrier against the redox reaction of methylviologen redox probe indicating a more complete palladium thin film and formation of stable alkanethiol based SAM.

In a second step, various methods for the preparation of mixed metal surfaces were studied, which consisted in (i) the electrochemical deposition of palladium on gold electrode, (ii) the co-deposition of palladium and gold from palladium-gold mixed deposition bath on GC electrodes, and (iii) the co-sputtering of palladium and gold onto silicon (100) substrates.

In line with sub-objective 2, a selective reduction desorption of alkanethiol from a mixed metal substrate was demonstrated. Mixed metal electrodes were prepared by electrodeposition of palladium onto gold electrodes for short deposition times. The presence of both palladium and gold atoms on the electrode surface was confirmed by electrochemical method. We demonstrated selective reductive desorption of SAM of 2-mercaptoethanol from the palladium domains of the mixed palladium-gold surface. Electrochemical DNA biosensors were constructed using these substrates and their performances compared to that of plain gold electrodes. For the biosensor configuration studied, the mixed metal substrates did not show improvement as compared to plain gold electrodes. Even though the surface nanostructuring with mixed metal substrates

ISBN:978-84-692-9758-2/DL:T-206-2010

did not show improvement on sensitivity of DNA biosensors, they my find other applications such as in catalysis. The mixed metal substrate prepared by co-evaporation of palladium and gold with various ratio may find application in catalysis.

In line with sub-objective 3, studies were conducted for electrochemical surface nanostructuring of carbon surface with metal particles. A method was developed to prepare nano-sized domains to act as substrates for the immobilisation of SAMs and optimised in order to increase nanoparticles number density while preventing the formation of aggregates. With the objective of realising highly sensitive genosensors, the nanostructuring approach allowed the creation of favourable conditions for the effective interaction of nanodomains of DNA capture probes attached to the nanoparticles with their target sequence.

The sequential electrochemical nucleation approach involved a number of electrochemical deposition and protection steps. Briefly, the first stage of electrochemical deposition of the metal nanoparticles on the glassy carbon surface was followed by protection of the particles by self-assembling of a thiol monolayer to prevent them from being used as seeds in subsequent deposition steps. In the next deposition step, new particles were formed on the glassy carbon surface due to the insulating action of the SAM on the particles deposited in the previous step. Optimal conditions regarding particle size, distribution and number density were studied by varying deposition parameters like deposition potential, deposition time and concentration of the deposition bath. An electroactive labelled thiol that selectively chemisorbed onto the metal nanoparticles was used to distinguish the glassy carbon electroactive surface from the gold nanoparticle surface.

We initially studied the sequential deposition of gold nanoparticles and further extended the developed methodology to the sequential deposition of palladium nanoparticles. A higher ferrocene signal enhancement was recorded when using sequentially deposited gold nanoparticles as compared to that recorded when using planar gold electrodes. Furthermore, sequential deposition of palladium using ferrocenyl alkanethiol protective

ISBN:978-84-692-9758-2/DL:T-206-2010

SAM showed markedly higher ferrocenyl signal enhancement (57.5 μC after fifth round) than gold nanoparticles (7.2 μC after fifth round) with the overall enhancement factor close to 48 fold when comparing the palladium nanostructured surface with the planar gold electrodes (1.2 μC) routinely used in electrochemical genosensors. The signal enhancement can be attributed to the unique properties of nanoparticles with the higher surface ratio of surface atoms not only making the self-assembling processes of thiol-based monolayers more effective on the nanoparticles than on bulk metals, but also contributing to signal enhancement due to the inherent enhanced catalytic activity.

As described in the introduction part of the thesis, surface nanostructuring could enhance hybridisation efficiency of DNA biosensors and improves the sensitivity of the biosensors. In line with sub objective 4, nanostructured surface using the sequential deposition method developed was used for genosensor applications. Electrode surface nanostructuring using sequentially deposited gold nanoparticles for signal enhancement and improving sensitivity of DNA biosensor was demonstrated. SAMs of 20 base thiolated DNA capture probe formed on the nanostructured surface were employed for the detection of a 63 bases oligonucleotides model target using horseradish peroxidase as enzymatic label. The electrochemical signal recorded was compared against a gold planar electrode prepared by electrochemical deposition of gold on glassy carbon electrode and higher sensitivity was observed for the nanostructured electrodes for detection of the target DNA with a sandwich assay using horseradish peroxidase enzyme label. Nanostructured electrode prepared following three rounds of deposition exhibited sensitivity of 44.89 (nA/nM) and linear range 0.53 nM to 25 nM, where as for the plain gold electrodes sensitivity was 13.67 nA/nM with a linear range extending from 5.22 nM to 25 nM. In another approach, for detection of ferrocene labelled target, the nanostructured electrode for three rounds of gold nanoparticles sequential deposition resulted in a 3.5 fold signal enhancement in comparison to the signal recorded using a plain gold electrode.

Overall, this work has contributed significantly to improvement of transducer surface which is a key element in the construction of a genosensors. The work presented in this thesis is focused on the basic understanding and characterisation of nanostructured

ISBN:978-84-692-9758-2/DL:T-206-2010

surfaces with simple alkanethiols and electrochemical interrogations. At the first stage of the work, preparation and characterisation of nanostructured surfaces was studied. The high surface reactivity of the electronucleated metal nanoparticles to form alkanethiol SAMs was confirmed. Strategies to increase the particles number density were developed. Based on these findings, genosensors were constructed with improved sensitivity than routinely used gold electrodes. As a model, genosensors for the detection of the lymphotoxin-alpha gene were constructed to investigate improvement of signal as a result of surface nanostructuring. The reason for the observed signal enhancement was explained by the high surface reactivity of the metallic nanoparticles to strongly bind with thiolated probe DNA, and availability of suitable environment for effective hybridisation with DNA target as a result of surface nanostructuring.

7.2. Future work

In the development of genosensors, the control of surface density and orientation of probe molecules is crucial for extracting the required signal as a result of the interaction with the target DNA/RNA sequence. The nanostructuring approach developed in this study may find applications in other biosensor applications such as immunosensors and aptasensors.

The sequential deposition approach of surface nanostructuring also offers the possibility of multianalyte detection, in which different capture probe SAMs could be formed in each stage of the sequential deposition. As the performance of a DNA biosensor from a single deposition stage is significantly better than a bulk gold electrode, with three deposition stages three non-cross reacting targets could be sensed as far as suitable multi-labels could be used.

The sequential deposition of metal nanoparticles developed in this work for surface nanostructuring provides a structured surface where sensing and anchoring domains are integrated on an electrode. The metallic nanoparticle domains are used for attaching the biomolecular probes, whereas the glassy carbon domains can be used for electrochemical sensing of the transduction process in cases where diffusion controlled

ISBN:978-84-692-9758-2/DL:T-206-2010

redox markers are used. As a result signal enhancement is achievable as compared to classical plain gold electrodes, where sensing of the diffusion controlled redox markers during the detection stage is reduced due to blocking of the surface with a back-filler monolayer or other protective layers.

Mixed metal surface structuring could find applications to construct biosensors where one of the metal domains is used as a platform for anchoring the biorecognition monolayer and the other metal domain is used for electrochemically catalysing the labels so that higher signal amplification could be achieved.

In this work, surface nanostructuring of glassy carbon electrodes with sequential deposition of metal nanoparticles has been demonstrated. The enhancement of signal for DNA biosensor application has been demonstrated. For mass production of these substrates, the glassy carbon electrode could be replaced with disposable screen printed carbon electrodes. Optimisation of deposition parameters for the particular screen printed carbon electrode will be required in order to use them as substrates for biosensor applications.

Surface nanostructuring is not the only solution for improving the sensitivity and reproducibility of biosensors. Improvement in surface immobilisation of biorecognition probes together with a favourable medium for the biorecognition event and advances in detection methods can give highly sensitive biosensors. Highly sensitive detection systems like nanoparticle labels[81], dual amplification strategy with enzymes[89, 202] should enhance the signal level of the developed nanostructured surface in genosensor applications.